

26+ Year Old Photovoltaic Power Plant: Degradation and Reliability

Evaluation of Crystalline Silicon Modules – South Array

By

Kolapo Olakonu

A Thesis Presented in Partial Fulfillment
of the Requirements for the Degree
Master of Science in Technology

Approved November 2012 by the
Graduate Supervisory Committee:

Govindasamy TamizhMani, Chair
Devarajan Srinivasan
Bradley Rogers

ARIZONA STATE UNIVERSITY

December 2012

ABSTRACT

As the use of photovoltaic (PV) modules in large power plants continues to increase globally, more studies on degradation, reliability, failure modes, and mechanisms of field aged modules are needed to predict module life expectancy based on accelerated lifetime testing of PV modules. In this work, a 26+ year old PV power plant in Phoenix, Arizona has been evaluated for performance, reliability, and durability. The PV power plant, called Solar One, is owned and operated by John F. Long's homeowners association. It is a 200 kW_{dc}, standard test conditions (STC) rated power plant comprised of 4000 PV modules or frameless laminates, in 100 panel groups (rated at 175 kW_{ac}). The power plant is made of two center-tapped bipolar arrays, the north array and the south array. Due to a limited time frame to execute this large project, this work was performed by two masters students (Jonathan Belmont and Kolapo Olakonu) and the test results are presented in two masters theses. This thesis presents the results obtained on the south array and the other thesis presents the results obtained on the north array. Each of these two arrays is made of four sub arrays, the east sub arrays (positive and negative polarities) and the west sub arrays (positive and negative polarities), making up eight sub arrays. The evaluation and analyses of the power plant included in this thesis consists of: visual inspection, electrical performance measurements, and infrared thermography. A possible presence of potential induced degradation (PID) due to potential

difference between ground and strings was also investigated. Some installation practices were also studied and found to contribute to the power loss observed in this investigation. The power output measured in 2011 for all eight sub arrays at STC is approximately 76 kW_{dc} and represents a power loss of 62% (from 200 kW to 76 kW) over 26+ years. The 2011 measured power output for the four south sub arrays at STC is 39 kW_{dc} and represents a power loss of 61% (from 100 kW to 39 kW) over 26+ years. Encapsulation browning and non-cell interconnect ribbon breakages were determined to be the primary causes for the power loss.

DEDICATION

This thesis is dedicated to the memory of my father (David Olaoye Olakonu), my uncle (Paul Owodunni), my grandmother (Ma Adekanmbi). Their impact in my life is incomparable.

I thank my wife, Grace and our children, Favored and Joelle-Anne, for their support throughout the duration of my academic program at Arizona State University.

ACKNOWLEDGMENTS

From a heart of gratitude, I wish to thank to Dr. Govindasamy TamizhMani for accepting me into the field of solar research. This opportunity has laid a great foundation for my career. Thanks to SRP (Salt River Project), and Mr. Ernie Palomino, Mr. John Hetrick, Mr. Don Pelley and Grant Smedley for the technical and funding support to execute the project successfully. We would like to thank the John F. Long's home owners association of the Solar One sub division for allowing students to work in their facility. Huge thanks to our highly experienced consultant Mr. Bill Kazseta from the industry without whom, the work in this document could not have been successful. I appreciate all I learned from Bill throughout the site work. Bill will continue to motivate me for years to come. Thanks to my committee members; Dr. Bradley Rogers and Dr. Srinivasan Devarajan for your help and time with my work throughout the program. Thanks to Mr. Joseph Kuitche, for the direction, guidance from start to finish. I appreciate the joint working partnership with Jonathan Belmont on this project. Thanks to Sai Tatapudi, for the time out with us in the field. Thanks to my mentors Mr. Randy Dunton and Mr. David Filani for the motivation to pursue this program at ASU, Suryanarayana Vasantha Janakeera, you've been helpful with the project on-site and at the Arizona State University Photovoltaic Reliability Laboratory (ASU-PRL). Jaya Mallineni, thank you for taking up the challenge to understudy this research work for future projects. Other students from the ASU-PRL,

Meena, Brett, Qurat-ul-ain, Amber, Sierrah and Jim John, I appreciate your help on this Solar One project.

TABLE OF CONTENTS

	Page
LIST OF TABLES	ix
LIST OF FIGURES	x
CHAPTER	
1 INTRODUCTION	1
1.1 Background	1
1.2 Statement of problem	2
1.3 Scope for investigation	3
2 LITERATURE REVIEW	5
2.1 Previous site work at Solar One power plant	5
2.1.1 Visual inspection.....	5
2.1.2 Electrical measurements	5
2.2 Bipolar array	6
2.3 Degradation studied	8
2.3.1 Degradation or failure of packaging materials.....	9
2.3.2 Degradation or failure caused by loss of adhesion	10
2.3.3 Degradation or failure of module interconnects	11
2.3.4 Degradation caused by moisture intrusion.....	12
2.3.5 Degradation or failure of the mono-crystalline silicon solar cells	12
3 METHODOLOGY.....	14
3.1 Power plant configuration	14

CHAPTER	Page
3.1.1 PV modules and array characteristics.....	16
3.1.2 Power conditioner characteristics.....	17
3.2 Field work	18
3.2.1 Overview of performed work	18
3.2.2 Equipment used.....	18
3.3 Measurement strategy.....	19
3.3.1 Eight sub arrays I-V curve measurement.....	19
3.3.2 One hundred panel group I-V curves measurement....	19
3.3.3 Analyses of monthly/annual energy-billing report	19
3.3.4 PID study	20
3.3.5 Visual inspection.....	20
3.3.6 Hotspots scan.....	20
3.3.7 Interconnect breakage determination.....	21
3.3.8 Low irradiance I-V measurements of sample PG's.....	22
3.3.9 Temperature and wind study.....	22
3.3.10 Wet and dry insulation test	23
3.4 Laboratory work.....	24
3.4.1 Baseline curve measurement.....	24
4 RESULTS AND DISCUSSION	25
4.1 Performance degradation.....	25
4.1.1 Performance of 4 south sub arrays	26
4.1.2 Performance of 100 panel groups.....	28

CHAPTER	Page
4.1.3 Annual performance degradation of the system	30
4.1.4 Performance at low irradiance.....	31
4.2 Visual inspection analysis	33
4.2.1 Failure modes observed.....	33
4.2.2 Overall array broken interconnect summary	33
4.2.3 Broken interconnects effects on Pmax, Isc and FF	36
4.3 Panel voltages for the south array.....	39
4.4 PV south array temperatures	41
4.5 Hot cell areas.....	43
4.6 High potential insulation test	47
4.7 I-V before and after repair	49
4.8 Overall performance degradation summary.....	49
5 CONCLUSION	53
5.1 Thermal fatigue and interconnect breakage.....	53
5.2 Encapsulant browning	54
5.3 Module replacements	55
REFERENCES	56
 APPENDIX	
A RESULTS OF SOLAR ONE ARRAY MEASUREMENTS	58

LIST OF TABLES

Table	Page
4.1 Results of 4 south sub arrays measurements	26
4.2 Results of high and low irradiance measurements.....	31
4.3 PV Array average temperature distribution	42
4.4 Lab experiment on back sheet ventilation	46
4.5(a) Hi-pot test resistance output in mega ohms (MΩ)	47
4.5(b) Hi-pot test current output in milliamps (mA)	48

LIST OF FIGURES

Figure	Page
1.1 Google Satellite Photograph of Solar One System	2
2.1 Solar One Bipolar array simplified schematic.....	8
2.2(a) Laminate-bus bar profile schematic.....	9
2.2(b) Laminate-bus bar details.....	9
2.3 Reliability failures and durability losses of PV modules	13
3.1 Solar One sub arrays layout.....	15
3.2 Left: Panel group layout on site. Right: PG schematic.....	17
3.3 Existing wind direction in Phoenix, Arizona	23
4.1 West and east south sub arrays output power summary	26
4.2 South sub arrays I-V curves summary [IVPC3].....	27
4.3 Sub arrays P-V curves summary [IVPC3].....	28
4.4 South array measured and normalized power summary	29
4.5 Degradation rate is 2.29% per year (outliers excluded).....	30
4.6 Degradation rate is 2.52% per year (outliers included).....	31
4.7 Effect of low irradiance on the PGs fill factor	32
4.8 Summary of physical defects counted on PV array.....	33
4.9 IR scans for determination of interconnect breakages.....	34
4.10 Summary of broken interconnects on PV array.....	36
4.11 Failure modes interactions on PV array.....	38
4.12 South array panel voltages measured under load.....	39
4.13 Bypass diode wiring schematic.....	40

Figure	Page
4.14 Temperature distribution pattern on the south array	43
4.15 Hot areas effect on PV array	45
4.16 Hot area cell effects on module back side	45
4.17 Hi-Pot Insulation Test wiring for positive (left) and negative (right) polarities above ground	48
4.18 I-V comparison of PG from new to degraded condition	49
4.19 Bus bar and panel pre-assembly error	50
4.20 Left: Bus bar cover repairs after module replaced. Right: Corrosion observed on B.O.S. front side due to moisture intrusion.....	51
4.21 Left: cracks on module interconnect. Right: breakages observed in module interconnects in the PV array.....	51
4.22 Left: cell browning with oxygen bleaching at edges and around cell cracks. Right: commonly observed extensive browning of the original PV modules	52
4.23 Left: Original module on top, replaced module at bottom. Right: Panel group with multiple replacement modules.....	52

Chapter 1

INTRODUCTION

1.1 Background

For Photovoltaic (PV) modules to be a commercially viable source of energy, their reliability over the warranted lifetime is vital. Most PV manufacturers today provide product warranties in excess of 20 years [1]. Degradation begins after installation and continues until the system is decommissioned. Solar One was contracted in 1985 by the John F. Long organization to install the PV power plant. They designed, built, and marketed homes in the Maryvale area of Phoenix since 1947. The Solar One concept is based on a micro grid system. It is made of a ground mounted Photovoltaic array and the system's power generated is shared by a neighborhood group of homes. The array is south facing and tilted at 17° . A building on the northwest side of the site houses the power conditioner and other PV system equipment as shown in Figure 1. A collaborative effort between the Atlantic Richfield Company and the J.F. Long organization guaranteed 10 years of 350,000 kWh energy production annually from the 200 kW_{dc} STC rated PV array. ARCO Solar Inc. was the PV system designer, installer, and supplier of PV modules. The Solar One power plant is comprised of a total of 4000 PV modules divided into 100 panel groups (PG's) or 8 sub arrays with a total rating of 200kW_{dc} (175 kW_{ac}). Organizations which previously performed studies on the power plant are: Electric Power Research Institute in 1991[2], the host

utility company SRP in 1993 [3], [4] and New Mexico State University.

After 26 years of power production, a large degradation has been observed at the Solar One Power Plant.



Figure 1.1: Google Satellite Photograph of Solar One System

1.2 Statement of problem

The Solar One PV system has presumably reached the wear-out stage of its operation and this could explain why there is a lower power output from the system. This thesis will identify the cause of the systems lower power output. However, degradation has occurred in an unusual pattern. It has been observed that there is more power loss at the east side of the

PV array than the west side. This raised many concerns as to how the degradation occurred over the 26 year lifetime of the PV modules. The power plant is composed of two arrays: a south array and a north array. The results obtained on the south array are presented in this thesis and the results obtained on the north array will be presented in another MS thesis.

1.3 Scope for investigation

The overall scope in this research work is to evaluate the entire system to:

- Calculate the performance loss over 26+ years based on the measured data and monitored data including:
 - Current-Voltage measurements of 100 panel groups (composed of 4000 PV modules) in collaboration with the other researcher (Jonathan Belmont)
 - Current-Voltage measurements of 8 sub arrays (composed of 4000 PV modules) in collaboration with the other researcher (Jonathan Belmont)
 - Panel groups (12-13 panel groups) mismatch loss in each sub array
 - Instant power data from the inverter on sunny days
 - Metered data supplied by the homeowner association
- Identify the durability and/or reliability causes for the performance loss through:

- Infrared scanning on every module for hotspot identification
- Infrared scanning on selected number of modules for non-cell interconnect breakages
- Panel group voltage measurement to detect failed panels
- Visual inspection for encapsulant browning, glass breakage, delamination, corrosion, broken non-cell interconnectors and module replacements over the 26+ years.

Chapter 2

LITERATURE REVIEW

2.1 Previous site work at Solar One power plant

A detailed inspection and performance of the PV system were conducted in 1989 by engineers from Ascension Technology and Southwest Technology Development Institute for the PV system installer, ARCO solar [2]. Activities performed in 1989 include:

2.1.1 Visual inspection

All components of the system were visually inspected for damages, loose wiring, evidence of changes to module laminate materials, fuses and switches located in the equipment building. The results are: no broken or damaged PV modules, no loose wiring or UV damage, no corrosion of galvanized supports, no connector problems found, and the entire system was said to be in an excellent condition [2].

2.1.2 Electrical measurements

Maximum power point tracking of the Toshiba power conditioner was tested and found to be working properly. At the time, all testing on the PV array was done with the power conditioner in operation thus limiting the ability to take I-V curves. A shading technique applied to the panels helped verify functioning of the bypass diodes. Results of this test found five non-functioning, open-circuited PV modules in the array, however with no visible sign of damage or degradation. Also, one bypass diode was found to have failed and in an open-circuit condition. Four other bypass

diodes had intermittent open-circuiting. Physically wiggling them restored connection to the module circuit. It was concluded that the array was in general good working condition.

Atlantic Richfield Company, the parent company to ARCO solar, inspected the system two times a year since 1985 for approximately ten years and some key maintenance lessons have been learned. They include documented cases of some vandalized modules which were replaced with the M54 Siemens 55 W modules, a replaced blocking diode in the collection box within the equipment building, and an instance of power conditioner failure in the summer of 1989. Details of energy output and performance degradation of the system will be given in the thesis work of Jonathan Belmont.

2.2 Bipolar array

The Solar One system consist of a bipolar PV array. Article 690.2 of the National Electric Code (NEC) defines a bipolar as a PV array that has two outputs each having opposite polarity to a common reference point or neutral center tap. This array consists of two monopole sub arrays which have two conductors in each output circuit, one positive and the other negative. Two monopole PV sub arrays are used to form the bipolar PV array in Solar One system.

Bipolar arrays are a way to stay within the NEC code yet have a high voltage on the inverter (>600V). Normally, grounded systems usually have

the negative point in the array connected to the grounded conductor, and the potential to earth is 0V during normal operation. Any part of the system cannot be greater than 600V above the potential of the earth by code (NEC). One way to have approximately 750V across the inverter input terminals as in the case of the Solar One system is to make the mid-point of the PV array 0V, connected to ground and then have +375V and -375V on either side of the PV array. This way one can have 750V across the inverter input (+375V to -375V = 750V), yet not have any part of the PV array be at more than 600V above the earth's potential. Therefore, all equipment used on any bipolar PV system can be 600V listed. Figure 2.1, below shows a simplified Solar One bipolar array schematic.

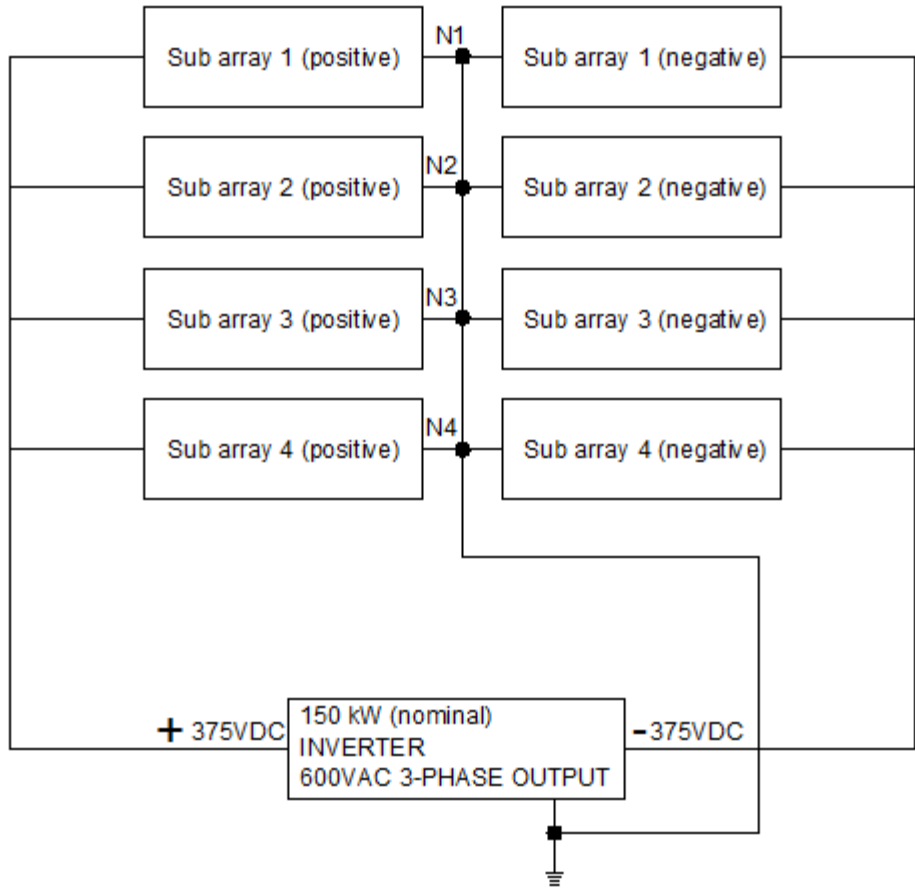


Figure 2.1 Solar One Bipolar array simplified schematic

2.3 Degradation studied

Over the 26+ year period, outdoor exposure to the weather has caused some failure of PV module components, including the bus bar interconnections. Figures 2.2(a) and (b) below show details of how laminates which are connected around the bus bar.

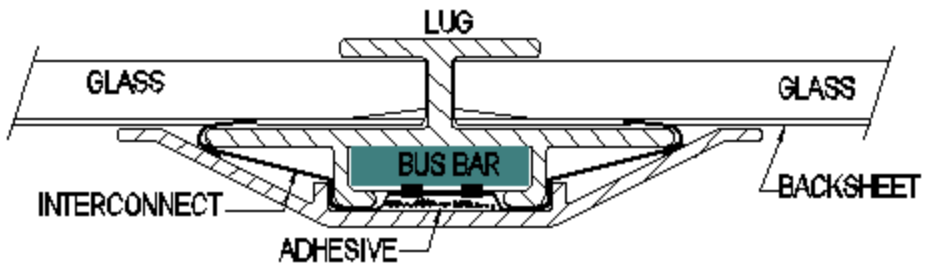


Figure 2.2(a) Laminated-bus bar profile schematic

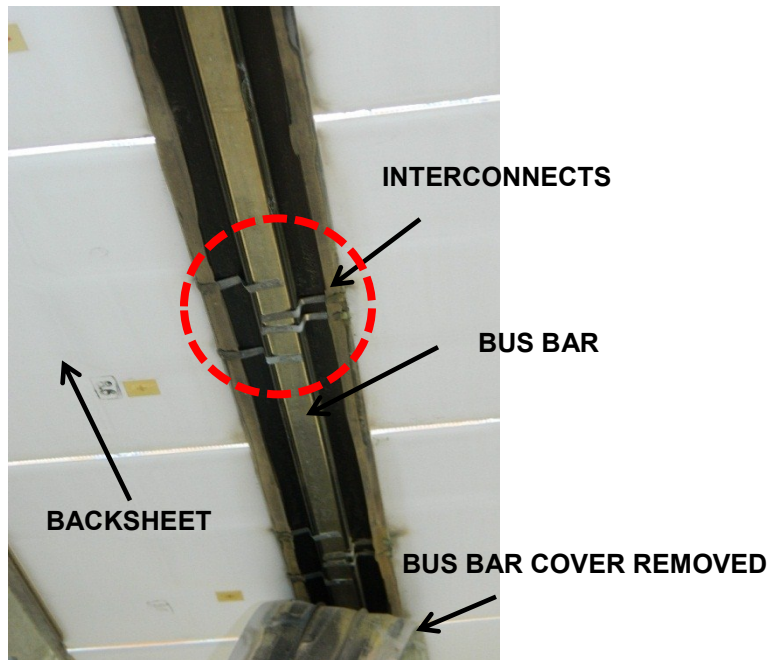


Figure 2.2(b) Laminated-bus bar details

The following degradation or failure types were investigated in this project:

2.3.1 Degradation or failure of packaging materials

Like any material exposed to the weather, degradation or failure occurs over time. Module packaging material degradation or failure includes glass breakage (failure), bypass diode failure (failure), encapsulant discoloration (degradation) or delamination (failure), and back sheet cracking (failure)

and crumbling (failure). These problems could also introduce safety hazards like ground faults or electric shock due to leakage current. Modules perform below rated capacity when encapsulant discoloration causes the reduction of light generated currents in the solar cells [5]. Safety hazards are a major issue in high voltage systems with module packaging material damage [6].

As shown in Figure 2.3, the PV module could experience both a degradation issue and/or a failure issue [7]. If the PV modules are removed (or replaced) from the field before the warranty period expires for any types of failures, then those failures may be classified as hard failures or catastrophic failures. In other words, all failures which qualify for warranty returns may be called reliability failures. If the performance of PV modules degrades but still meets the warranty requirements, then those losses may be classified as soft issues or degradative losses. Towards the end-of-life, multiple degradative mechanisms may operate and lead to wear out failures. Overall, the durability losses may be defined as degradative and wear out issues which meet the warranty requirements and the reliability failures may be defined as catastrophic and wear out failures which do not meet the warranty requirements.

2.3.2 Degradation or failure caused by loss of adhesion

The primary failure mode in this degradation type is delamination. This is defined as the disintegration of bond between material layers that make up the PV module [6].

Front side or back side delamination interferes with uniform and efficient heat dissipation from the module. Higher cell temperatures will ultimately shorten the useful life of the module and reduce power output of affected modules. A hotspot issue due to excessive temperatures causes solar cells to operate at 30⁰C or higher than other cells in the module [6]. This contributes to a mismatch in an array setup such as Solar One.

2.3.3 Degradation or failure of module interconnects

High conducting materials like copper are soldered using alloys of tin and lead (SnPb) onto the metallization of semiconductor device or solar cell surface. Solar One cell interconnects are made of tin coated copper ribbons. Soldered joints are made on cell to ribbon or ribbon to ribbon within the module. As the module continues to experience thermal cycling, joint coarsening occurs and the joint material and its physical properties are affected. Thermo-mechanical fatigue leads to the formation of larger grains and possible cracks on grain boundaries, causing possible joint failure. Module interconnects are usually made with several redundant joints, which provides least resistance to the light generated current out of the module. Solar One modules used interconnect ribbons to connect to the bus bars. Since there are no cables or junction boxes, both cell interconnects and module interconnect ribbons were studied in this

project. Failure of these interconnects observed led to high series resistance in the electrical circuit, and several hotspots in solar cells [6].

2.3.4 Degradation caused by moisture intrusion

Moisture intrusion usually follows the aforementioned degradation or failure types. Moisture permeation through module back sheet or edge of laminates like the Solar One frameless modules causes leakage currents. If the leakage current is very small, it could cause potential induced degradation (PID) depending on the array polarity and the relative humidity of the site. If the leakage current is high, it could cause a safety hazard including electrical shock or ground fault. Retained moisture also causes adhesion strength failure of packaging materials and significant power performance loss in the module due to delamination. Corrosion due to high operating potential (PID) is a major effect of moisture intrusion. Some metallization materials have a high sensitivity to moisture thus fostering corrosion [6].

2.3.5 Degradation or failure of the mono-crystalline silicon solar cells

The crystalline silicon semiconductor materials have field record of high performance stability. After the initial light induced degradation (LID) of the c-Si solar cells, only few changes that affect performance can be associated with the semiconductor device. These include reverse-bias cell heating (hotspots), chemically assisted diffusion of phosphorus atoms,

and the n-type cell dopant to the cell surface. This has been known to correlate with loss of adhesion at the cell/encapsulant interface. Cracking of the c-Si semiconductor material is also commonly observed in field aged modules causing electrical isolation. However, with improvements in manufacturing, cell crack occurrence has reduced significantly. [5, 6].

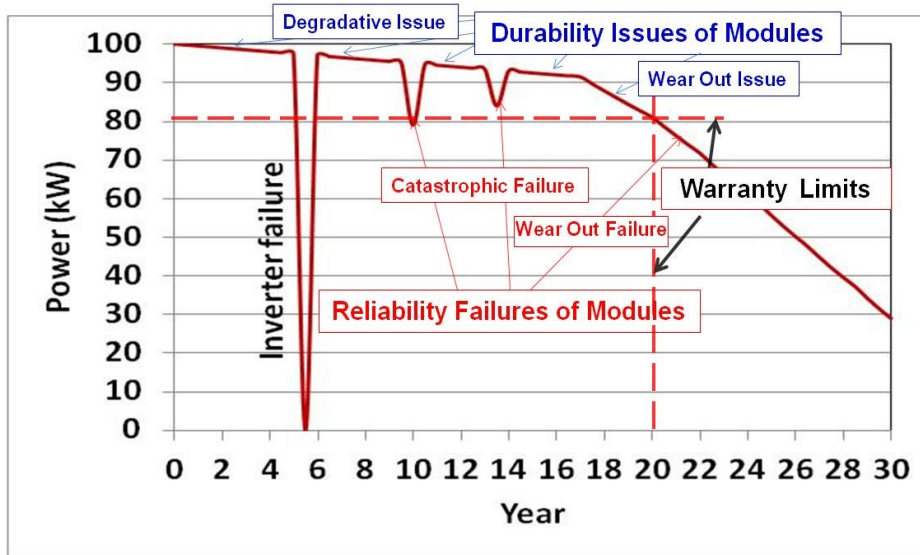


Figure 2.3 Reliability failures and durability losses of PV modules. Source: [7].

Chapter 3

METHODOLOGY

3.1 Power plant configuration

The Solar One PV system is a 200 kW (DC) PV array installed, which yields a 175 kVA (AC) 3-phase 600V inverter output from a 150 kW (DC) nominal inverter input. Positive sub arrays have 13 panel groups and negative sub arrays have 12 panel groups. Sub arrays 1 and 2 are to the south, and sub arrays 3 and 4 are to the north. The west side of the array has 2 positive and 2 negative sub arrays, just as the east side of the array has 2 positive and 2 negative sub arrays. See Figure 3.1.

Power is fed from the array into a power conditioner or inverter through underground copper cables feeding into the equipment building. Other balance-of-system (BOS) equipment located within the equipment building include: a collection box for termination of array wiring, and 3 disconnects with fuses. Also outside the building on concrete pads are: a utility grade switchgear components which interfaces the PV system to the SRP power system, a 600V to 12.5kV transformer, vacuum circuit breaker, metering cabinet and points of interconnection to three 50kVA transformers that supply power to the Solar One homes.

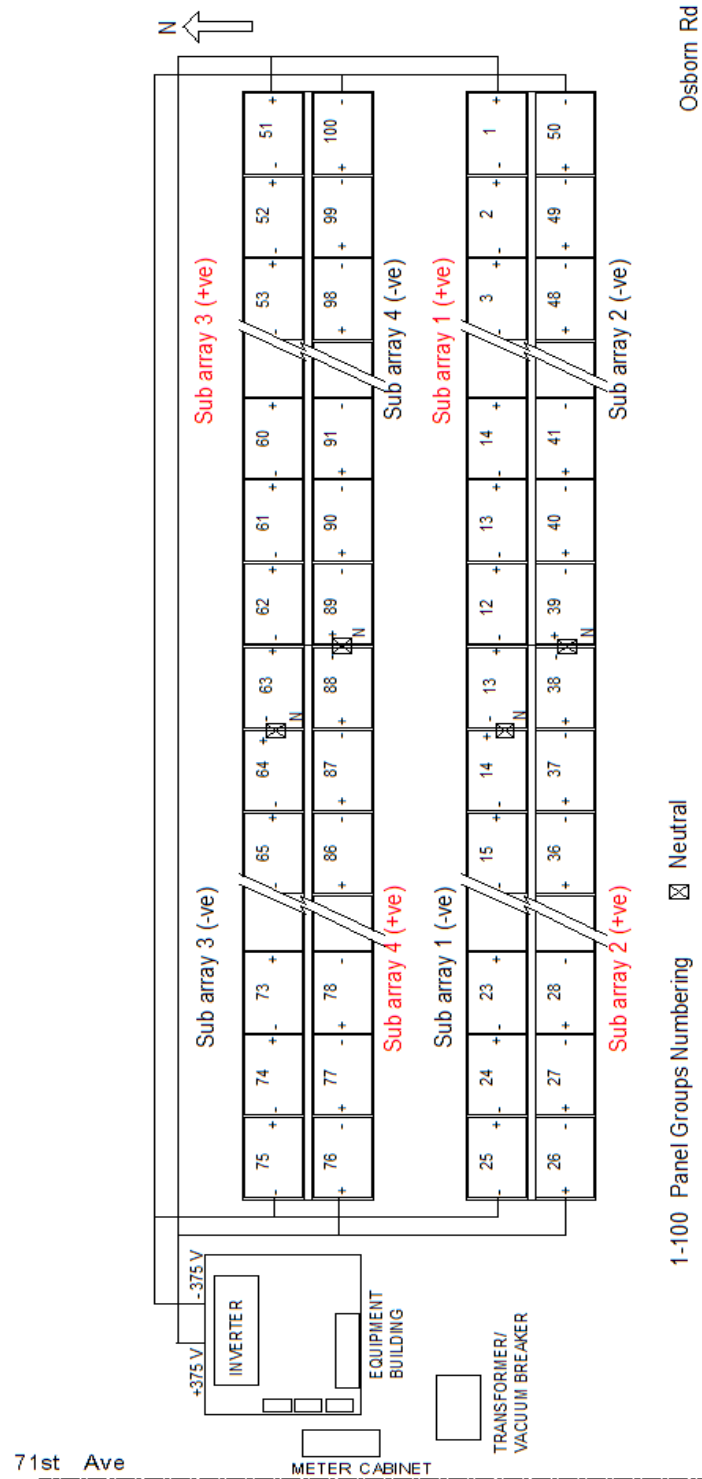


Figure 3.1 Solar One sub arrays layout

3.1.1 PV modules and array characteristics

The Power Plant is made of 4000 frameless mono-crystalline PV modules. Ten modules are connected in parallel to form a panel. Four of these panels are series connected to form a panel group. Series connection of panels are made by riveting module interconnects unto bus bars. A sub array has 12 panel groups for negative biased sub arrays and 13 panel groups for positive biased sub arrays. A total of 8 sub arrays make up the power plant. There are challenges from previous research associated with frameless crystalline silicon modules from the durability point of view. They are more fragile with higher probability of moisture intrusion than the framed type. The certification test that is used for mechanical durability of frameless modules is the IEC 61646. These modules are supported directly on the rear glass surface to the mounting structure which could create a lot of stresses around the support on the glass. This may eventually affect the cells within the module [6]. Infrared images show damages to cells above the two middle supporting structures of the panels, see Figure 4.15. Figure 3.2 below shows the panel group layout at Solar One. The PV module specifications used at Solar One at STC conditions of $1,000 \text{ W/m}^2$ irradiance and 25°C cell temperature are:

Open circuit voltage = 7.3 V

Maximum power voltage = 5.8 V

Maximum power current = 8.6 A

Short circuit current = 9.6 A

Rated power = 50 W

Fill factor = 0.71

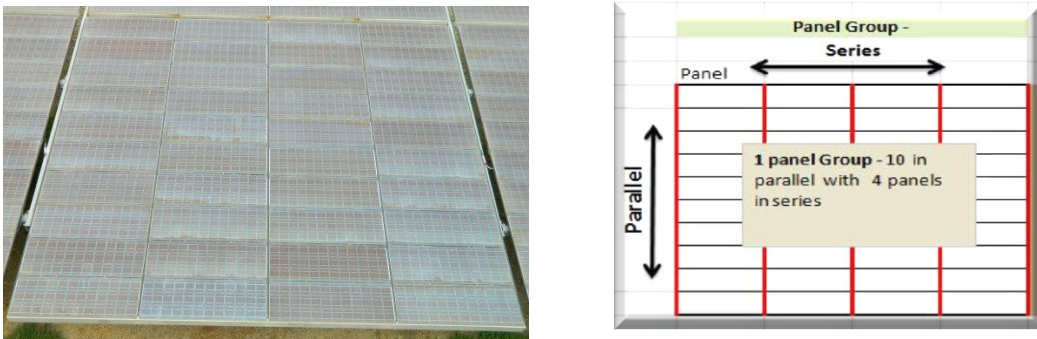


Figure 3.2 Left: Panel group layout on site. Right: PG schematic

3.1.2 Power conditioner characteristics

The Toshiba inverter built in August 1985 has a nominal input power rating of 150 kW at 375V DC, housed in three cabinets within the equipment building. Analog meters on one of the enclosures display instantaneous DC and AC current, voltage and power of the PV system. System status and diagnostics are read from an LED display in front of the inverter. The inverter also has a maximum power point tracking (MPPT) circuitry, and can be switched to a manual mode in order to adjust array voltage in the range of 250V to 470V.

The inverter output is rated at 175 kVA at 3-phase 600V AC. The ground fault detection within the inverter is no match to modern power plant inverters deployed to PV systems in recent times. There is no ground fault detection on the DC side of the inverter and the AC side has a breaker for about 5-10 Amps of leakage current, thus posing a safety

concern within the system during wet conditions. Details of ground fault tests carried out will be given in chapter four.

3.2 Field work

3.2.1 Overview of performed work

Preliminary field work to determine the performance of the PV system included: eight I-V curves of the sub arrays, one hundred I-V curves of the panel groups, analyses of monthly/annual energy generated and billing reports, and a PID study.

Based on the results of the tests above, we went further to investigate the following over the entire PV array: visual inspection, hotspots scan, interconnect breakage determination, temperature and wind study, low irradiance I-V curve study of six sample panel groups (two best case, two average case and two worst case), and high potential wet/dry resistance insulation tests. Results from these tests are given in details in chapter four.

3.2.2 Equipment used

The following equipment was used in data acquisition:

- Daystar DS-100C current-voltage (I-V) curve tracer
- Fluke TI-55 Infrared (IR) camera
- Thermo couples and IR thermometer
- Digital multimeters
- Ideal 61-795 Digital Insulation Tester

3.3 Measurement strategy

3.3.1 Eight sub arrays I-V curve measurement

Data was always collected at near full sun meaning $1000\text{W}/\text{m}^2$ irradiance. This allowed the power characteristics of the array to be optimized for measurements. The standard procedures for measuring I-V curves, including normalization were followed which includes a mono crystalline reference cell set in the plane of array. The 8 sub arrays I-V curves were measured using the I-V curve Daystar DC-100C machine at the collection box where all the arrays wiring terminate in the equipment building.

3.3.2 One hundred panel group I-V curves measurement

I-V curves for the 100 individual panel groups were measured and normalized to STC for a common reference point of comparison. Normalization was based on ASTM E 1036-96 [8]. Standard procedures were followed. The data obtained include; STC values of maximum power, short circuit current, open circuit voltage and fill factor for the entire PV system, and summary given in chapter four and the appendix.

3.3.3 Analyses of monthly/annual energy-billing report

Available data from 1988 to 2010, and the measurements made in 2011 were examined and plotted in order to determine the annual degradation rate. The slope of the curves for both data with and without outliers produced some figures distinctive of Solar One PV system

3.3.4 PID study

From the unusual power drop on the east side of the array, an initial thought suggested a PID issue. After a detailed study of the I-V curve measurements, PID was not considered to be the issue. Since both east and west arrays have 2 positive sub arrays and 2 negative sub arrays each, it is easy to rule out the possibility of Potential Induced Degradation (PID), which occurs more often on a high negatively biased array in a humid condition. Both positively and negatively biased sub arrays on the east side of the PV array were observed to have degraded considerably compared to the sub arrays on the west.

3.3.5 Visual inspection

After I-V measurements were completed, a detailed visual inspection was carried out. This involved assessments of broken modules, cracked cells, back sheet delamination, cell corrosion, metal blossoming, interconnect breakage and hotspot issues on the PV array. A table of failure modes was developed from the information obtained from the visual inspection. The interactions of the different failure modes were studied and explained in chapter four.

3.3.6 Hotspots scan

Hotspots on solar cells are caused by power dissipation from not shaded or unaffected solar cells into the shaded solar cells. Since lower current is produced from a shaded cell, the current in the series string of cells is limited by the affected cell thus causing a higher voltage in the

good cells which in turn reverse bias the shaded cell [5]. Though there is no apparent shading of solar cells at Solar One, all panel groups have steel support framing behind the modules, which has prevented adequate ventilation of solar cell directly above them. These cells operated at higher cell temperatures than the rest of the cell in the panel groups and could be responsible for considerable performance degradation of the PV system. These effects are seen using the infrared camera on the front surface of the panel groups under load.

3.3.7 Interconnect breakage determination

During the visual inspection stage, it was observed that some bus bar covers were opened, making the module interconnects visible. Some of these were fully or partially broken. It was decided to investigate and estimate the total amount of broken interconnects in the system for the 100 panel groups. The method used involves the IR camera by scanning through unopened bus bar covers in order to reveal the condition of the module interconnects-bus bar joints. Connected interconnects shows a hotspot point of connection to the bus bar or where the ribbon kinks/folds while broken interconnects showed no hotspot. Current flowing through the connection point has a higher temperature than the surrounding surface on the bus bar. This method was very useful in finding broken interconnects without the need to break open any bus bar cover within the PV array.

3.3.8 Low irradiance I-V measurements of sample PG's

Effect of shunt resistance becomes important at low light levels. With less light generated current, equivalent resistance (or characteristic resistance) of the solar cell approaches the shunt resistance, increasing the fractional power loss due to shunt resistance [5]. The method used in carrying out this low irradiance experiment involved the use of transmittance calibrated mesh screens which were laid on the panel groups before I-V curves were taken in order to reduce irradiance to about 150-200 W/m². During these measurements, the reference cell was not covered with mesh screen to avoid the non-uniformity issue on the small area (4 cm²) cell. A high irradiance IV-curve was taken immediately after the mesh screen was removed in order to compare results.

3.3.9 Temperature and wind study

Existing data from Luke Air force base in west Phoenix near the Solar One power plant showed that prevalent wind direction is from the south west. See Figure 3.3. Measurements made under the array during summer of 2012 agree with the existing data. There is a slight increase in the temperature of panel groups on the east side than the west side of the PV array. The approach used was a walk through while holding a multimeter with thermocouple and measuring ambient temperature under the PG's.

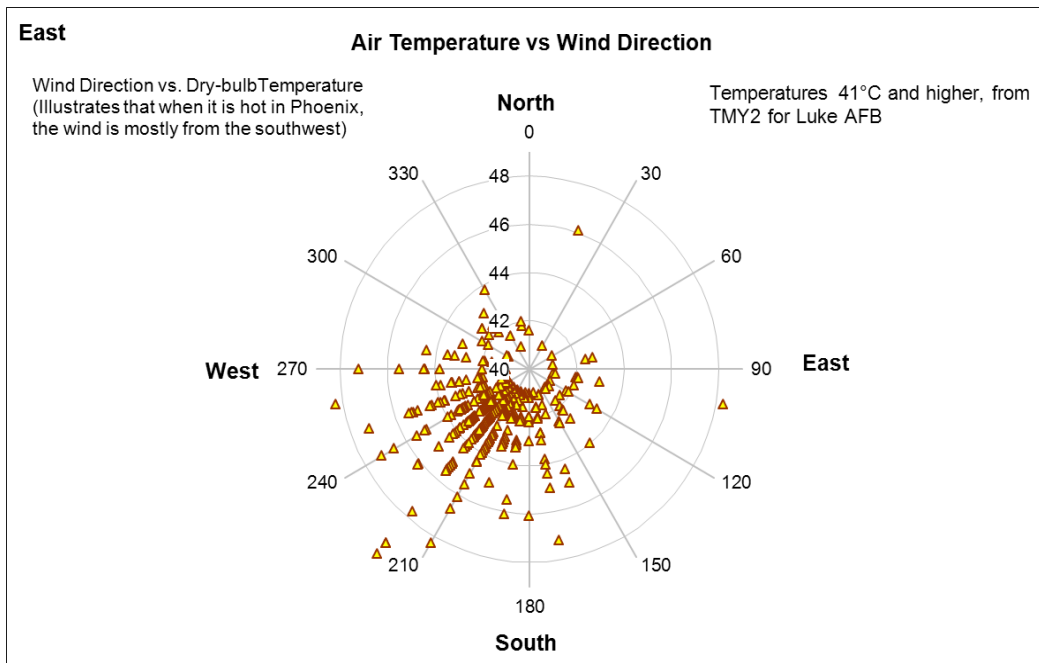


Figure 3.3 Existing wind direction in Phoenix, Arizona

3.3.10 Wet and dry insulation test

Insulation test was conducted to verify the effectiveness of the array packaging material. The PV array has several modules broken, with cracked and delaminated back sheets. Since there was obvious exposure of bus bars operating at very high voltages and currents, personnel safety became a concern with the array particularly during wet conditions of rain and morning dew. The approach was to use an Ideal 61-795 digital insulation tester, and connect according to Figure 4.11. The results obtained are contained in Tables 4.5 (a) and (b) in chapter four.

3.4 Laboratory work

3.4.1 Baseline curve measurement

Some new Arco M54 modules (55Watts) which were used for the replacement in the early 1990's were obtained from the HOA, and were analyzed for comparison with nameplate data at the ASU-PRL for their electrical characteristics, and the temperature coefficients. The table of results showing the temperature coefficients for 8 sample modules measured at Standard Testing Conditions (STC) is given in the appendix.

Chapter 4

RESULTS AND DISCUSSION

4.1 Performance degradation

It has been observed that more degradation occurred on the east sub arrays than the west sub arrays as shown in Figure 4.1. In order to understand the reasons for this unusual difference between east and west sub arrays, various measurements and tests which are given below, were carried out and the discussions that follow help in analyzing the data obtained. This thesis work from this point shall concentrate on the south array, with results presented hereafter.

Current voltage (I-V) curve is the basic electrical output of a PV module. The curve signifies all possible voltage and current operating points at any given irradiance and cell temperature [9]. Figures 1.2, 1.3 and 1.4 in Appendix A, shows approximated I-V curves representative of 1) a new module, 2) new panel group (PG), and (3) the entire array. This approximation was done using the fresh modules which were stored indoor since early 1990's. The present array performance I-V curve shown as part of Figure 1.4 in appendix A was modeled from the results of measurements made on the system in 2011.

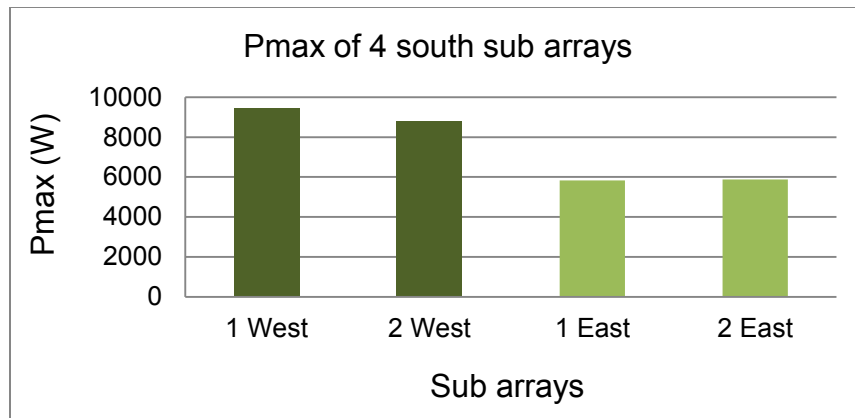


Figure 4.1 West and east south sub arrays output power summary

4.1.1 Performance of 4 south sub arrays

The measurements of the performance for the 4 sub arrays were taken on the 12th of October 2011 at the Solar One power plant around 10:35 am and 11:15 am. It was a very clear day. The plane of array irradiance recorded was between 849 W/m² and 905 W/m² with average of 877 W/m². Air mass was calculated to be 1.5. The results in the table below form the basis for further investigation for the cause of more power loss in the 2 east sub arrays.

Table 4.1 Results of 4 south sub arrays measurements.

	Sub array number	Number of PG's	STC Isc (A)	STC Voc (V)	STC Pmax (W)
SOUTHWEST ARRAY	1-negative	12	68	320	12,155
	2-positive	13	66	343	11,672
Average			67	331	11,913
Total	2	25			23,827
SOUTHEAST ARRAY	1-positive	13	58	342	7,628
	2-negative	12	61	316	7,443
Average			59	329	7,535
Total	2	25			15,071

- There is more power output from the west sub arrays than the east sub arrays
- Pmax sum of all 4 south sub arrays at STC = 39 kW
- Southwest sub arrays = 24 kW
- Southeast sub arrays = 15 kW
- Southeast sub arrays = 63.5% of West sub array power output
- North array output = 37 kW
- Combined array output = 76 kW
- Inverter reading for north and south array STC output = 62.1 kW
- Sub arrays mismatch losses = $(76 - 62.1 / 76) = 18\%$

Below are the I-V and P-V curves superposition for the south sub arrays, based on the measurements in Table 4.1.

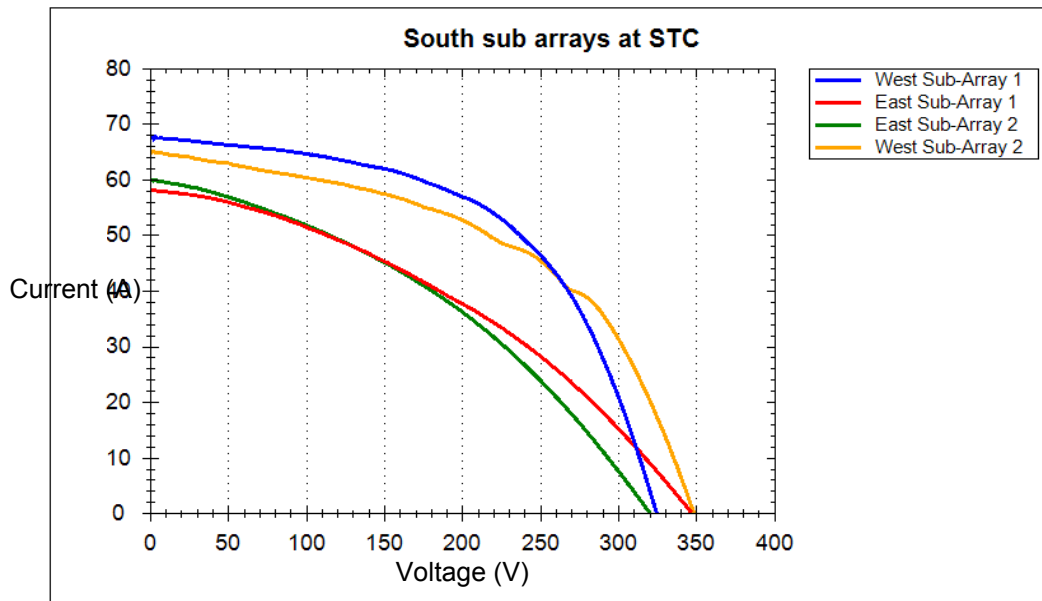


Figure 4.2 South sub arrays I-V curves summary [IVPC3]

- West sub arrays have similar I-V curves
- East sub arrays have similar I-V curves
- Positive sub arrays have higher Voc because of one additional panel group
- Lower Isc in east sub arrays due to more module interconnect breakage
- High operating cell temperatures on east sub arrays to be discussed later

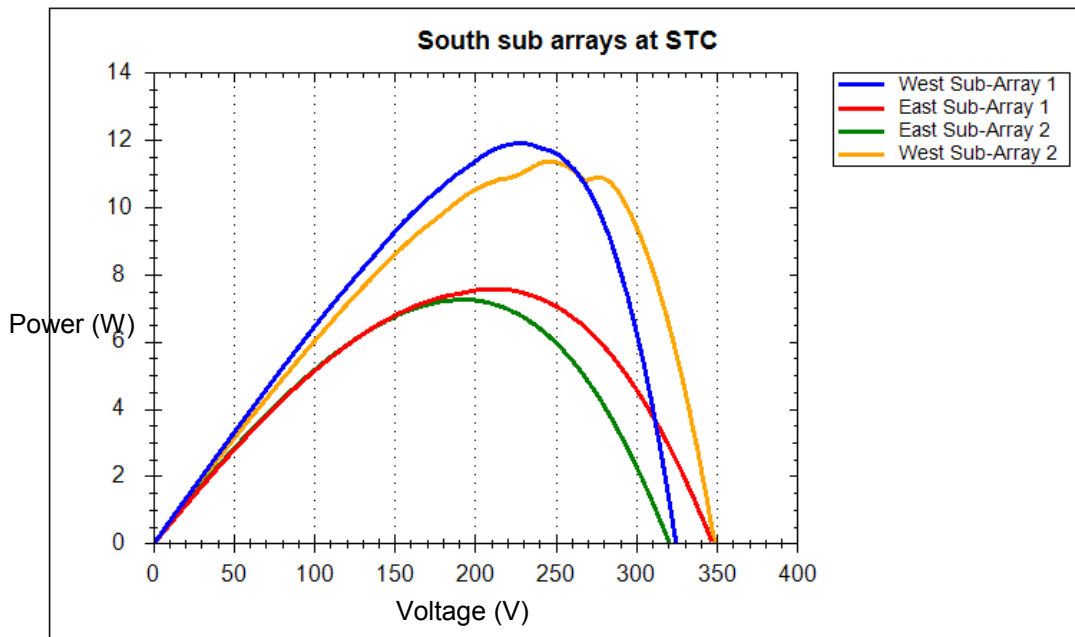


Figure 4.3 Sub arrays P-V curves summary [IVPC3]

4.1.2 Performance of 100 panel groups

The measurements of the performance for the 100 panel groups were taken on the 26th of October 2011 at the Solar One power plant around 10:56 am and 13:50 am. The Irradiance recorded was between 740 W/m² and 918 W/m² with average of 829 W/m². The calculated air mass at the

time of measurement was very close to 1.5. Figure 4.4 below gives the summary of measurements obtained for the south array. The table of data corresponding to the 100 panel groups is given in appendix A.

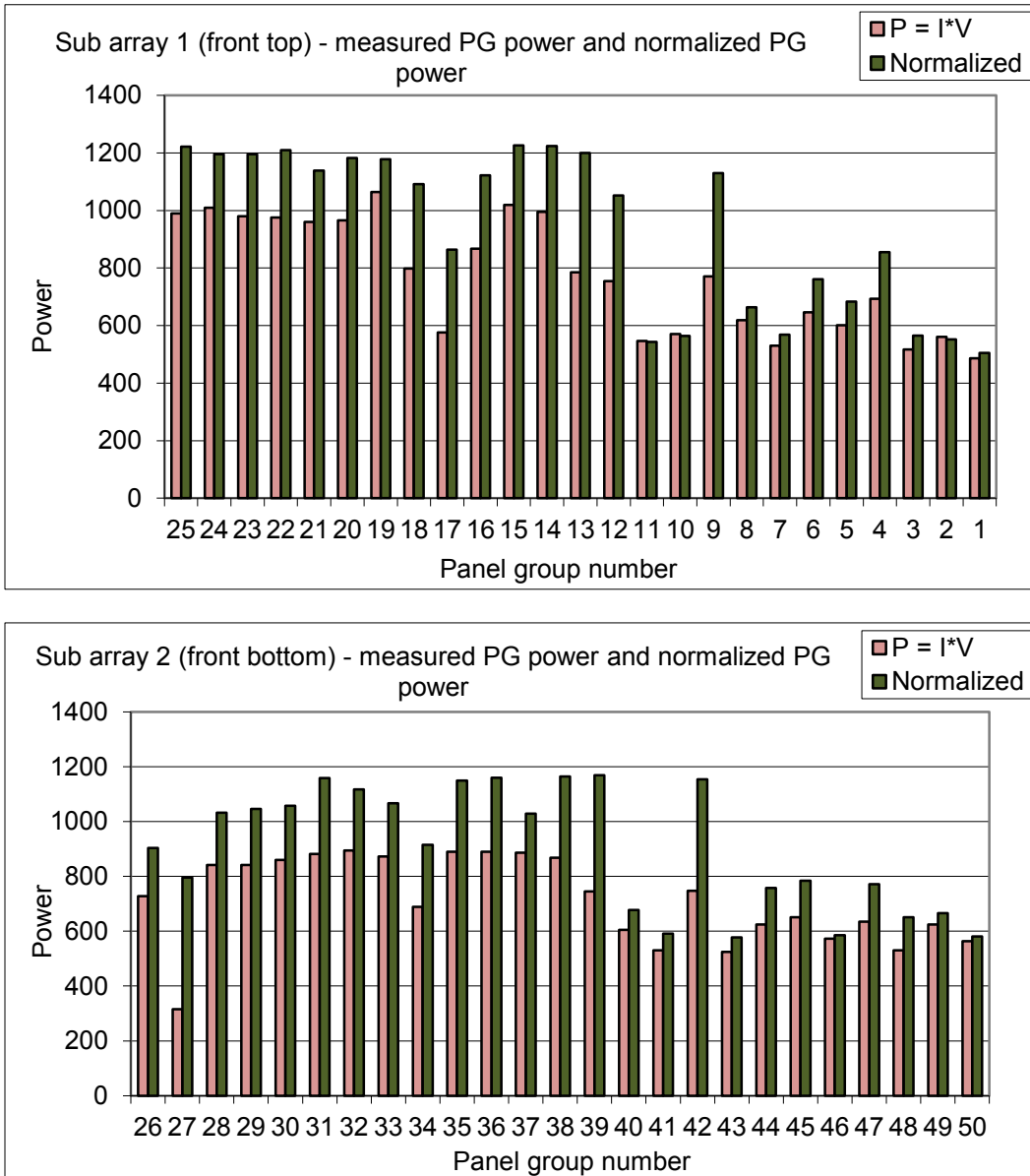


Figure 4.4 South array measured and normalized power summary

- Pmax sum of all 100 panel groups at STC = 88 kW

- Pmax sum of all 8 sub arrays at STC = 76 kW
- Panel group mismatch loss = $[(88 - 76) / 88] = 13.6\%$
- Lowest performing panel group PG 91 = 325 W (east)
- Highest performing panel group PG 15 = 1225 W (west)

4.1.3 Annual performance degradation of the system

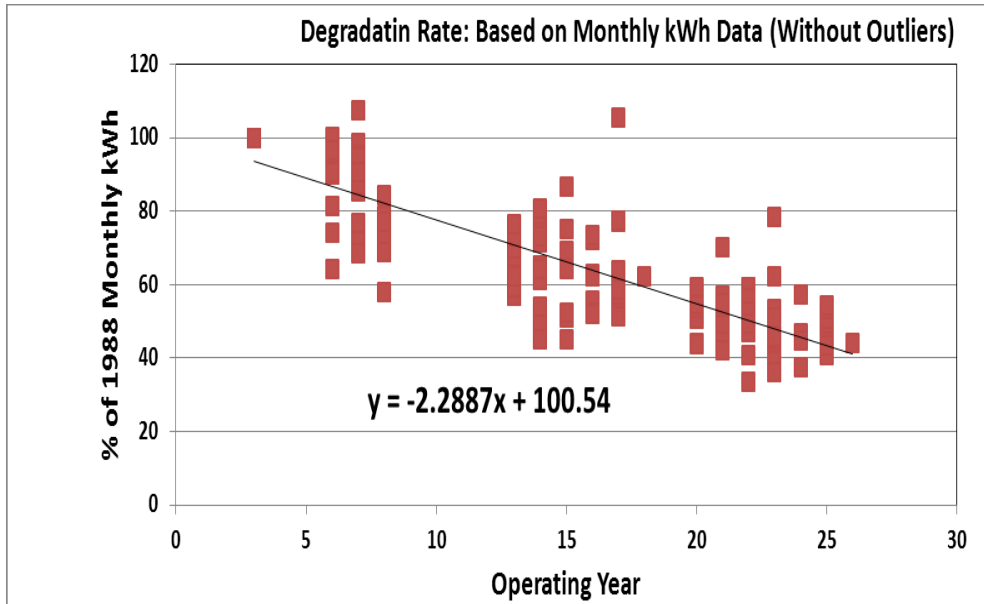


Figure 4.5 Degradation rate is 2.29% per year (outliers excluded) [10]

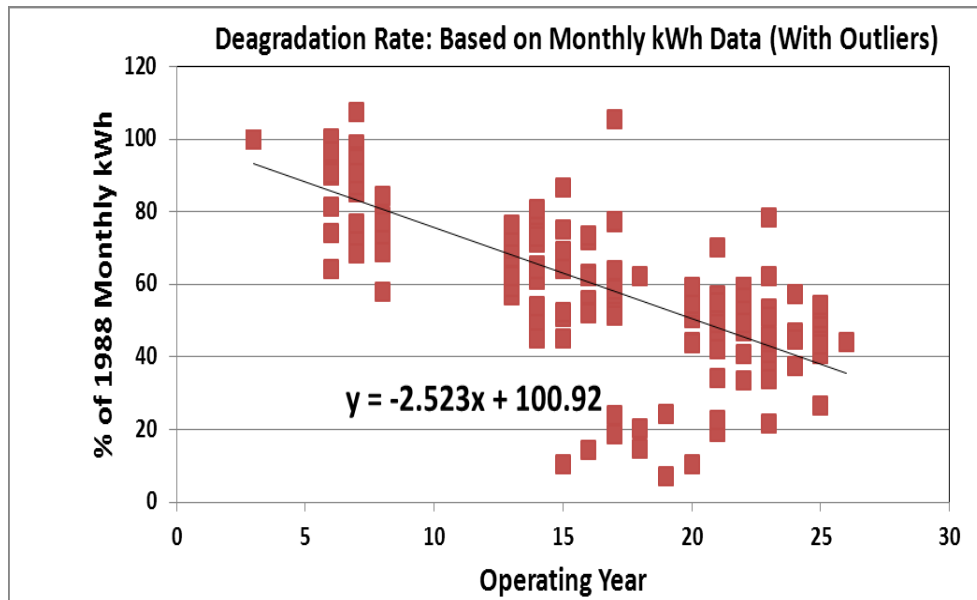


Figure 4.6 Degradation rate is 2.52% per year (outliers included)

- Annual average energy production is about 112 MWh for the past 10 years (1988 = 321 MWh)

4.1.4 Performance at low irradiance

Low irradiance measurements help to characterize solar cells for series and shunt resistance related problems. Fill factor was observed to go up in the low irradiance results for the following sample panel groups: PG91, PG97, PG55, PG14 but PG58 shows a reduction in fill factor at low irradiance. The fill factor increases with reduced series resistance issue at low light levels due to low current generation from the modules with high level non-cell interconnect failures, which carry current from modules to the external circuit.

The output of both high and low irradiance measurements were normalized and provided in Table 4.2 and Figure 4.4 below.

Table 4.2 Results of high and low irradiance measurements.

HIGH IRRADIANCE					
	worse	worse	worse	average	best
Panel Group	PG91	PG97	PG55	PG58	PG14
Voc	29.1	28.6	28.1	28.3	28.9
Isc	51.0	54.4	58.5	85.0	73.8
Fill Factor	23.4	38.4	24.8	43.7	54.8
Peak Power	347.7	597.3	407.9	1053.2	1165.5
Vpeak	12.3	17.7	16.4	20.6	21.1
Ipeak	28.3	33.7	24.8	51.2	55.1
Irradiance	1,000	1,000	1,000	1,000	1,000
Cell Temp.	25	25	25	25	25
LOW IRRADIANCE					
Voc	25.6	25.8	21.6	24.7	25.0
Isc	12.2	12.9	8.3	49.1	13.3
Fill Factor	35.7	49.5	64.8	18.6	66.7
Peak Power	111.3	164.4	115.6	225.9	221.6
Vpeak	17.3	19.6	14.8	19.0	19.5
Ipeak	6.4	8.4	7.8	11.9	11.3
Irradiance	200	200	200	200	200
Cell Temp.	25	25	25	25	25

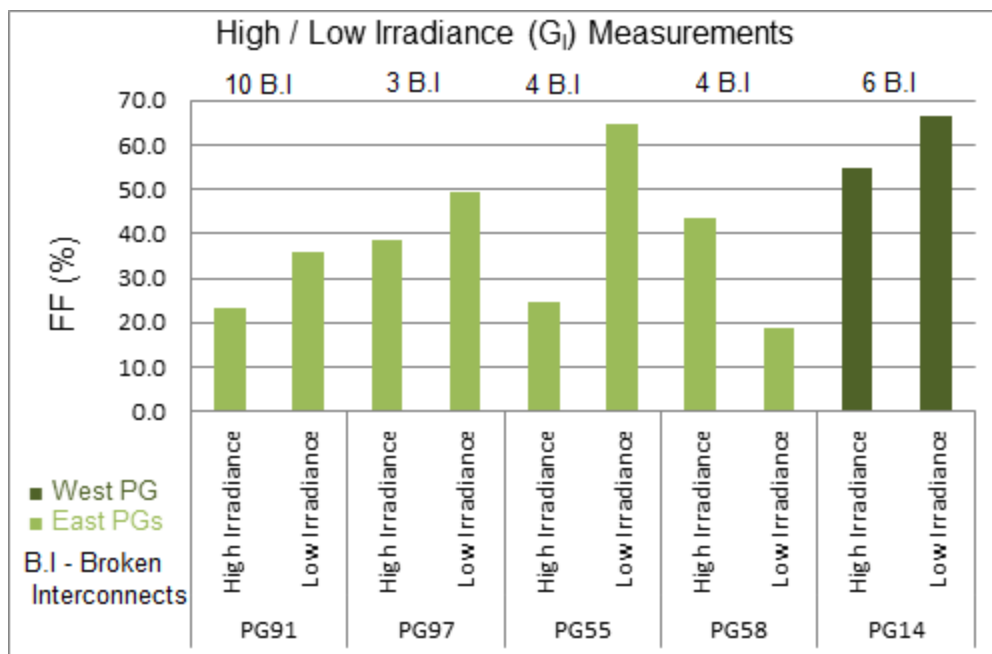


Figure 4.7 Effect of low irradiance on the PGs fill factor

- Increased fill factor with reduced series resistance effect at low irradiance
- PG58 has unusually high I_{sc} at low irradiance responsible for fill factor drop
- Fill factor is better for high interconnect failure modules due to reduced series resistance issue.

4.2 Visual inspection analysis

4.2.1 Degradation or failure modes observed

Physical observations on the PV array included the following:
Replaced modules, glass breakage, cell/metallization corrosion, encapsulant browning, cell cracks, back sheet delamination, broken interconnects, hotspots etc. Figure 4.8 gives a quantitative analysis of failure modes on the PV array.

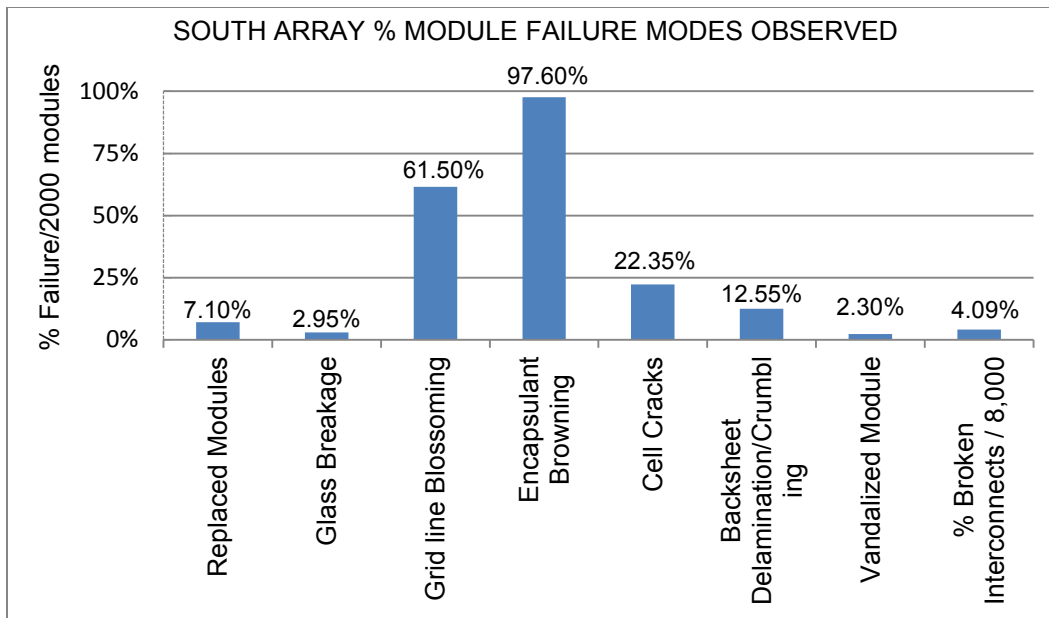


Figure 4.8 Summary of physical defects counted on PV array

4.2.2 Overall array broken interconnect summary

During the visual inspection stage, it was observed that some bus bar covers where opened, making the module interconnects visible. Some of these were fully or partially broken. Each module has 4 interconnect ribbons, therefore the south array has a total of 8000 interconnects being investigated using IR scan imaging. The probable cause is thermal fatigue and corrosion on the exposed bus bars during rainy days (this site receives rain only 3-4 times a year with only about 8-inch rain level). More broken interconnects were found to have occurred within some sealed bus bar covers. The method to estimate the damaged interconnects involved the use of infrared scanning. Connected interconnects shows a hotspot point of connection to the bus bar or where the ribbon kinks/folds while broken interconnects showed no hotspot. Current flowing through the

connection point has a higher temperature than the surrounding surface on the bus bar. This method was very useful in finding broken interconnects without the need to open any bus bar cover within the PV array. Figure 4.9 below show sample IR images of interconnect damages.

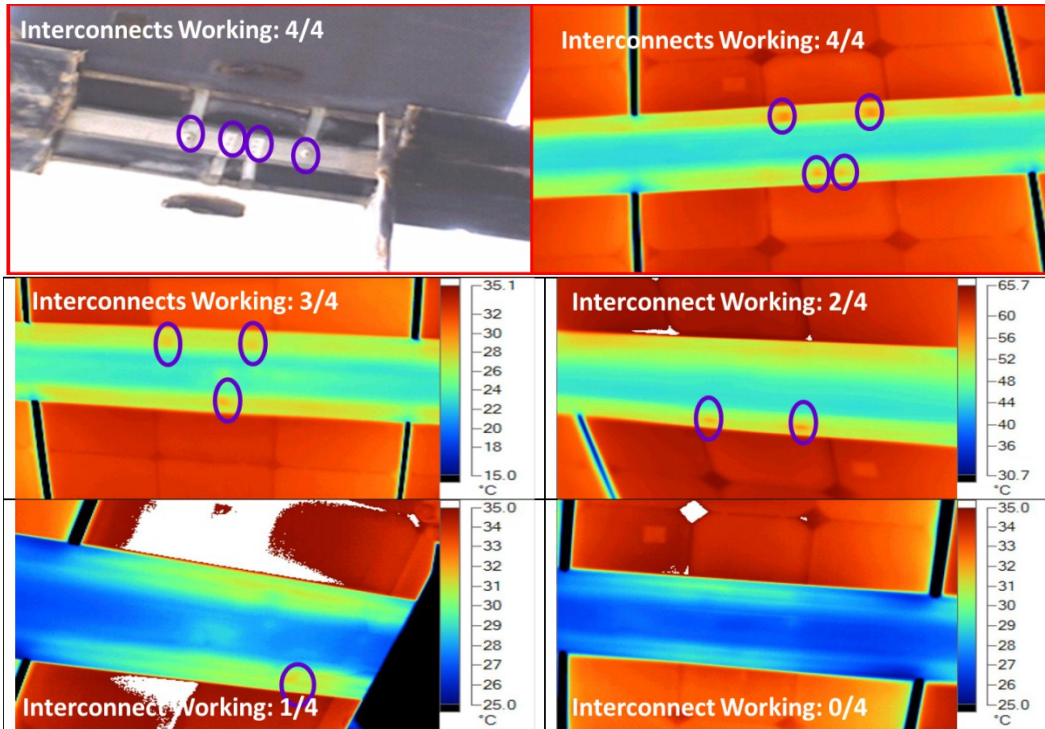


Figure 4.9 IR scans for determination of interconnect breakages

A summary of total broken interconnects is shown in the Figure 4.10 below. The east sub arrays have more detected broken interconnects. Performance degradation increases when more current is forced through fewer interconnections causing higher series resistances in the affected panel groups. The panel groups in the east array have lower fill factors than the panel groups in the west side of the array.

The reason for higher level of broken interconnects on the east array is not known but a possible hypothesis could be due to improper sealing of the back cover over the interconnect-bus bar area after the replacement of failed modules with new modules in early 1990's. The improper sealing would lead to severe corrosion of interconnects during rainy days leading to interconnect breakages. The Google aerial photograph indicates that more modules had been replaced in the east sub arrays as the encapsulant discoloration was found to be less than that of the original modules. Higher module replacement would have led to higher interconnect breakage due to improper sealing of the back cover in early 1990's.

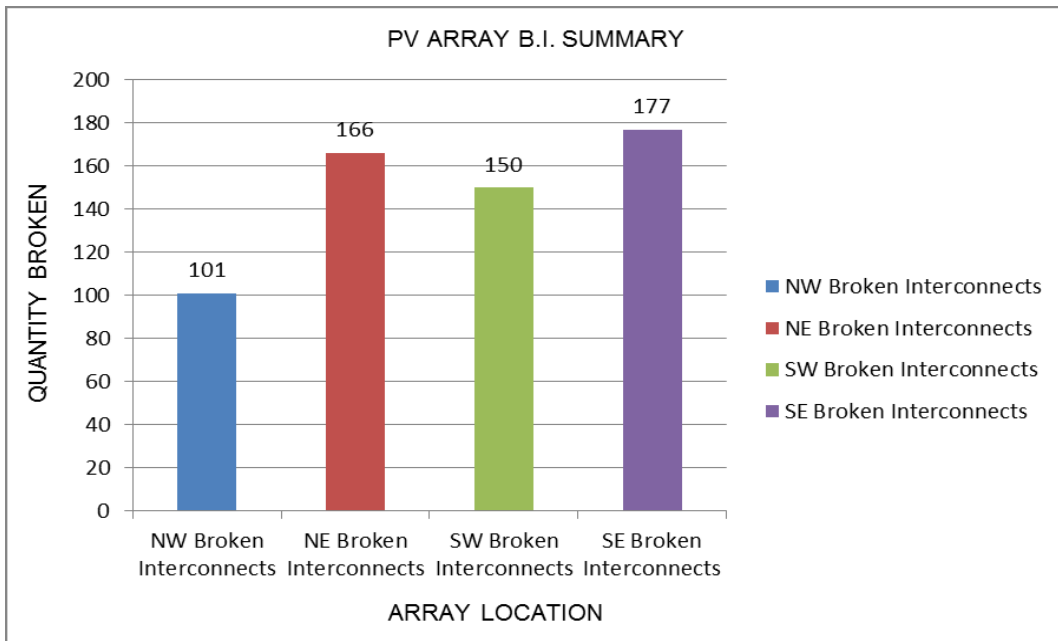
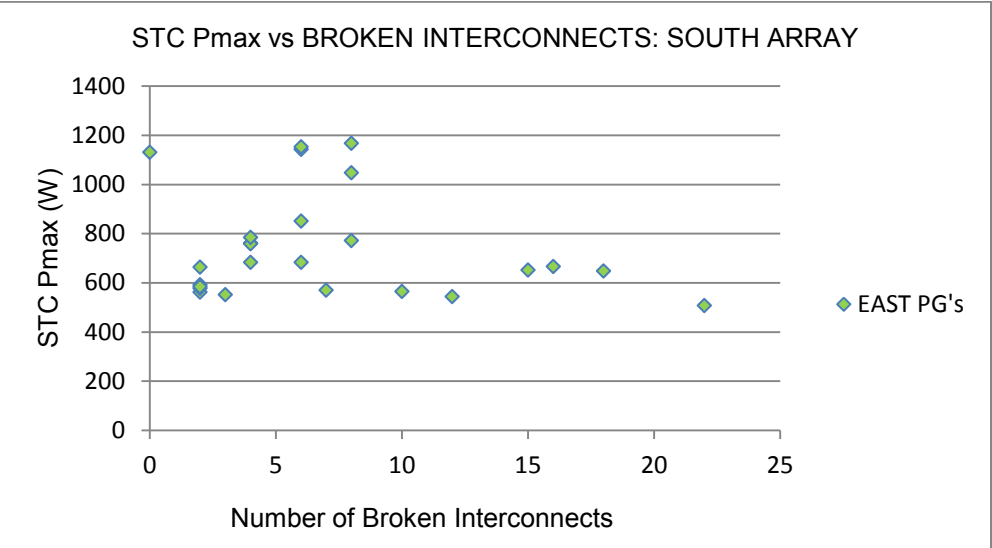
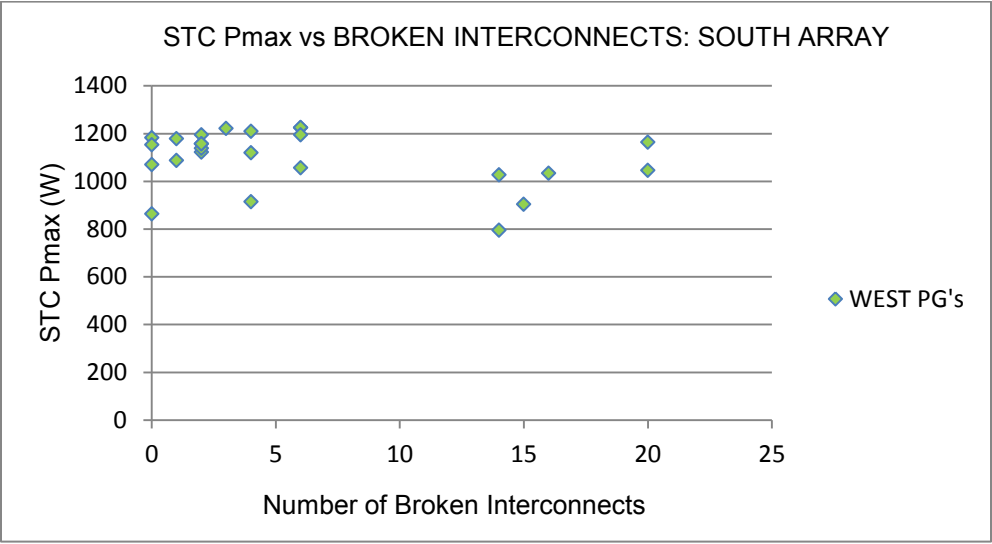
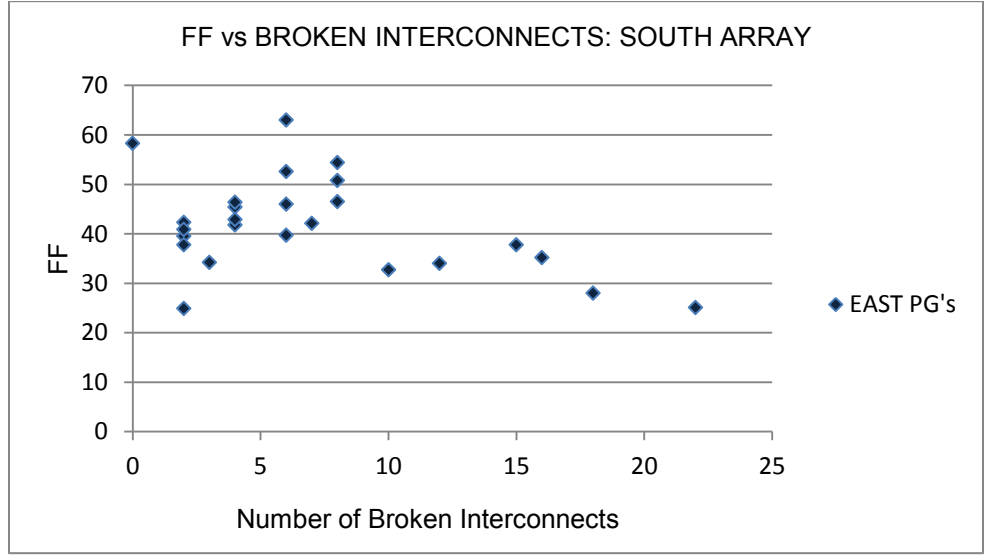
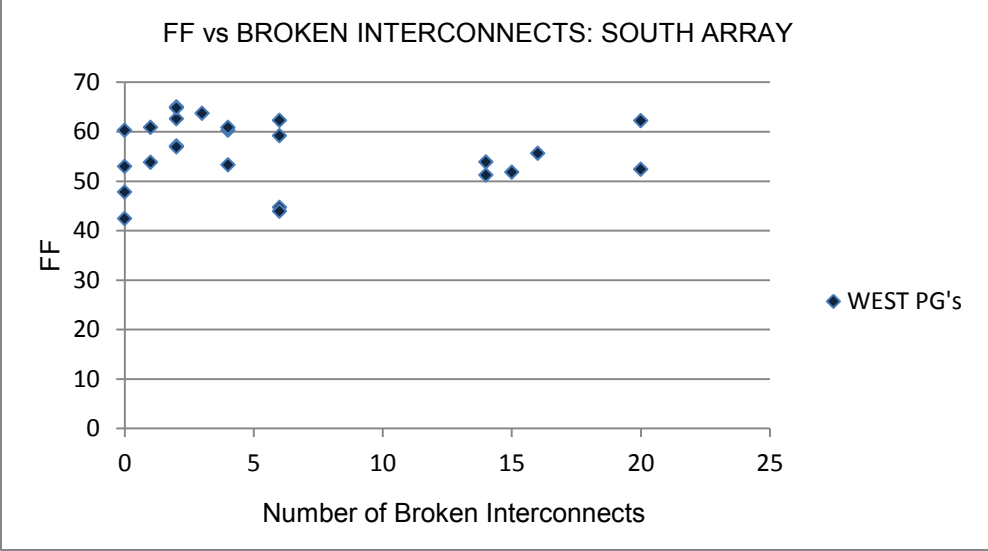


Figure 4.10 Summary of broken interconnects on PV array

4.2.3 Broken interconnects effects on Pmax, Isc and FF





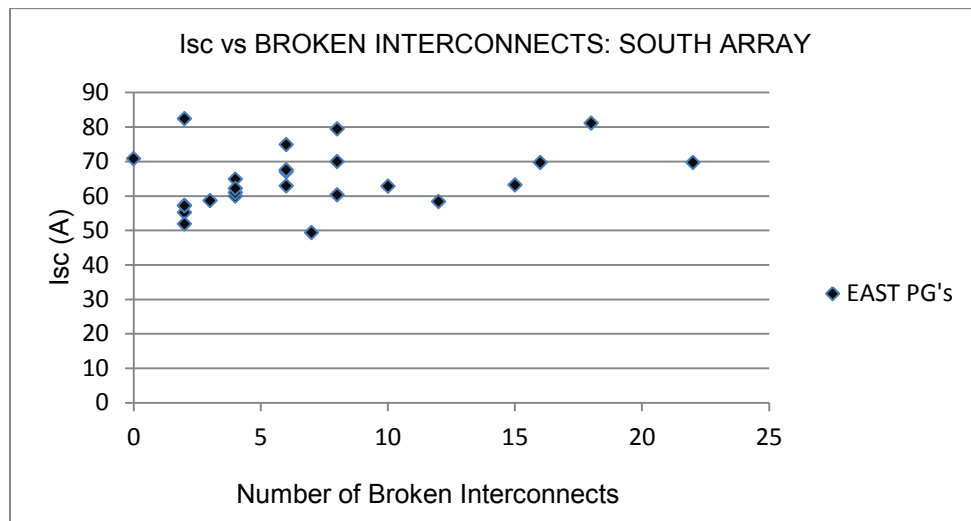
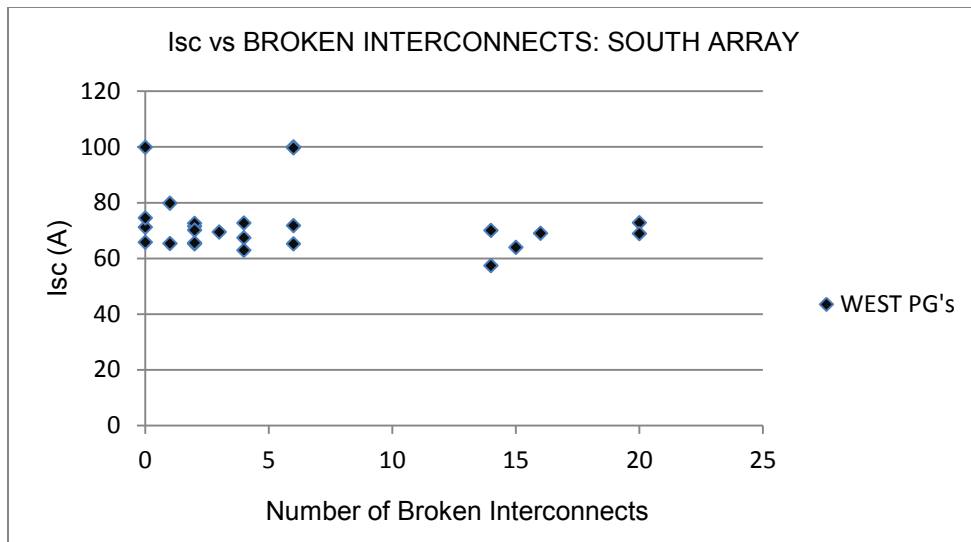


Figure 4.11 Failure modes interactions on PV array

4.3 Panel voltages for the south array

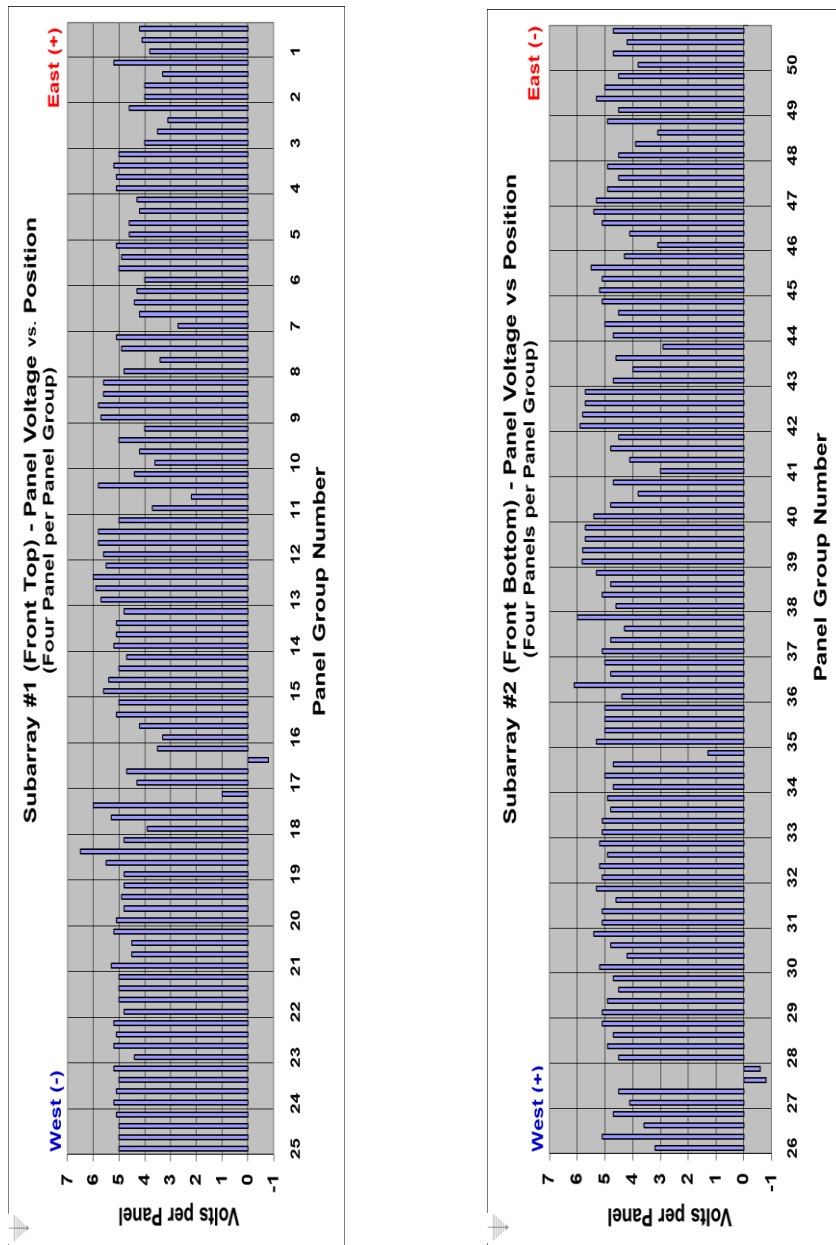


Figure 4.12 South array panel voltages measured under load

Sub arrays with positive bias have 13 PGs or 52 panels and negative bias sub arrays have 12 PGs or 48 panels all connected in series. As

panel voltages add up in series, the last panels on either ends of a sub array have open circuit voltages (V_{oc}) of approximately +380 V and -350 V respectively. These are under ideal conditions. As degradation occurred in the system, shunt resistances caused V_{oc} drop in affected panels. Two bypass diodes are externally wired into the panel group as shown in Figure 4.13 below. The wiring is permanently attached to the bus bars within the panel group. With this configuration, panels 1 or 2 failure due to shunting or hotspot failure will cause bypass diode 1 to conduct and if panels 3 or 4 fail, bypass diode 2 will conduct. Panel group 53 in the north array was found to have a conducting bypass diode. Other panels shown to have negative voltages had conducting bypass diodes as well.

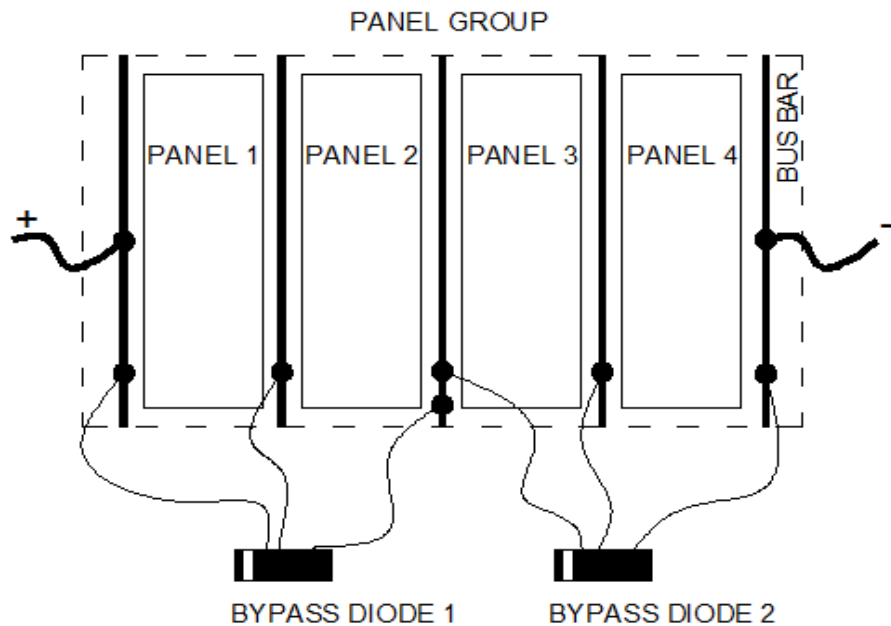


Figure 4.13 Bypass diode wiring schematic

The panel voltages were measured using a digital multimeter, carefully inserting the pointed positive terminal into the wiring and the negative

terminal to ground. A cumulative voltage read out was obtained for each panel from the center tap to the end of the sub array. A Microsoft excel spreadsheet was used to record all the data and necessary subtraction was done to determine voltages generated by each panel. Infrared images of the panels were compared to the panel voltages and there was observed a voltage drop generated by panels with hot areas.

4.4 PV south array temperatures

As with all PV arrays, operating cell temperatures are a function of the ambient temperature, incident sunlight on the array and the type of mounting used. Solar One PV system is a rack mounted system with the lowest point on array approximately two feet from the ground, while the highest point is about nine feet from the ground.

Due to high summer temperatures in Phoenix Arizona, and for the 26+ of field operation much thermal degradation has been observed on the solar array. The Arrhenius model for thermal degradation characterizes the pattern of failure observed on the array [11].

Table 4.3 PV Array average temperature distribution

South Array PG's Average Ambient Temperatures																											
DATE	WEST AVERAGE	West - Sub array 1 PG's												East - Sub array 1 PG's												EAST AVERAGE	
		25	24	23	22	21	20	19	18	17	16	15	14	13	12	11	10	9	8	7	6	5	4	3	2		1
Day 1 05/03/2012		47.0	47.0	47.0	46.0	47.0	46.0	46.0	46.0	46.0	47.0	46.0	45.0	46.0	48.0	48.0	47.0	48.0	47.0	47.0	47.0	47.0	47.0	47.0	45.0	45.0	
	46.5	50.0	47.0	47.0	47.0	46.0	46.0	46.0	46.0	46.0	46.0	46.0	46.0	48.0	48.0	47.0	47.0	47.0	47.0	47.0	47.0	47.0	48.0	45.0	44.0		
		48.5	47.0	47.0	46.5	47.0	46.0	46.0	46.0	46.5	46.0	45.5	47.0	47.0	47.0	47.5	47.0	47.0	47.0	47.0	47.0	47.5	46.0	47.0	45.0	44.5	
Day 2 05/04/2012		44.0	44.0	44.0	44.0	45.0	44.0	44.0	45.0	44.0	44.0	44.0	44.0	45.0	45.0	45.0	45.0	45.0	45.0	45.0	45.0	45.0	45.0	46.0	48.0		
	44.2	44.0	43.0	44.0	44.0	44.0	44.0	44.0	44.0	44.0	44.0	44.0	44.0	45.0	45.0	45.0	45.0	45.0	45.0	46.0	46.0	45.0	45.0	45.0	47.0		
		44.0	43.5	44.0	44.0	44.5	44.0	44.0	44.0	44.5	44.5	44.0	44.0	45.0	45.0	45.0	45.0	45.0	45.0	45.5	45.5	45.5	45.0	45.5	47.5		
OVERALL AVERAGE	45.3																										46.0

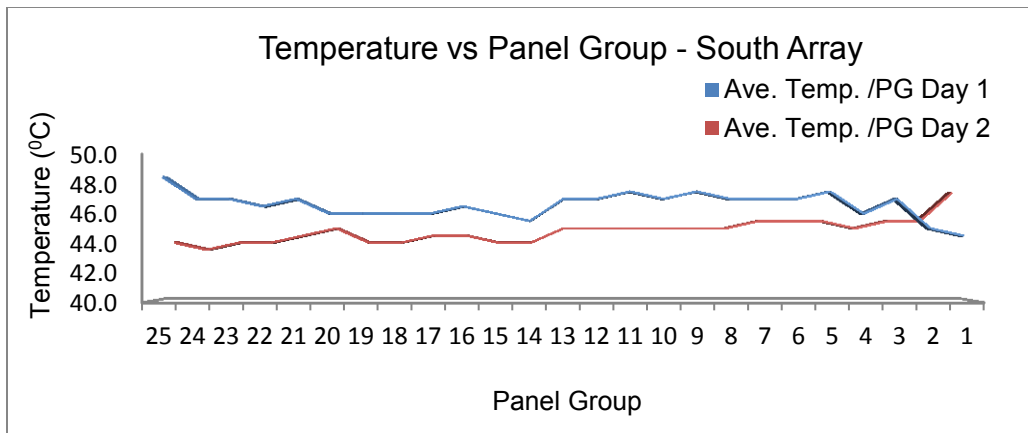
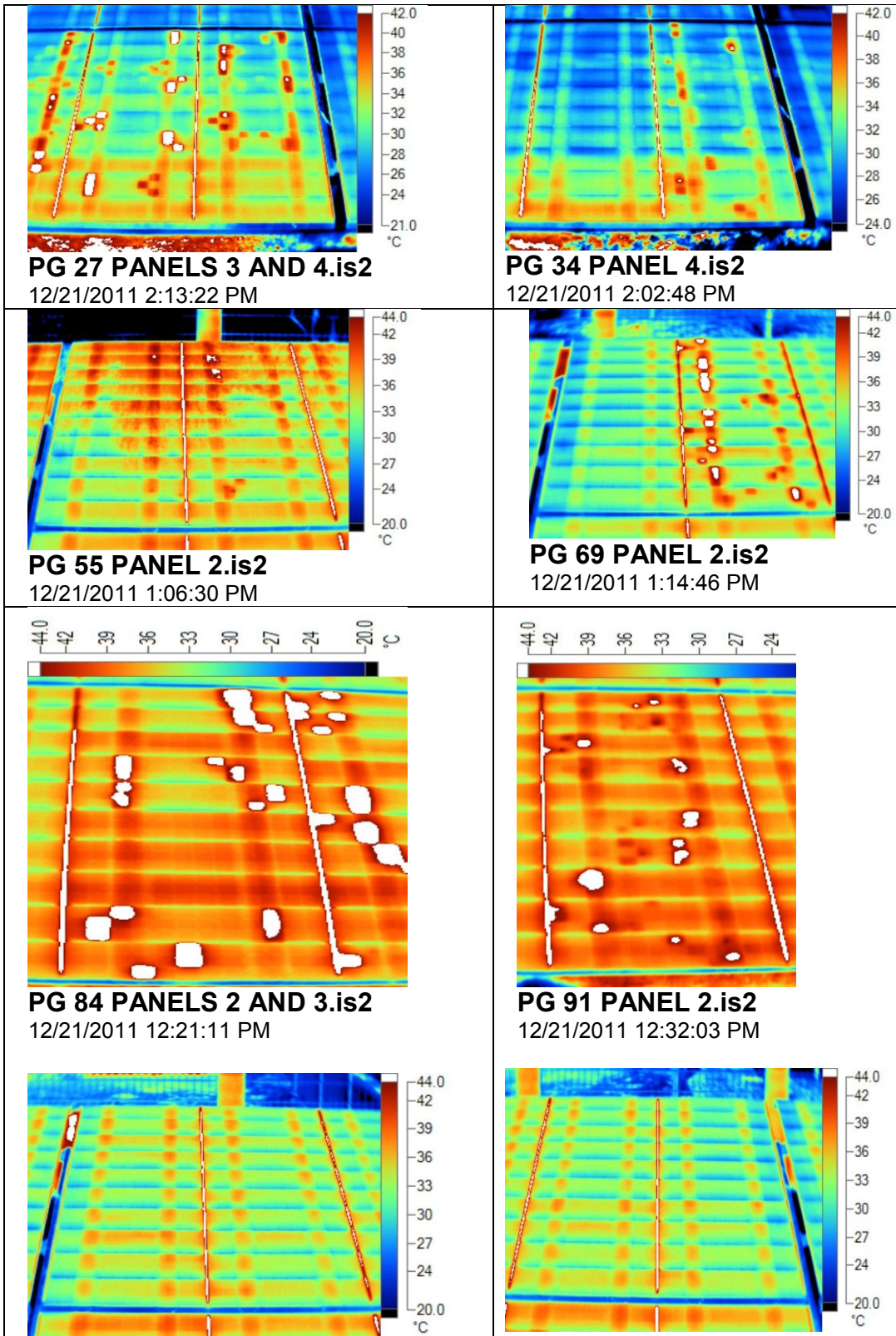


Figure 4.14 Temperature distribution pattern on the south array

4.5 Hot cell areas

Infrared (IR) image of panel groups were taken while the array is under load, to determine the extent of degradation from hot areas. The panels with high hot areas observed were also low in panel voltages. The images of the specific panels below can be compared with the above panel voltages in Figure 4.12. Some of the panel voltages affected are found to be reversed biased. Panel IR images from panel groups 27, 34, 55, 69, 84 and 91 shown in Figure 4.15 below with more severe hot areas are shown and the 4 panels of panel group 58 which has mild hot areas are shown for comparison. The affected panel samples have low panel voltages and corresponding power outputs.



PG 58 PANELS 1 AND 2.is2
12/21/2011 1:08:41 PM

PG 58 PANELS 3 AND 4.is2
12/21/2011 1:08:28 PM

Figure 4.15 Hot areas effect on PV array

Panels within the panel groups are numbered 1 to 4 in the direction of increasing panel group numbers. There are 19 panels within the south array having critical hot area issues found during the physical inspection using IR camera on the array connected to load. This was executed in December 21st 2011 between 11:00 am and 2:00 pm, with hot areas ranging from 50 to 60^o Celsius. The rest of the panel groups have mild to medium hot area effects due to the support framing discussed earlier.

Hot areas for the whole array generally developed on the module cells just above the steel frame supporting the modules on the structural support for the array. The back side of the module in Figure 4.16 highlights this observation, as the cells do not have enough ventilation on the backsheet in the area enclosed by the supporting frame. A lab experiment was carried out to be verify effect of high temperatures on cells with low ventilation (or high thermal insulation) on the PV array as shown in Figure 4.16 below.



Figure 4.16 Hot area cell effects on modules back side (Left: In the field. Right: Simulated in the lab)

The result showed an average of 1.6 W power drop from a partially insulated sample module SM54 with 41.6 W measured peak power without insulation, results given in the Table 4.4 below:

Table 4.4 Lab experiment on back sheet ventilation

	No-insulation	No-insulation	Cells insulated on the back side	Cells insulated on the back side
Curve ID:	1	2	3	6
Date:	6/8/2012	6/8/2012	6/8/2012	6/8/2012
Time:	13:37:40	13:42:15	13:59:33	14:09:38
Voc:	6.27	6.25	6.06	6.04
Isc:	10.14	10.13	10.28	10.29
Fill Factor:	66.88	66.80	65.62	65.44
Peak Power:	42.48	42.27	40.87	40.69
Irrad 1:	1,053	1,053	1,059	1,065
Cell Temp	56	56.9	68	73.2

4.6 High potential insulation test

High potential (Hi-pot) test was carried out to investigate the safety of the PV array in wet and dry conditions. During the test, a very wet condition was simulated by throwing water from buckets onto the panel group and allowing to run down to the ground and covering the backside, frame support on the rear side of the PG with water to saturate the PG being tested. For the mild wet conditions, water was sprayed using a spray bottle both on top of the laminates and the backsides just enough to evaporate easily without any dripping to the ground. The results in Table 4.5 (a) are given in Mega Ohms for the resistances measured for dry and both wet conditions simulated. Broken glass reduced resistances in PG 14 and 55. A 500V DC was applied to the PGs using a Meggar tester. Tables 4.5 (a) and (b) give resistance output of the test and calculated current respectively using the formula:

$$V = I \times R \text{ and } I = V / R.$$

Table 4.5(a) Hi-Pot test resistance output in mega ohms (MΩ)

PGs TESTED	DRY CONDITION		VERY WET CONDITION (RAIN)		MILD WET CONDITION (DEW)	
	M +	M-	M +	M-	M +	M-
*14	192.5	371	0.014	0.002	-	-
97	330	190	0.035	0.015	-	-
4	209.4	244.5	0.048	0.08	-	-
*55	177	181	-	-	13.3	36.56
91	183	232	-	-	48	44
58	179	176	-	-	10.5	63.8

* Panel Group has one module with broken glass

Table 4.5(b) Hi-pot test current output in milliamps (mA)

PGs TESTED	DRY CONDITION		VERY WET CONDITION (RAIN)		MILD WET CONDITION (DEW)	
	M +	M-	M +	M-	M +	M-
*14	0.0026	0.0013	35.714	250.000	-	-
97	0.0015	0.0026	14.286	33.333	-	-
4	0.0024	0.0020	10.417	6.250	-	-
*55	0.0028	0.0028	-	-	0.038	0.014
91	0.0027	0.0022	-	-	0.010	0.011
58	0.0028	0.0028	-	-	0.048	0.008

* Panel Group has one module with broken glass

M+ means meggar tester output for positive polarity above ground

M- means meggar tester output for negative polarity above ground

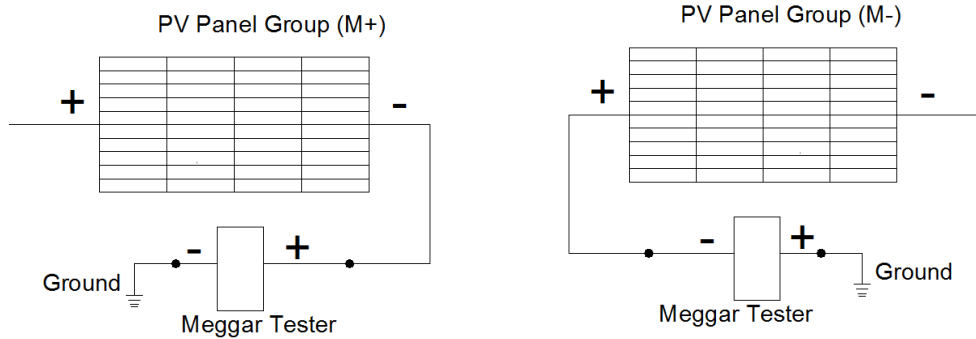


Figure 4.17 Hi-Pot Insulation Test wiring for positive (left) and negative (right) polarities above ground

- High leakage current on rainy days
- Inverter shutdown will most likely occur
- Most leakage on PG with broken module
- PV system not safe when wet

4.7 I-V before and after repair

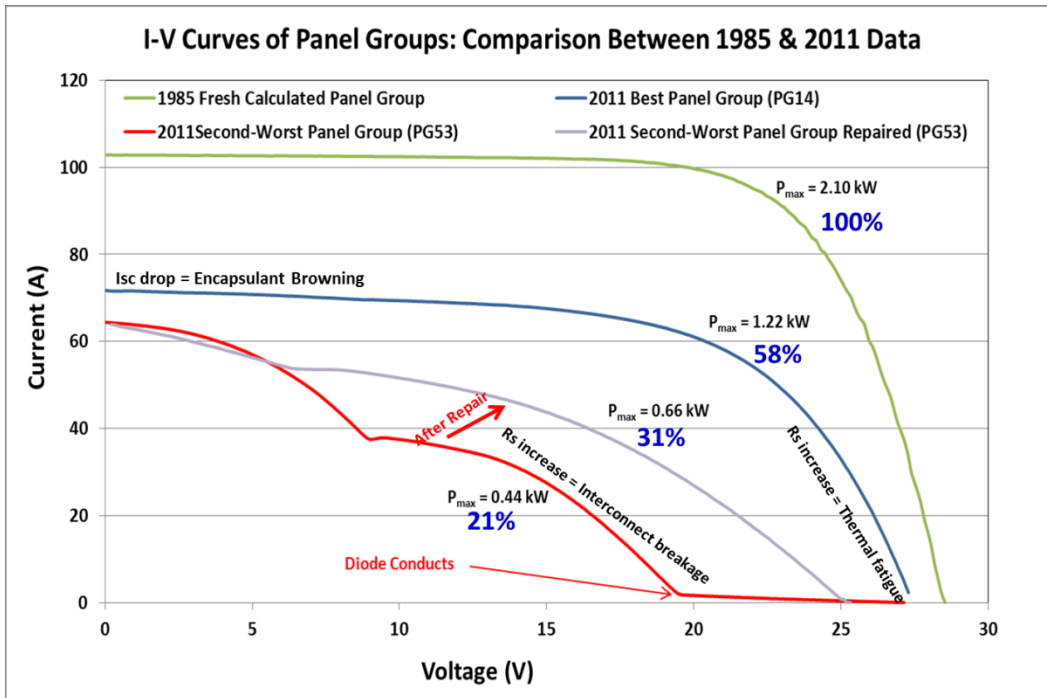


Figure 4.18 I-V comparison of PG from new to degraded condition

Figure 4.18 above shows what the IV curve of the original panel group characteristic is in 1985 when installed. After 26+ years, the best measured performing panel group (PG 14) has 58% of original power. One of the worst measured performing panel group (PG 53) had 21% of original power. Some interconnect repairs made to PG53 which contained many open circuit modules restored 50% of the 21% original power measured.

4.8 Overall performance degradation summary

After all the tests were concluded at the site, the primary findings indicate that the significant power drop was attributable to thermo-

mechanical fatigue and rain induced corrosion both leading to interconnect breakages.. In addition, encapsulation browning all over the entire array also contributed to the power loss (excessive level of browning on the original modules and significant level of browning on the replaced modules in the early 1990s).

It was observed that the installation of the bus bar which contains the terminal for the bypass diode connection was moved or displaced about a quarter inch in order for the hole on the bus bar cover to fit the diode terminal. This displacement was performed after the modules interconnection ribbons have been pre-fabricated thus causing some stresses on the ribbons as a result of this displacement from the fixed module position. The detail of displacement is shown in the Figure 4.19.



Figure 4.19 Bus bar and panel pre-assembly error

Also, several stress cracks on the module ribbon tabs are evident as observed on panel group 53. 80% of the modules were found to be in open circuit. The IV curve of PG53 shows diode activity as a result of interconnects failure.

The images below give examples of the findings on the array studied.

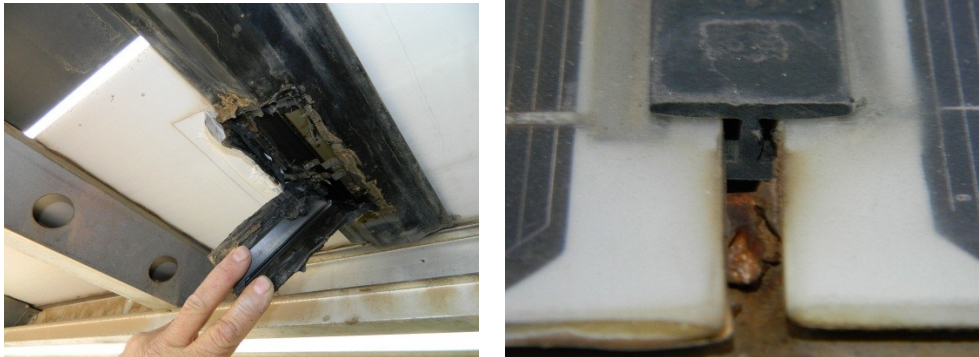


Figure 4.20 Left: Bus bar cover repairs after module replaced. Right: Corrosion observed on B.O.S. front side due to moisture intrusion



Figure 4.21 Left: cracks on module interconnect. Right: breakages observed in module interconnects in the PV array



Figure 4.22 Left: cell browning with oxygen bleaching at edges and around cell cracks. Right: commonly observed extensive browning of the original PV modules



Figure 4.23 Left: Original module on top, replaced module at bottom. Right: Panel group with multiple replacement modules.

Chapter 5

CONCLUSION

Four thousand modules installed in 1985 have been investigated after 26+ years of outdoor exposure in Phoenix, Arizona. The climatic conditions are hot and dry. The south array comprising of 2000 modules (50 panel groups at approximately 2000 W each originally) show an average of 1098 W per PG to the west and 744 W per PG to the east. This is approximately 30% less power on the east side than the west. Major possible/hypothetical reasons for more degradation observed in the east array are presented in the following:

1. Higher thermal fatigue (possibly due to slightly higher operating temperature) and interconnects breakage on the east side leading to high series resistance
2. Extensive encapsulant browning (possibly due to slightly higher operating temperature) leading to lower light transmittance and drop in operating current
3. Modules replacements (in early 1990's with opening and re-sealing of bus bar cover in the field for soldering of the modules on to the bus bars) leading to higher interconnect breakage and series resistance

5.1 Thermal fatigue and interconnects breakage

The effect of thermal fatigue and resulting cracking and breaking of non-cell interconnects on the bus bars have been observed to cause a major power drop on the east array. About 251 interconnect breakages were found on the west array and 343 breakages on the east array. This seems to agree with the hypothetically stated effect of module replacement explained below.

Annual temperature ranges of PV components including interconnection ribbons and bus bars within the PV array in Phoenix, Arizona can be from 0°C to 75°C. Over a period of 26+ years thermal cycling aging has occurred day and night and winter and summer leading to severe non-cell interconnect failures.

5.2 Encapsulant browning

Degradation of the Ethylene vinyl acetate (EVA) material resulted in browning on the solar cell surface. EVA has additives that absorb ultraviolet rays (UV) from the sun light incident on the PV modules. These additives could disappear after several years of high UV exposure in desert climatic condition due to photochemical reactions within the encapsulation. Once the additives are gone, browning starts mildly first by a change in the clear colorless to a brown discoloration.

Almost all the PV laminates in the Solar One array have a high degree of browning. The least affected are the replaced and broken (but not replaced) modules and therefore very easy to identify the total replaced

modules in the PV array. Browning causes loss of short circuit current and maximum power point current which in turn affect the electrical performance of the module and hence the system. The effect of oxygen bleaching of the encapsulant around cracks in PV cells has been observed. The diffused oxygen through backskin and cell cracks induce a counter-browning reaction leading to higher light transmittance near the cell cracks.

5.3 Module replacements

Over the 26+ years of the PV system life, 118 modules have been replaced in the east array, and 72 modules replaced in the west array. ARCO maintenance manual procedure for module replacement is intrusive, followed by an after repair with glue. Most module replacements made, leave the entire bus bar length exposed to moisture intrusion such as rainfall. This has led to corrosion of bus bar, interconnects connections to the bus bar and other supporting balance of system components. This has caused increased series resistance (lower fill factor at high irradiance and higher fill factor at low irradiance) and performance loss with safety hazard during wet conditions. Higher interconnect breakage in the east sub arrays is hypothetically attributed to improper re-sealing of the non-cell interconnect covers during module replacements in early 1990's. Ninety modules were replaced on the east side due to throwing-stone

vandalism. The throwing-stone vandalism is presumably higher on the east side because of lower wall height.

REFERENCES

- [1] Sanchez-Friera, P., Piliouline, M., Pelaez, J., Carretero, J. & Sidrach De Cardona, M. (2011). *Analysis of degradation mechanisms of crystalline silicon PV modules after 12 years of operation in Southern Europe*. Malaga: Wiley Online Library.
- [2] Russell, M. C. & Kern, Jr., E. C. (1990). *Lessons learned with residential photovoltaic systems*. Waltham, Massachusetts: IEEE Photovoltaic Specialists Conference
- [3] Chalmers, S. M. (1994). *Solar 1 photovoltaic system evaluation report*. Salt River Project Internal Report, Arizona.
- [4] Salt River Project (1993). *Solar One Subdivision Photovoltaic System Ownership Analysis*, - Salt River Project, Arizona
- [5] Honsberg, C. & Bowden, S. (2010). *PV education.org*. Retrieved October 10, 2012 from Arizona State University, Solar Power lab Web site: <http://www.pveducation.org/pvcdrom>
- [6] Quintana, M. A., King, D. L., McMahon, T. J. & Osterwald, C. R. (2002). *Commonly observed degradation in field-aged photovoltaic modules*. : IEEE Photovoltaic Specialist Conference.
- [7] TamizhMani G., Kuitche J. (2012) "*Background Review and Analysis on: Accelerated Lifetime Testing of Photovoltaic Modules*," Solar ABCs Study Report (DRAFT).
- [8] ASTM E 1036-96 (1996) Standard Test Methods for Electrical Performance of Non-Concentrator Terrestrial Photovoltaic Modules and Arrays Using Reference Cells
- [9] Dunlop, J. P. (2010). *Photovoltaic systems*.: American Technical Publishers, Inc.

[10] Rosenthal, A. L., Thomas, M. G. & Durand, S. J. (1993). *A ten year review of performance of photovoltaic systems*. Louisville, KY: IEEE Photovoltaic Specialists Conference.

[11] Kurtz, S., Whitfield, K., Tamizhmani, G., Koehl, M., Miller, D., Joyce, J., Wohlgemuth, J., Bosco, N., Kempe, M., Zgonena, T. (2011). *Evaluation of high-temperature exposure of photovoltaic modules*. : Progress in Photovoltaics: Research and Applications.

APPENDIX A
RESULTS OF SOLAR ONE ARRAY MEASUREMENTS

TABLE 1 - RESULTS OF SOLAR ONE ARRAY MEASUREMENTS

[PANEL GROUP	STC Isc (A)	STC Voc (V)	STC Pmax (W)	PANEL GROUP	STC Isc (A)	STC Voc (V)	STC Pmax (W)
1	69.7	28.9	507.6	51	71.9	28.9	584.5
2	58.6	27.4	551.5	52	71.8	27.2	571.9
3	62.8	27.4	564.9	53	64.3	27.2	438.2
4	67	27.6	851.2	54	59.7	27.1	784.6
5	59.9	27.2	683.2	55	40.8	26.8	421.2
6	60.9	27.4	761	56	52.8	27	475.1
7	49.3	27.3	568.9	57	51.6	27.3	539.8
8	57.2	27.4	663.4	58	88	27.6	1213.8
9	70.8	27.3	1130.2	59	63.7	27.3	919
10	82.4	27.3	561.2	60	75.7	27.2	452.2
11	58.3	27.3	543.2	61	50.4	27.1	487.2
12	69.9	27.4	1047.4	62	83.6	27.5	1012.6
13	74.9	28.9	1142	63	64	28.4	1083.4
14	71.7	27.3	1223.9	64	63.1	27.2	984.1
15	100	27.4	1225.7	65	81.5	27.5	987.9
16	71.5	27.4	1122.3	66	75.5	27.4	984.8
17	65.8	27.4	863.9	67	63.7	27.5	968.2
18	65.3	27.3	1088.1	68	65.2	27.4	943.2
19	79.8	27.4	1178.1	69	87.8	27.2	1035.4
20	71.2	27.4	1182.3	70	74.9	27.2	1047.4
21	72.5	27.5	1138.7	71	74.8	27.2	1048
22	72.6	27.6	1210	72	63	26.9	928.7
23	70.1	27.2	1194.9	73	68.9	27.4	990.7
24	99.7	27.2	1194.1	74	66.1	27.6	1034.5
25	69.4	27.5	1221.5	75	67.1	27.7	1100.7
26	63.9	27.2	903.8	76	66.2	27.6	1036.3
27	57.4	27	795.7	77	100.8	27.6	967.7
28	69	26.9	1034	78	69.4	27.4	984.8
29	72.8	27.4	1046.3	79	70.2	27.1	1015.5
30	65.2	27.3	1057.1	80	80.1	27.2	1048.6
31	65.2	27.3	1157.8	81	84	27.2	1031.6
32	67.4	27.2	1119.1	82	78.1	27.5	917.3
33	74.5	27	1069.5	83	63.6	27.5	965.7
34	62.9	27.2	914.6	84	57.1	27.6	725.6
35	99.9	27.2	1153	85	65.1	27.4	953.7
36	65.5	27.2	1157.7	86	81.8	27.4	1036.7
37	70	27.1	1027.8	87	62.2	27.5	890.4
38	68.9	27.1	1164.2	88	63.9	27.6	1000.4
39	79.4	28.9	1167	89	74	28.6	1083.8
40	62.9	27.3	682.4	90	51.3	27.1	492
41	55.2	27.1	591.6	91	51	26.9	325.3
42	67.5	27	1153.2	92	62.9	27.3	924
43	51.8	27.2	577.6	93	98.4	26.6	804.3
44	64.8	27.2	757.6	94	69.4	27.2	675.2
45	62.1	27.2	784	95	52.9	26.7	484.7
46	57.1	27	583.8	96	55.6	27.2	582.3
47	60.3	27.4	771.4	97	60.2	26.8	648.7
48	63.2	27.2	651.3	98	64.5	26.7	827.8
49	69.7	27	665.7	99	58.8	25	634.8
50	81.1	28.4	648	100	79.1	28.8	648.8

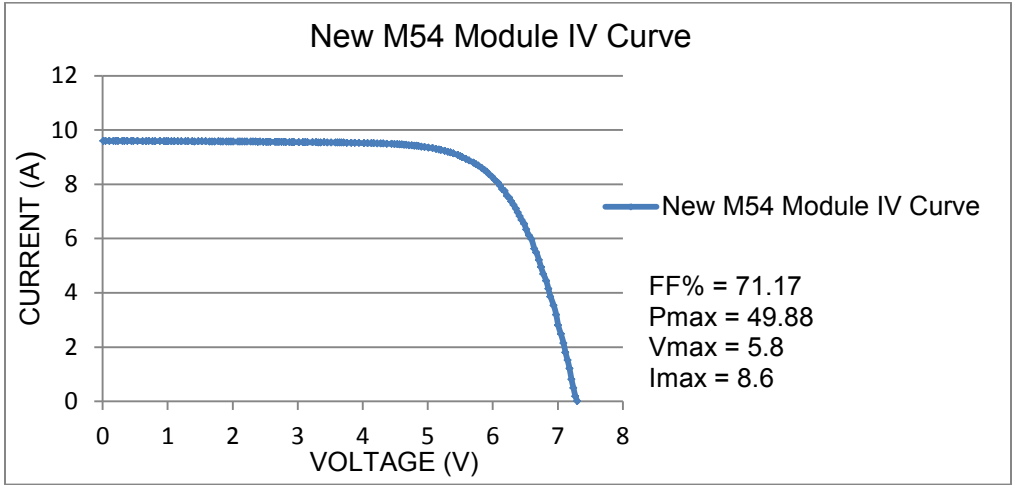


Figure 1.2 I-V curve of M54 mono-crystalline silicon laminate

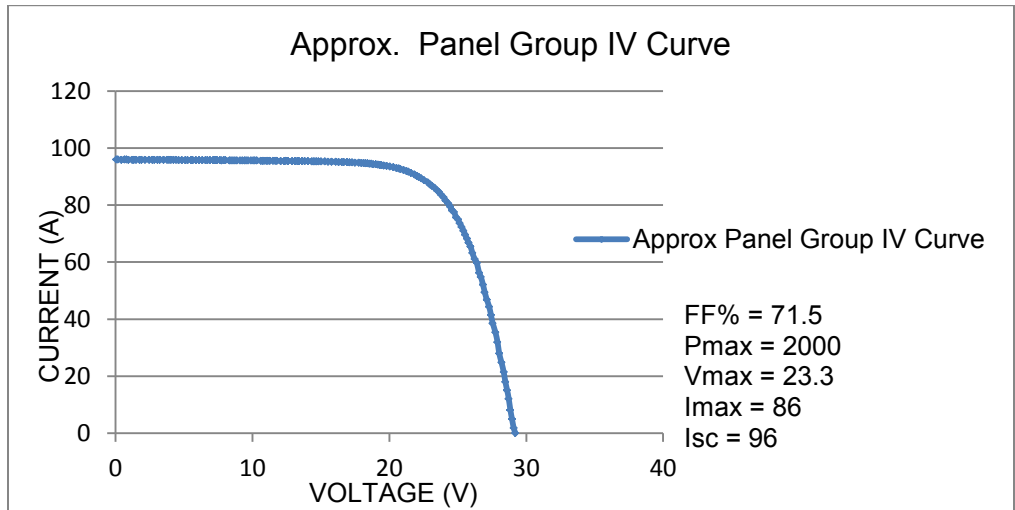


Figure 1.3 I-V curve of panel group of 40 module laminates

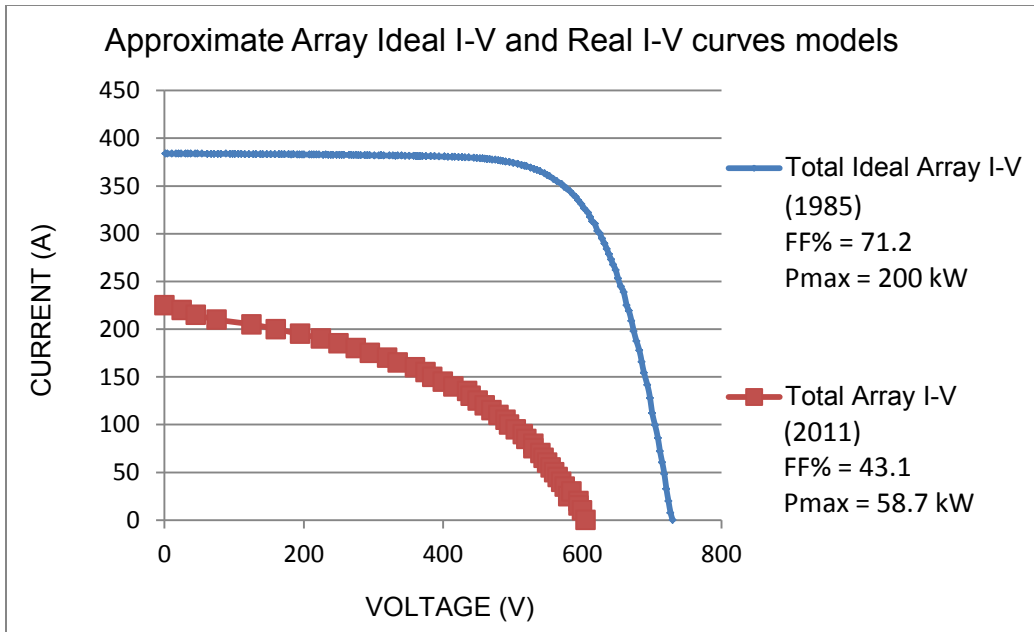


Figure 1.4 Approximate new I-V and measured I-V array models

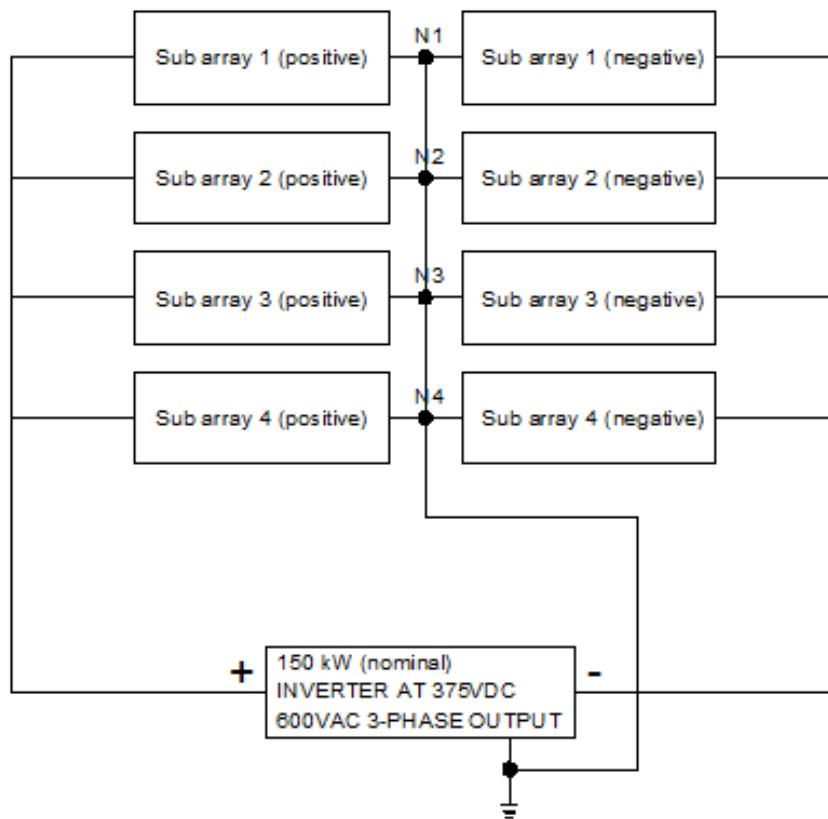


Figure 2.1 Bipolar arrays layout

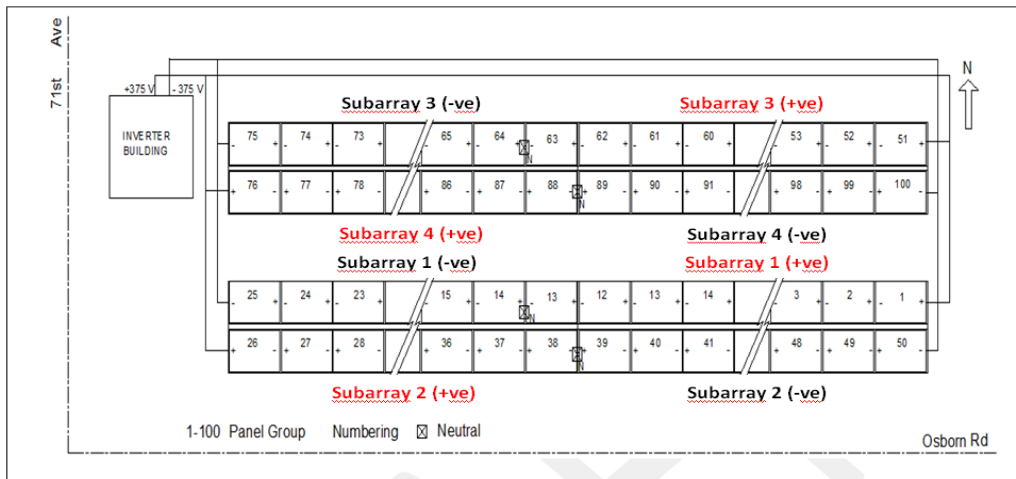


Figure 2.1.1 Sub array layout

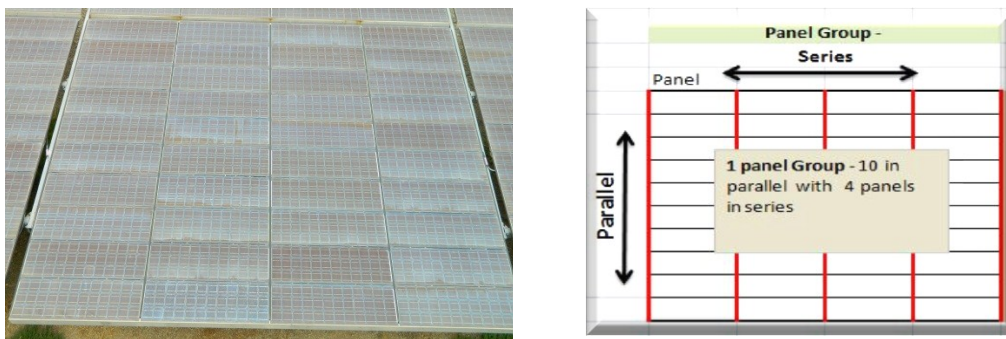


Figure 2.1.2 Panel group layouts

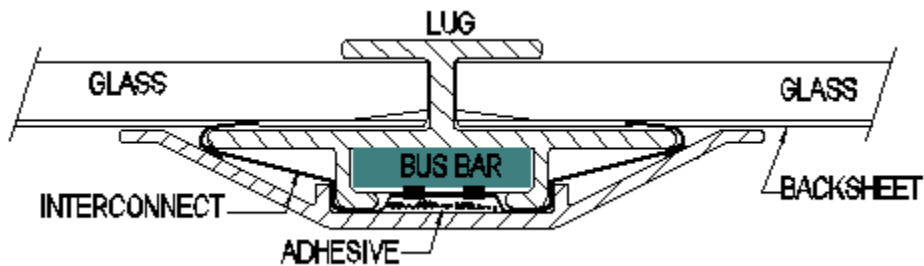


Figure 2.1.3 Laminate-bus bar profile schematic

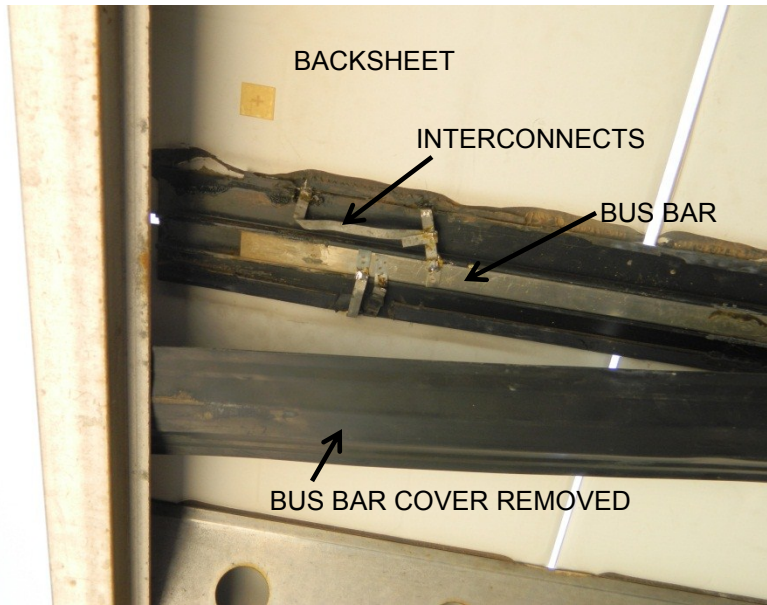


Figure 2.1.4 Laminate-bus bar details

TABLE 2 Temperature coefficients of 8 new sample modules

Results of Electrical Performance and Temperature Coefficient Test on 9/23/2011												
Module Power Rated @ STC		10.34	7.3	9.45	5.8	73.4	55.0					
Module S/N	Performance Measured at STC (1000W/m ² , 25°C)						Temperature Coefficients at Measured at STC (25°C)					
	Isc	Voc	Imp	Vmp	FF	Pm	Isc	Voc	Imp	Vmp	FF	Pm
	A	V	A	V	%	W	A/°C	V/°C	A/°C	V/°C	%/°C	W/°C
1955	9.97	7.2	9.10	5.7	72.2	51.9	0.0025	-0.0283	-0.0059	-0.0287	-0.1499	-0.2913
1957	9.95	7.2	9.02	5.7	71.7	51.4	0.0018	-0.0275	-0.0017	-0.0299	-0.1432	-0.2782
1971	10.09	7.2	9.03	5.8	71.8	52.3	0.0029	-0.0285	0.0031	-0.0330	-0.1389	-0.2830
1974	10.18	7.3	9.23	5.8	71.9	53.1	0.0010	-0.0310	-0.0063	-0.0313	-0.1413	-0.3241
2031	9.95	7.4	9.05	5.8	72.2	52.9	0.0008	-0.0351	-0.0046	-0.0373	-0.1761	-0.3611
2033	9.81	7.4	8.99	5.8	72.6	52.3	0.0035	-0.0289	-0.0041	-0.0294	-0.1519	-0.2836
2038	9.85	7.1	9.00	5.6	71.1	50.0	0.0027	-0.0229	-0.0049	-0.0214	-0.1059	-0.2159
2046	10.09	7.2	9.21	5.6	71.4	51.6	0.0026	-0.0263	-0.0033	-0.0276	-0.1409	-0.2697

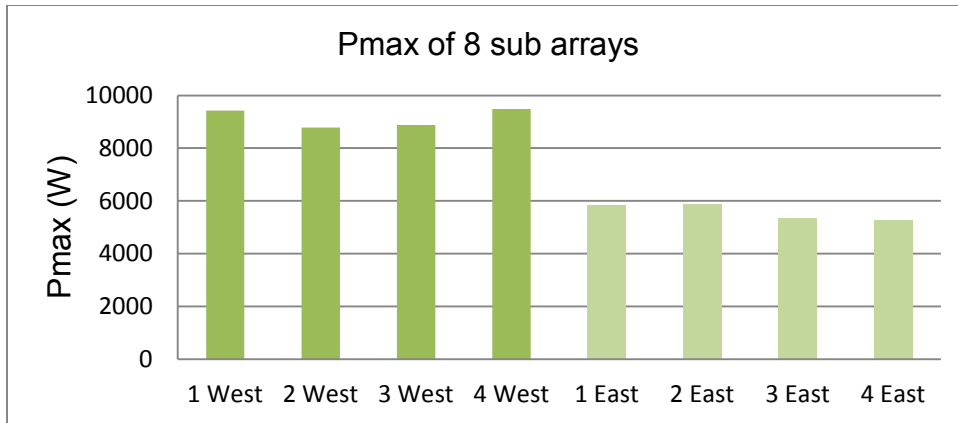


Figure 2.1.5 Sub arrays output power summary

TABLE 3 Result of 8 sub arrays measurements

	Sub array number	Number of PG's	STC Isc (A)	STC Voc (V)	STC Pmax (W)
WEST ARRAY	3-negative	12	65	316	11,139
	4-positive	13	67	344	12,427
	1-negative	12	68	320	12,155
	2-positive	13	66	343	11,672
Average			67	331	11,848
Total	4	50			47,393
EAST ARRAY	3-positive	13	55	340	6,833
	4-negative	12	57	315	6,572
	1-positive	13	58	342	7,628
	2-negative	12	61	316	7,443
Average			58	328	7,119
Total	4	50			28,476

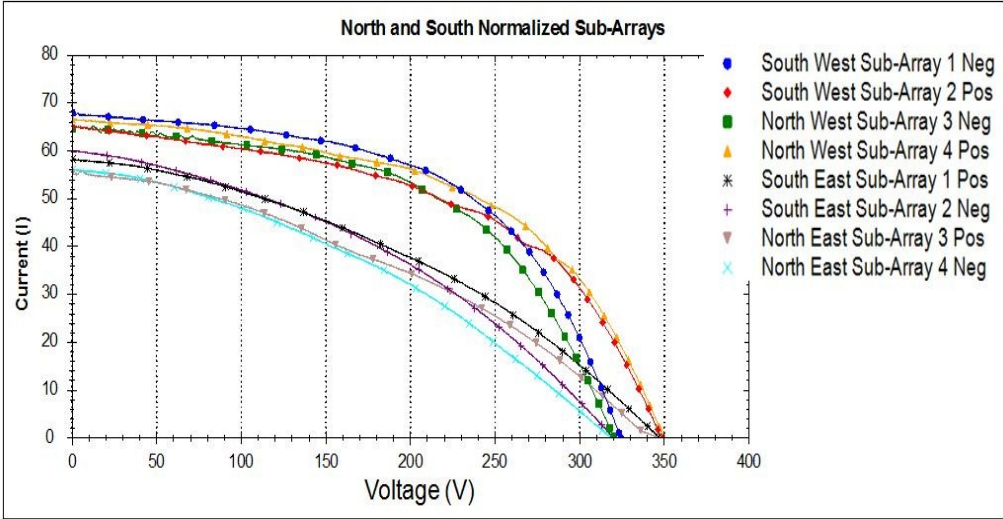
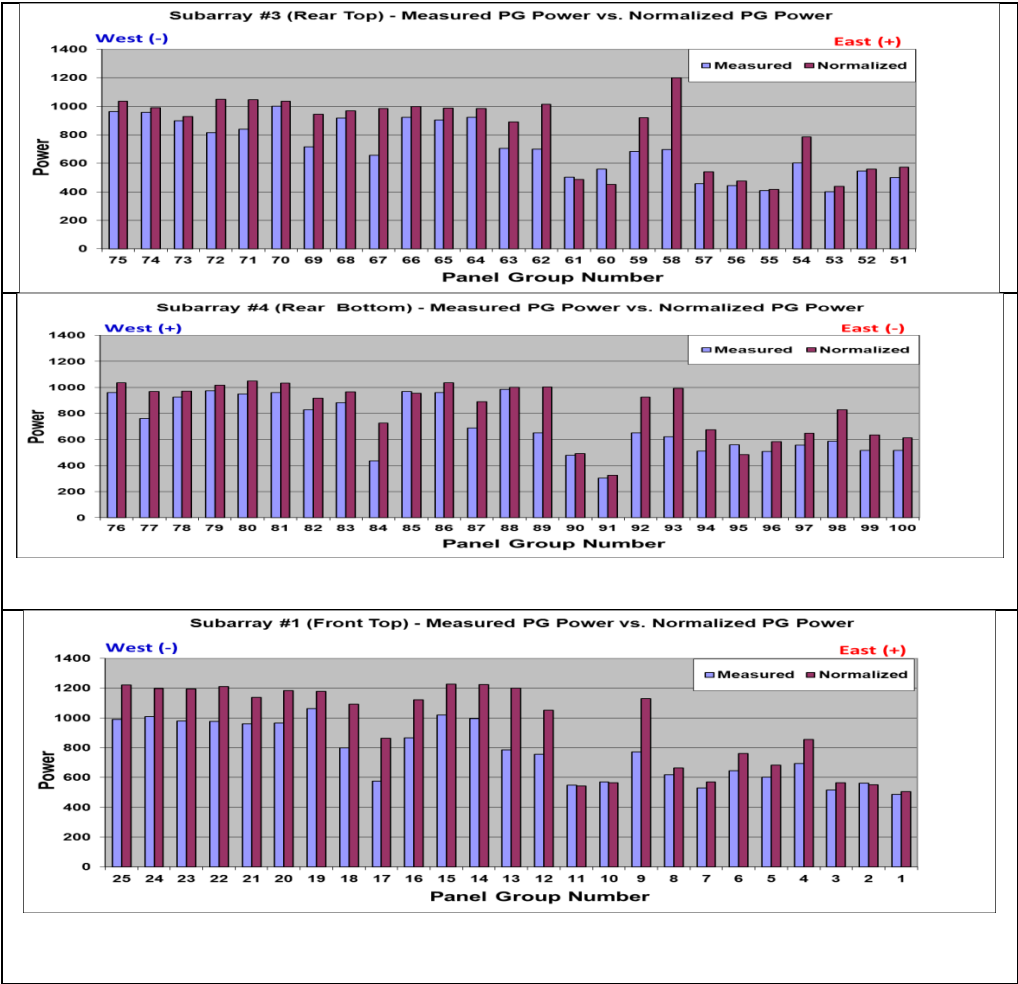
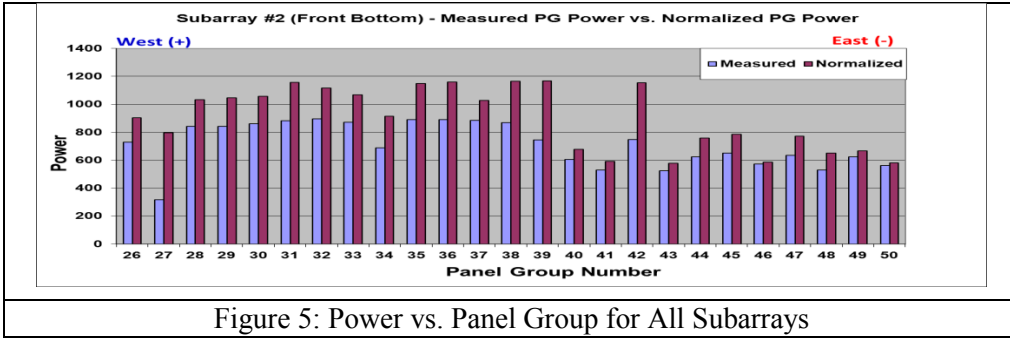
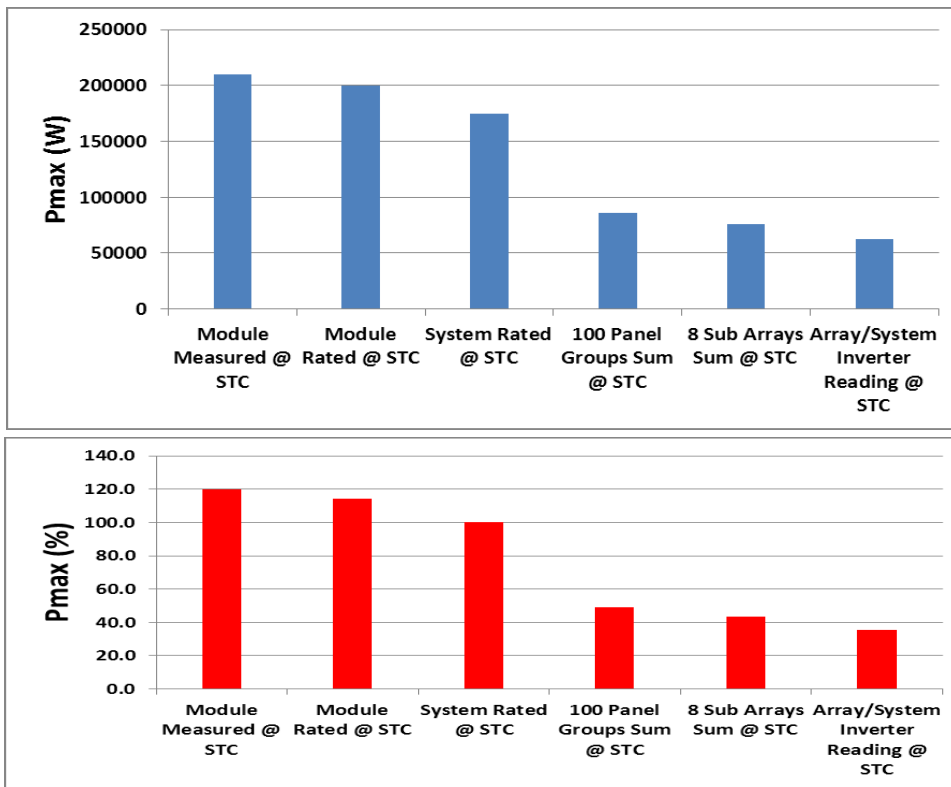


Figure 2.1.6 Sub arrays I-V and P-V curves summary [IVPC3]

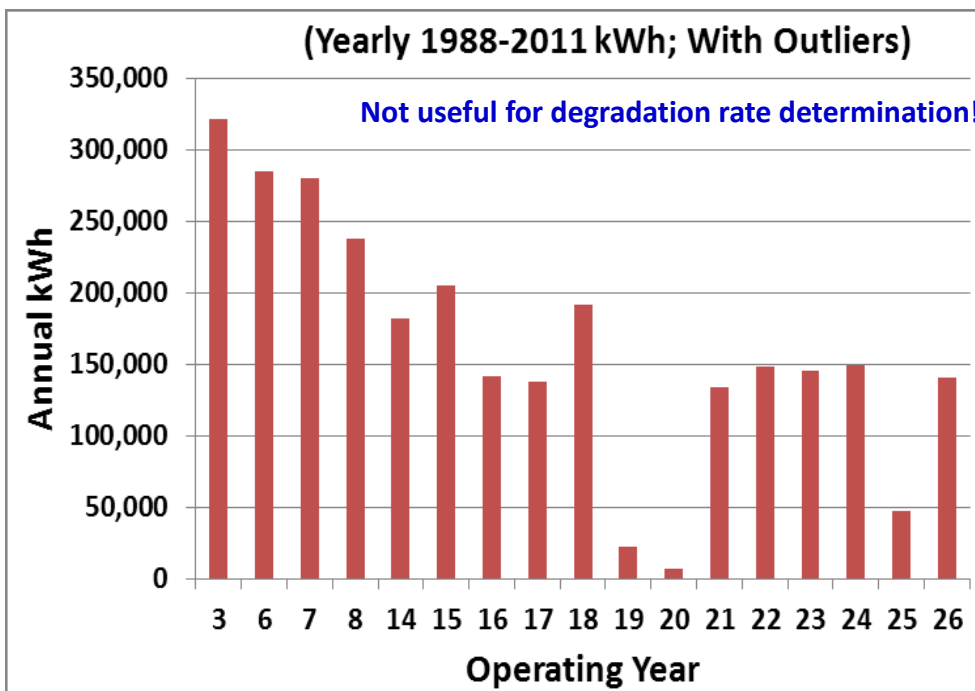
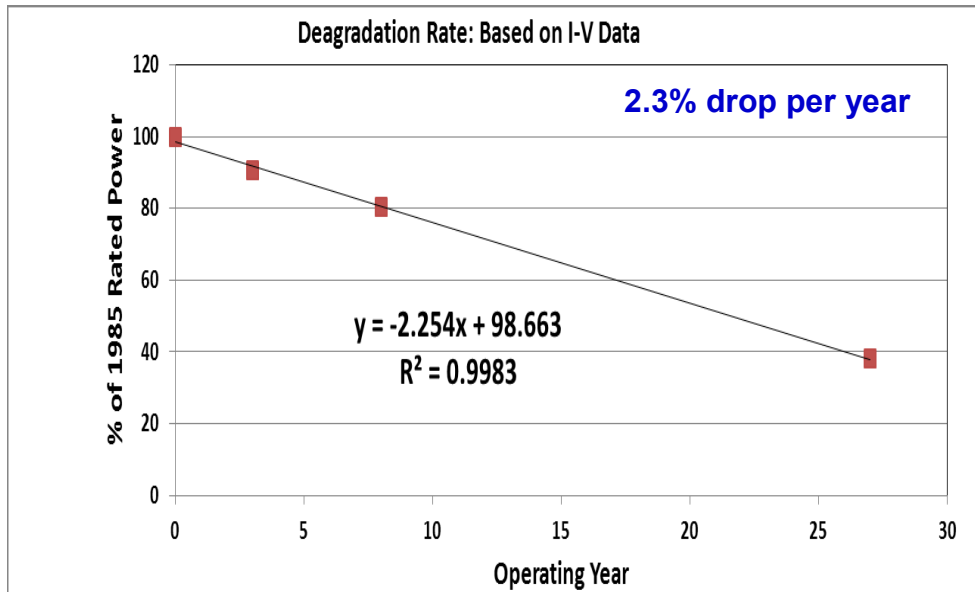


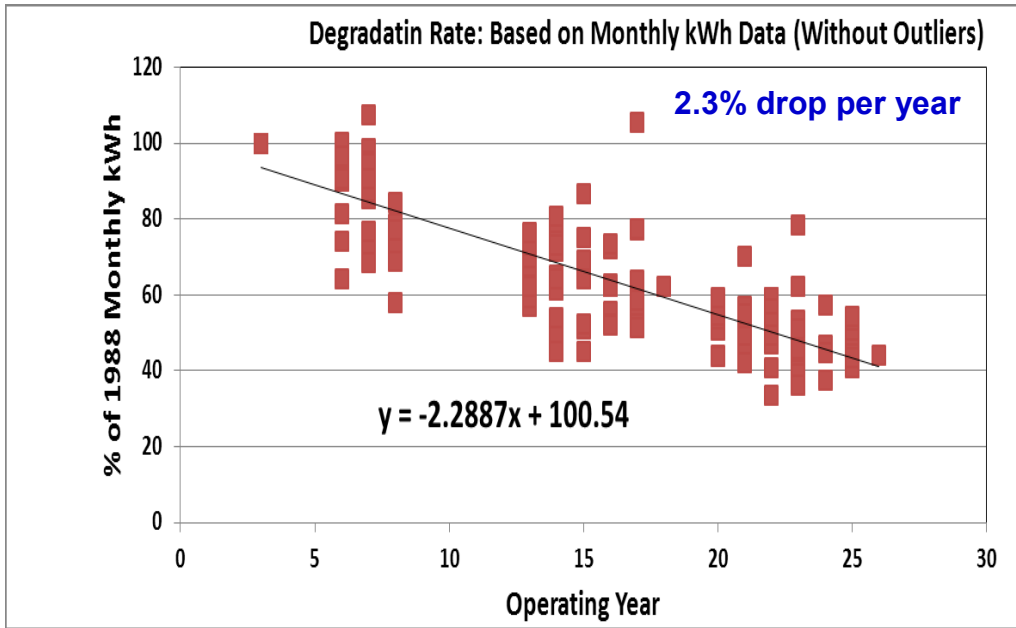


Quantification of mismatch losses

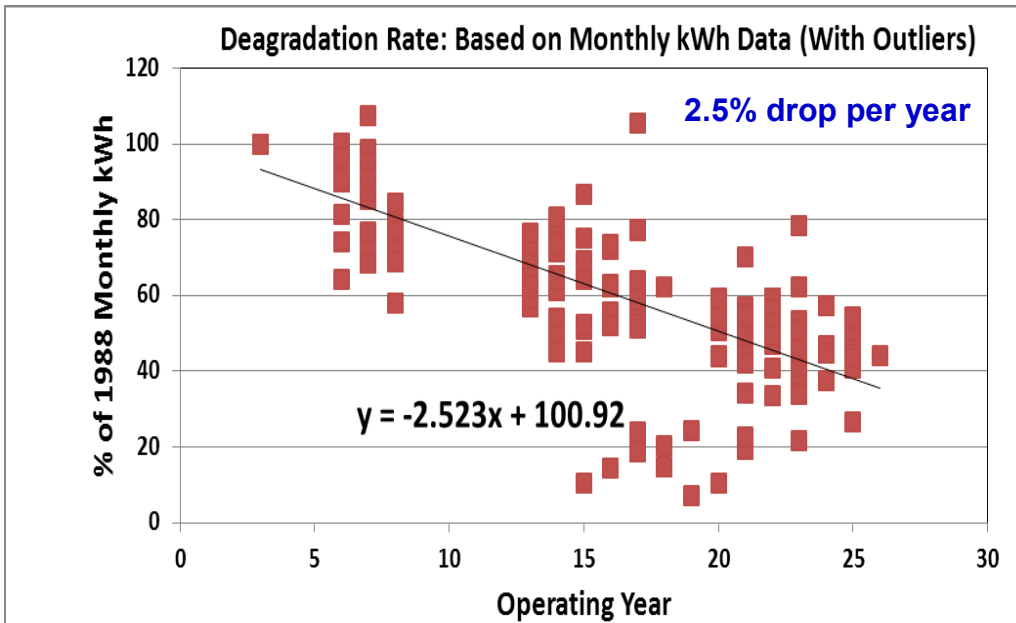


Annual performance degradation of the system





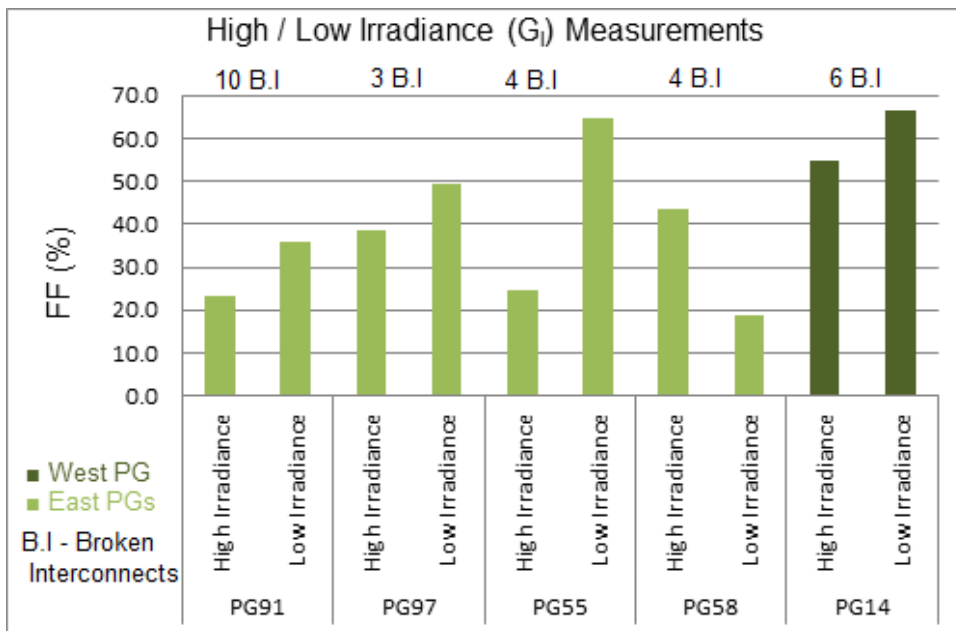
Degradation rate is 2.29% per year (outliers excluded)



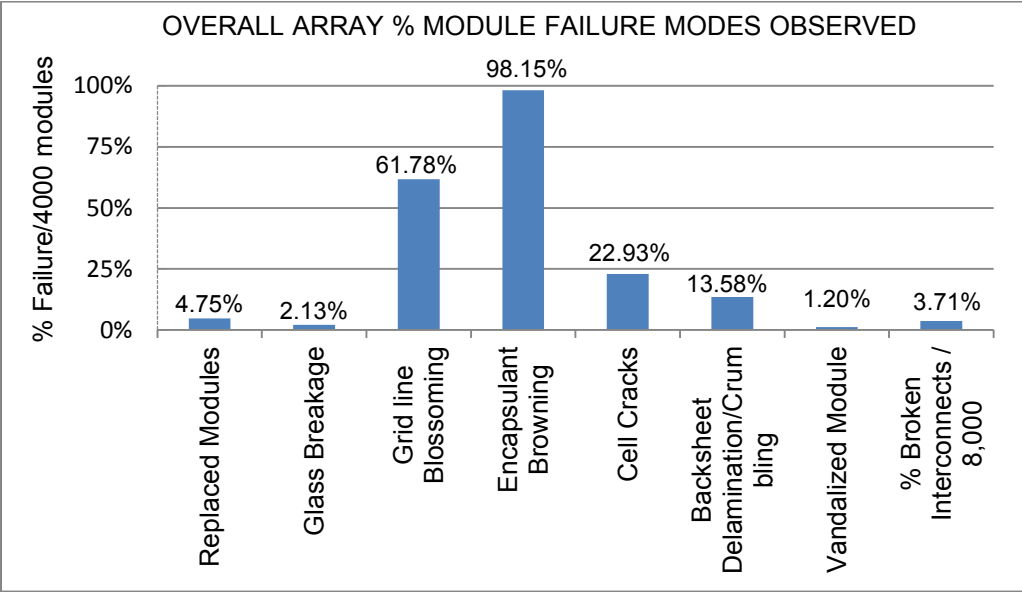
Degradation rate is 2.52% per year (outliers included)

Result of high and low irradiance measurements.

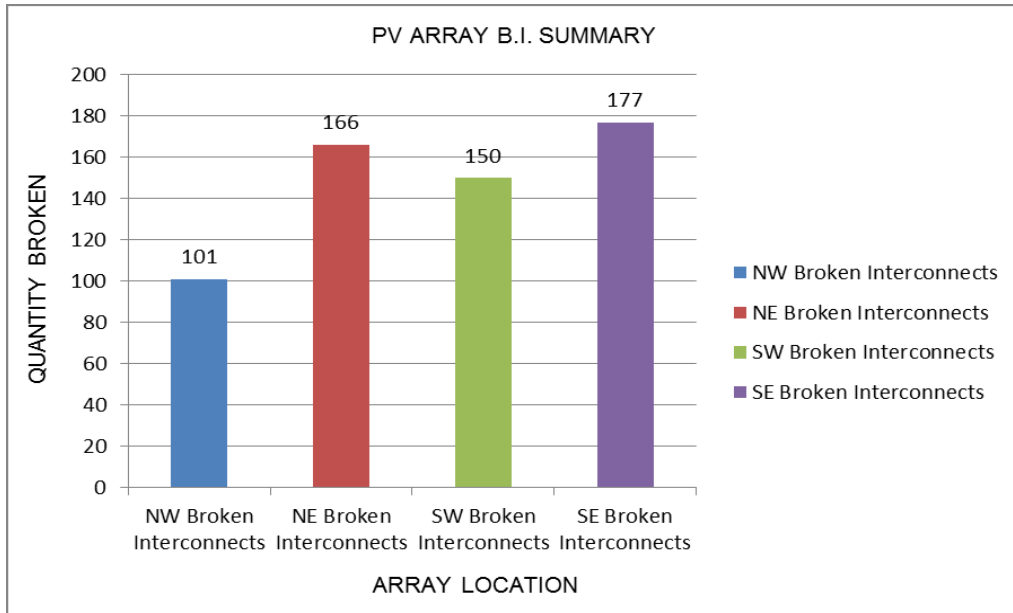
HIGH IRRADIANCE					
Panel Group	PG91	PG97	PG55	PG58	PG14
Voc	29.1	28.6	28.1	28.3	28.9
Isc	51.0	54.4	58.5	85.0	73.8
Fill Factor	23.4	38.4	24.8	43.7	54.8
Peak Power	347.7	597.3	407.9	1053.2	1165.5
Vpeak	12.3	17.7	16.4	20.6	21.1
Ipeak	28.3	33.7	24.8	51.2	55.1
Irradiance	1,000	1,000	1,000	1,000	1,000
Cell Temp.	25	25	25	25	25
LOW IRRADIANCE					
Voc	25.6	25.8	21.6	24.7	25.0
Isc	12.2	12.9	8.3	49.1	13.3
Fill Factor	35.7	49.5	64.8	18.6	66.7
Peak Power	111.3	164.4	115.6	225.9	221.6
Vpeak	17.3	19.6	14.8	19.0	19.5
Ipeak	6.4	8.4	7.8	11.9	11.3
Irradiance	200	200	200	200	200
Cell Temp.	25	25	25	25	25



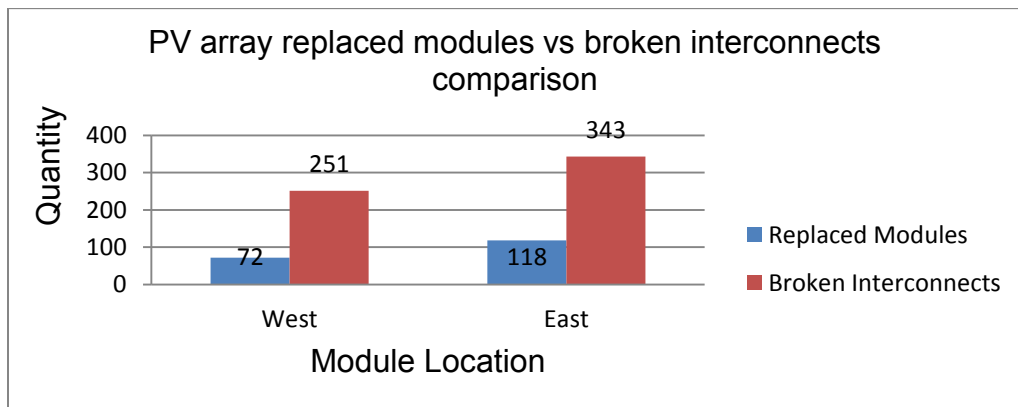
Effect of low irradiance on the PG's fill factor

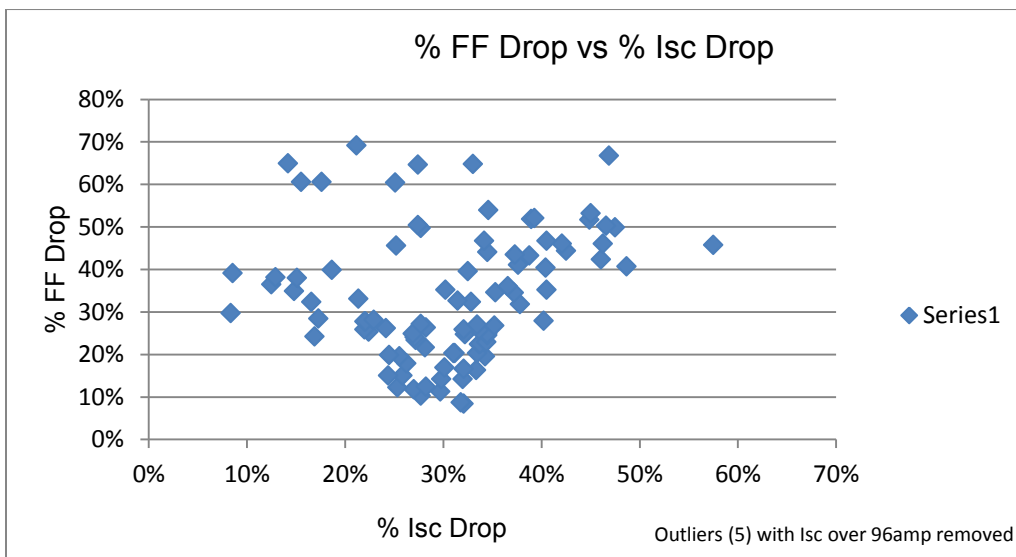
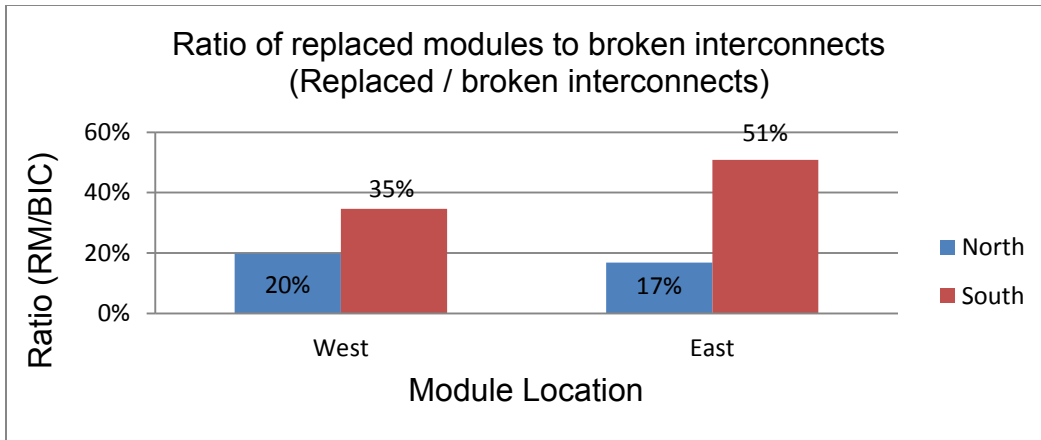


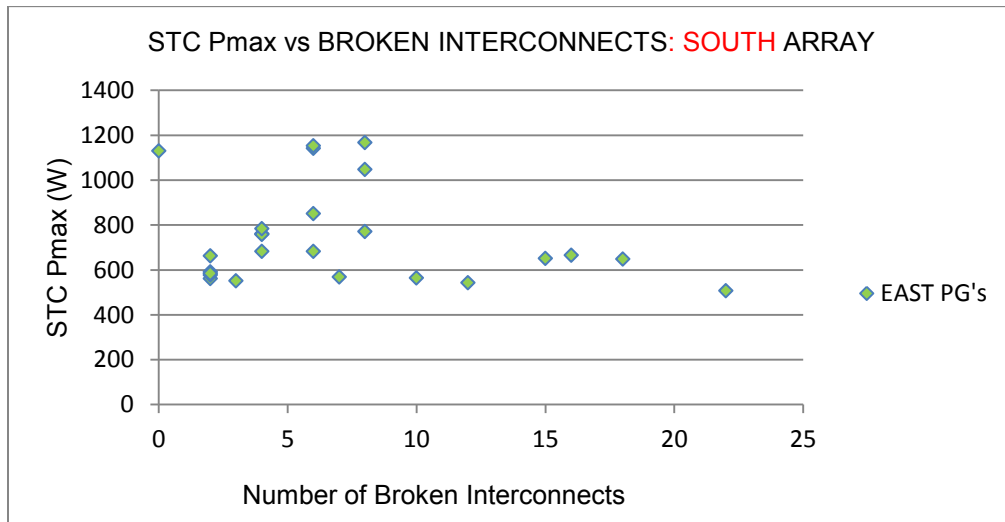
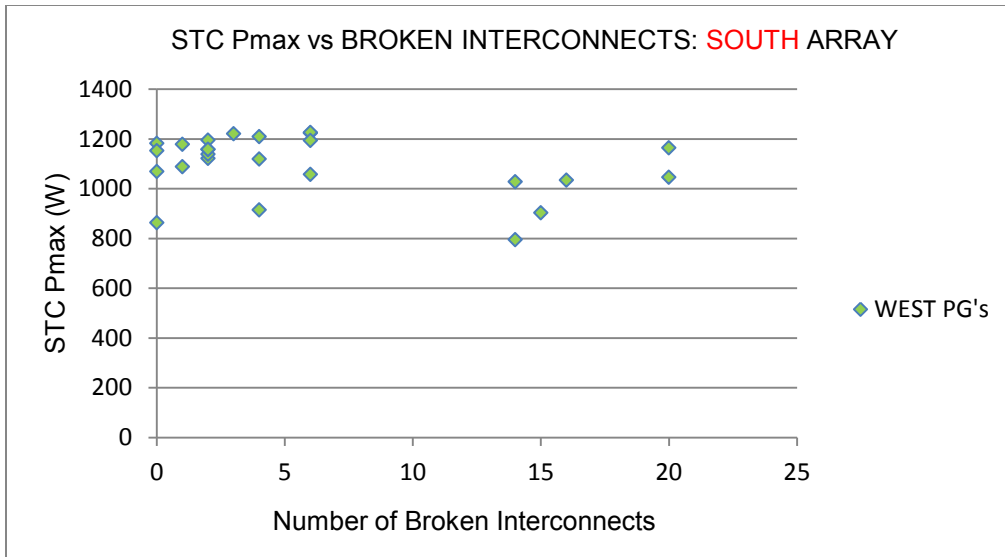
Summary of Physical defects counted on PV array

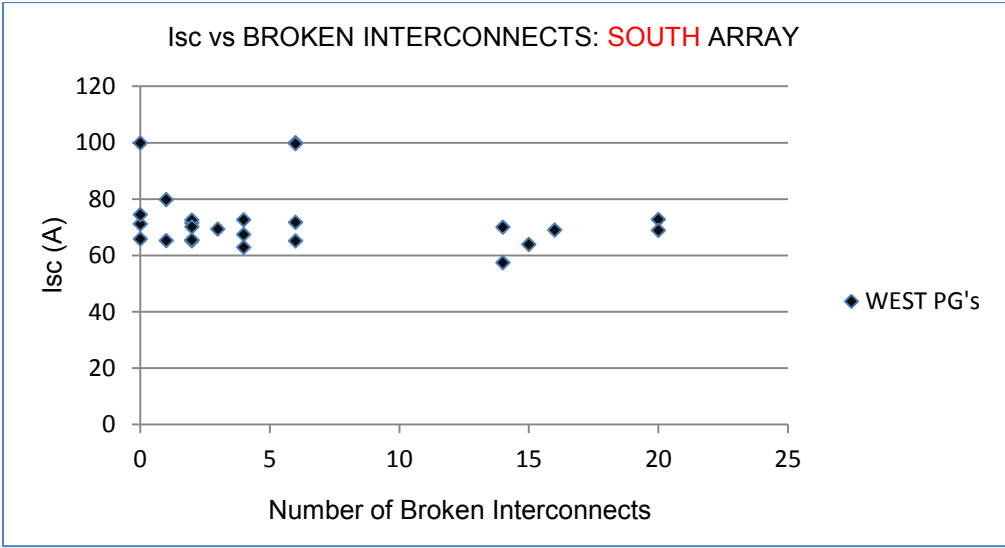
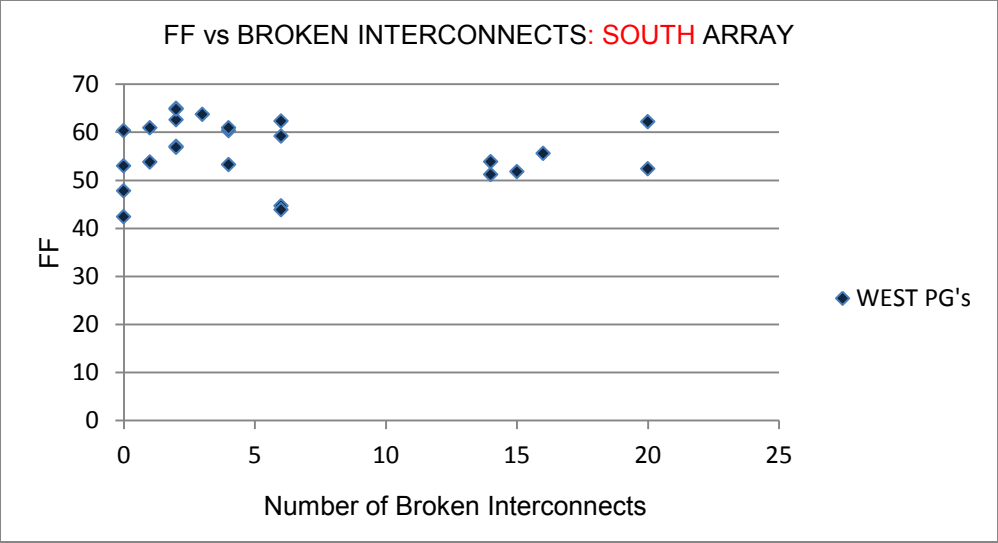


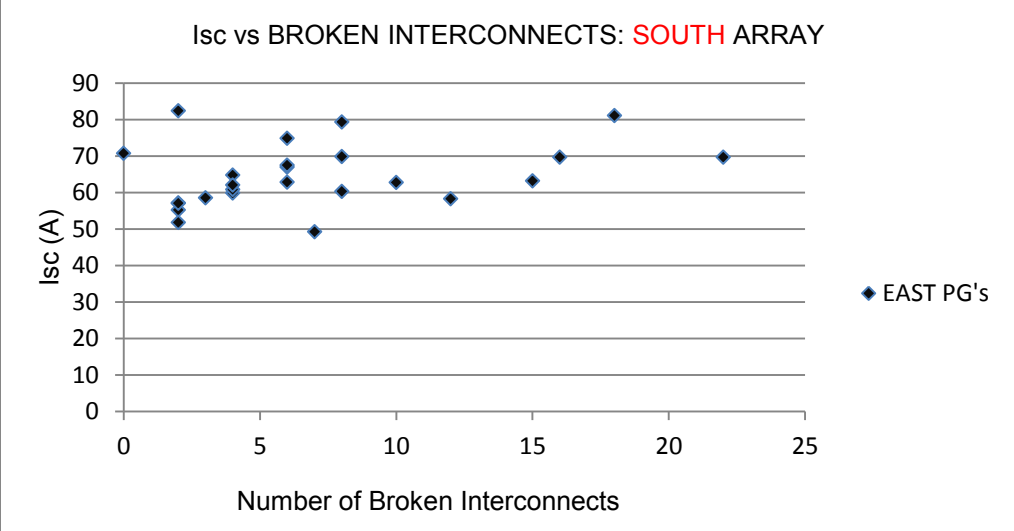
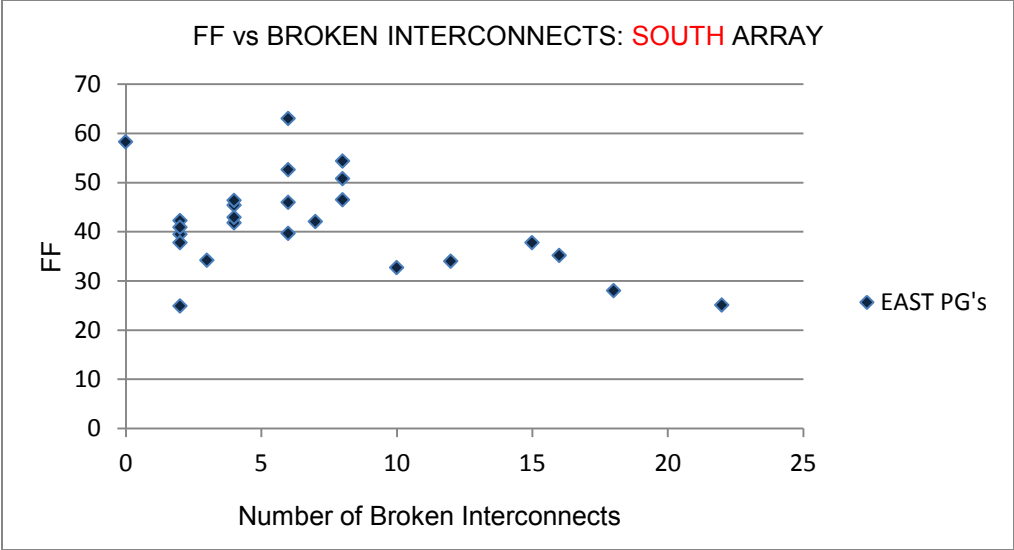
Summary of broken interconnects on PV array

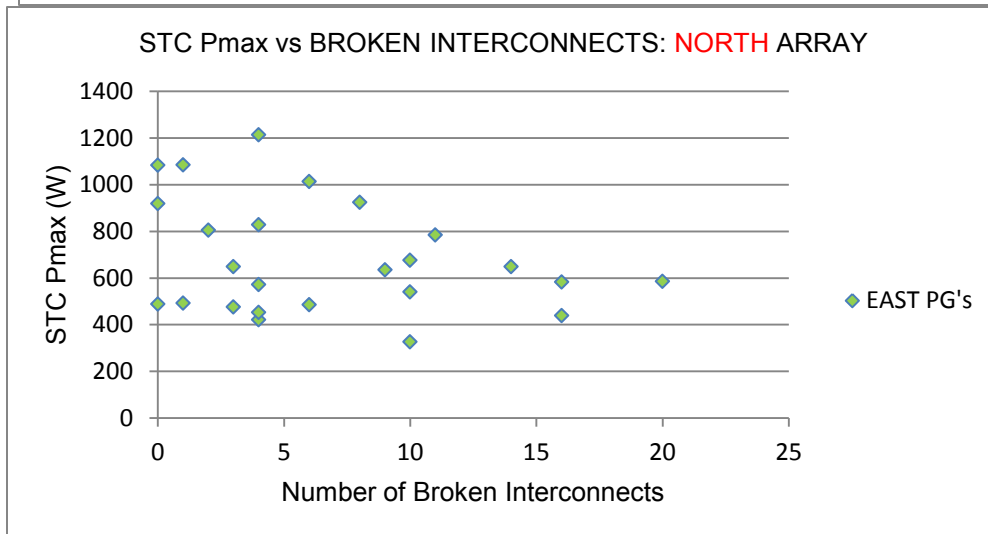
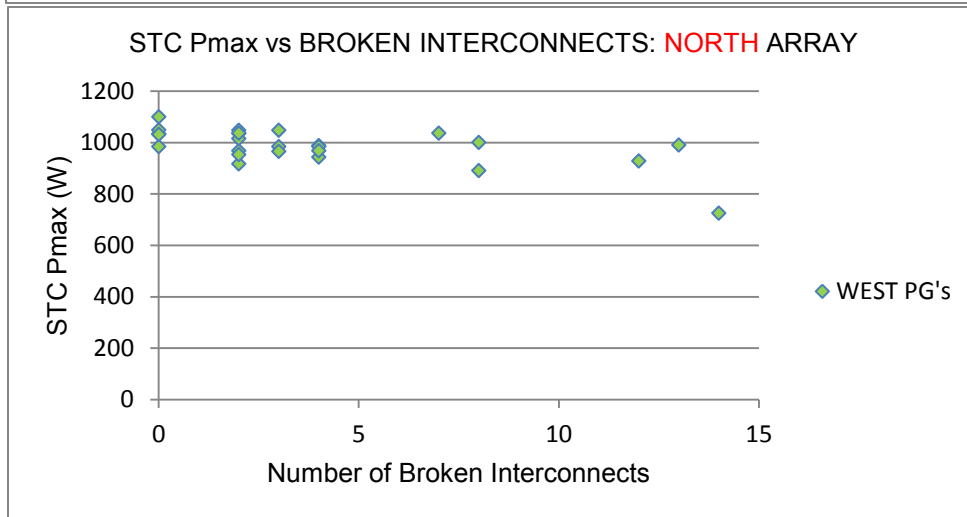
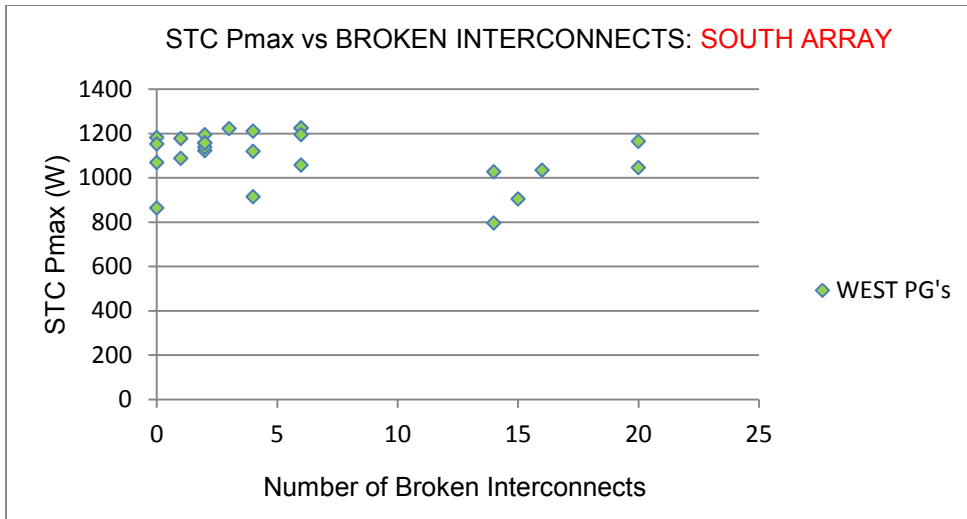


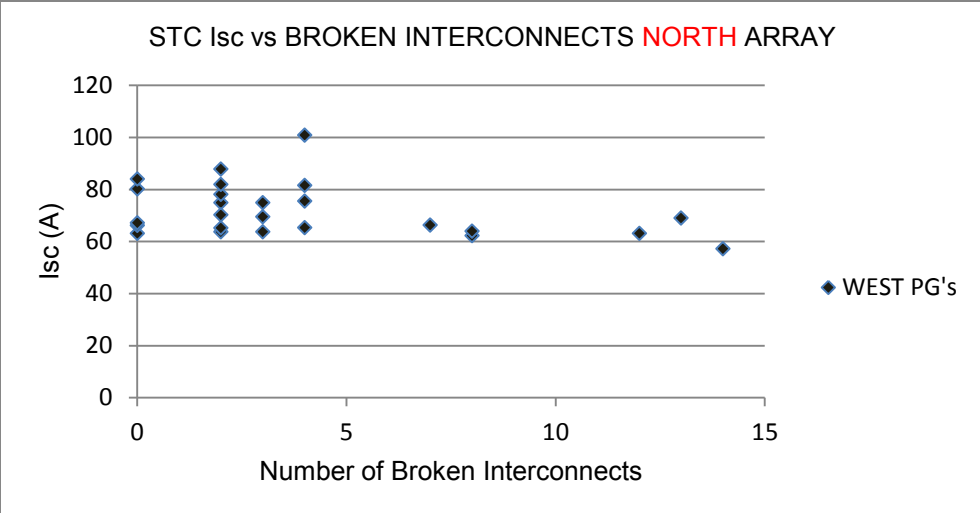
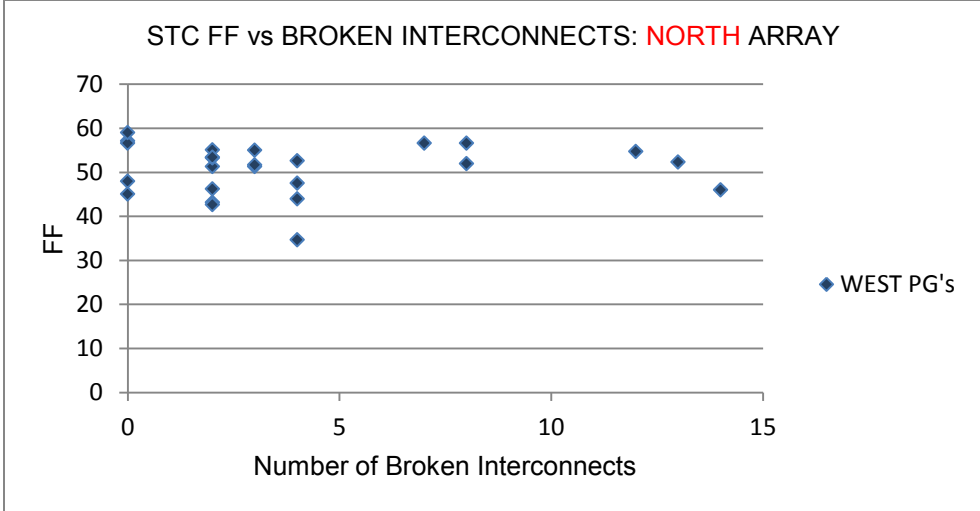


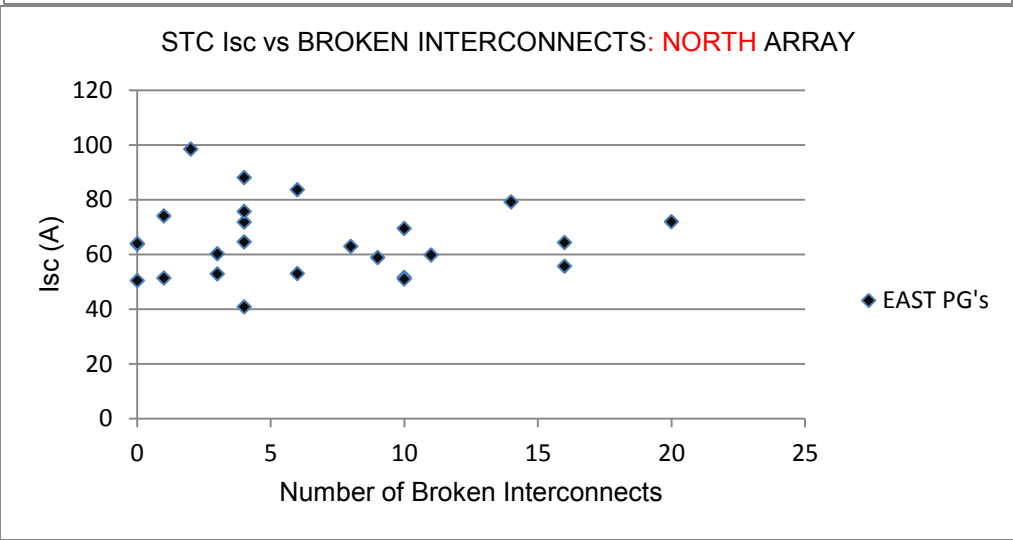
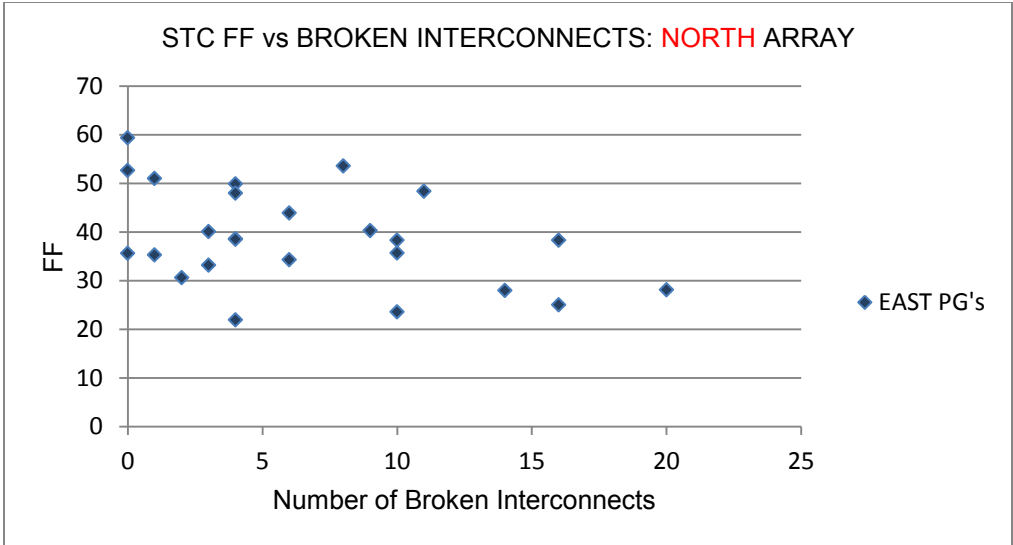


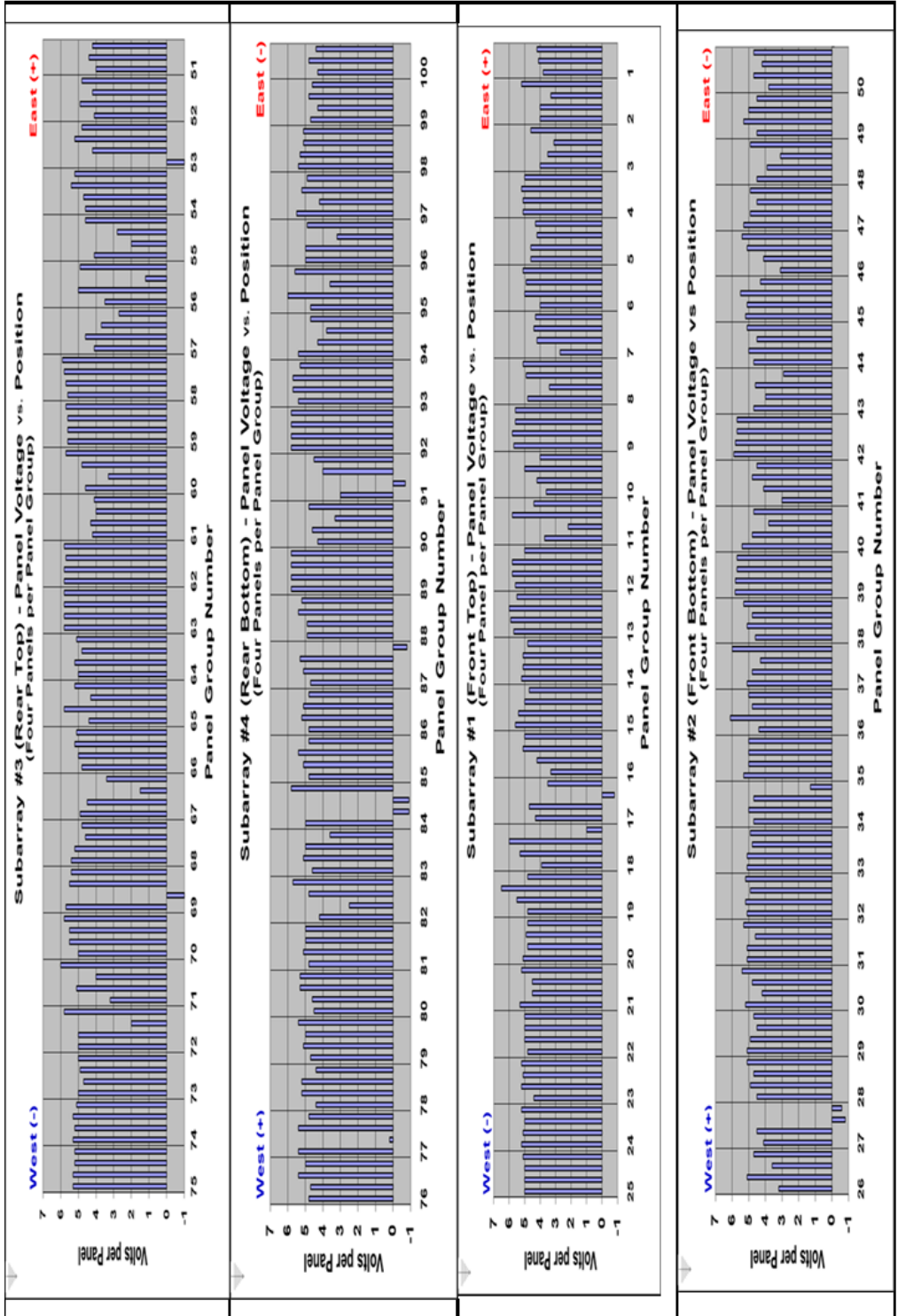






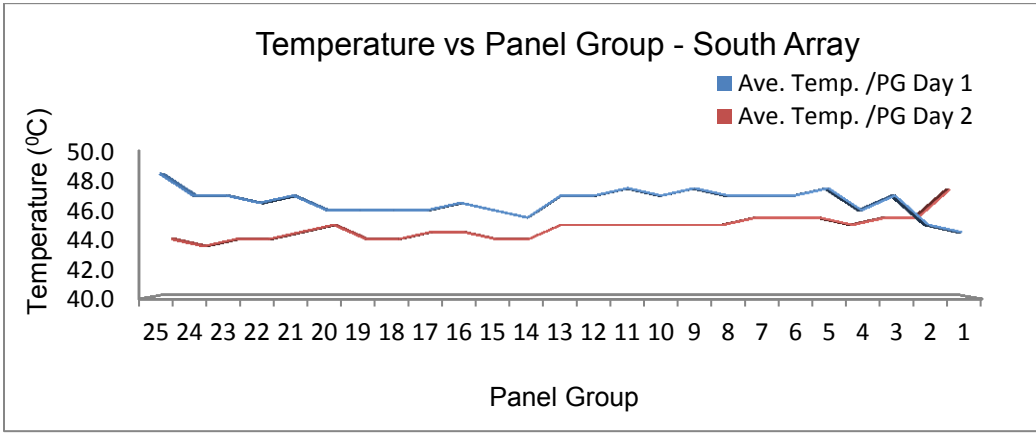
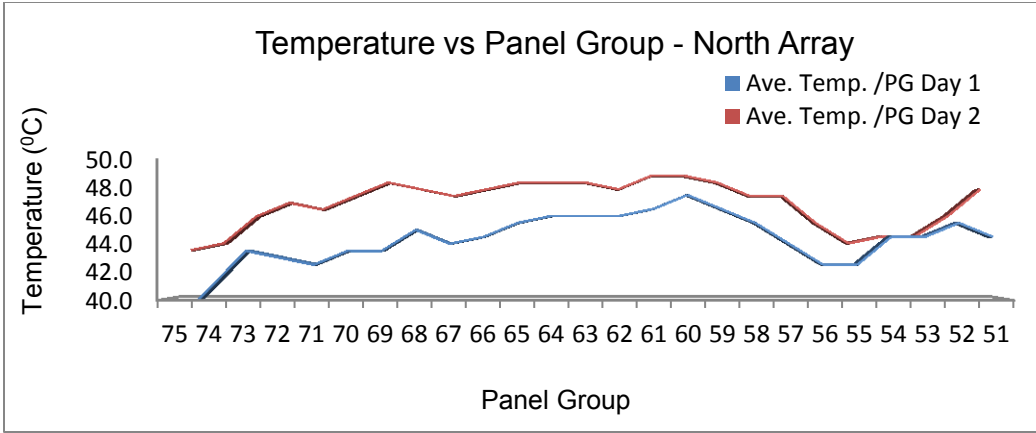


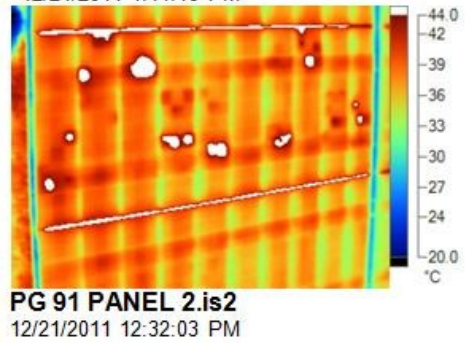
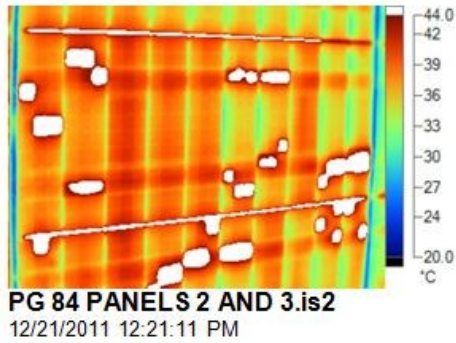
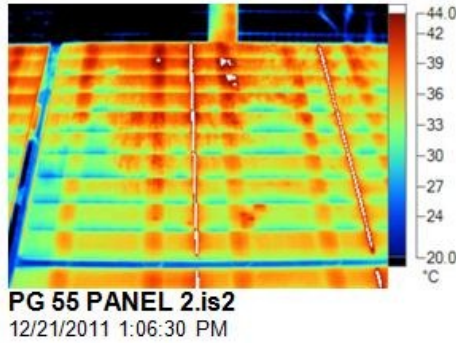
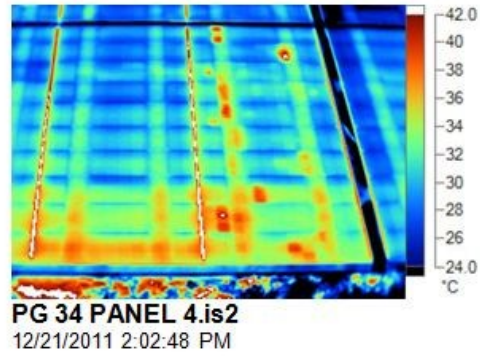
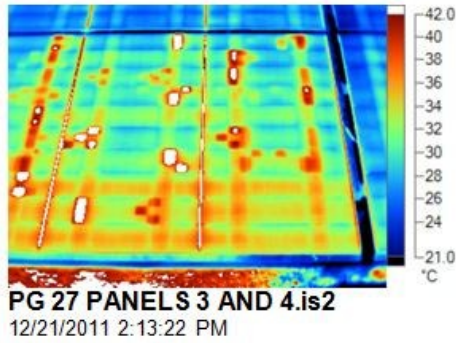




South array panel voltages measured under load

North Array PG's Average Ambient Temperatures																																
DATE	WEST AVERAGE	West - Sub array 3 PG's - Top Beam IR															East - Sub array 3 PG's - Top Beam IR															EAST AVERAGE
		75	74	73	72	71	70	69	68	67	66	65	64	63	62	61	60	59	58	57	56	55	54	53	52	51						
Day 1 05/03/2012		39.1	40.0	44.0	44.0	42.0	42.0	43.0	43.0	43.0	45.0	43.0	44.0	45.0	46.0	46.0	46.0	47.0	47.0	46.0	46.0	46.0	45.0	43.0	42.0	43.0	44.0	46.0	44.0			
		38.0	42.0	43.0	44.0	44.0	44.0	44.0	45.0	45.0	45.0	46.0	46.0	46.0	46.0	46.0	46.0	48.0	47.0	45.0	43.0	42.0	43.0	46.0	45.0	45.0	45.0	45.0	45.0			
	43.4	38.6	41.0	43.5	43.0	42.5	43.5	43.5	45.0	44.0	44.5	45.5	46.0	46.0	46.0	46.5	47.5	46.5	46.5	44.0	42.5	42.5	44.5	44.5	44.5	44.5	44.5	44.5	45.1			
Day 2 05/04/2012		44.0	44.0	46.0	47.0	46.0	47.0	48.0	48.0	47.0	48.0	48.0	49.0	48.0	48.0	48.0	49.0	48.0	48.0	48.0	48.0	45.0	44.0	44.0	44.0	46.0	47.0					
		43.0	44.0	46.0	47.0	47.0	48.0	49.0	48.0	48.0	48.0	49.0	48.0	49.0	48.0	50.0	49.0	49.0	47.0	47.0	46.0	44.0	45.0	45.0	46.0	49.0						
	47.0	43.5	44.0	46.0	47.0	46.5	47.5	48.5	48.0	47.5	48.0	48.5	48.5	48.5	48.0	49.0	49.0	48.5	48.0	47.5	45.5	44.0	44.5	44.5	46.0	48.0	47.0					
OVERALL AVERAGE	45.2																															46.0
South Array PG's Average Ambient Temperatures																																
DATE	WEST AVERAGE	West - Sub array 1 PG's - Top Beam IR															East - Sub array 1 PG's - Top Beam IR															EAST AVERAGE
		25	24	23	22	21	20	19	18	17	16	15	14	13	12	11	10	9	8	7	6	5	4	3	2	1						
Day 1 05/03/2012		47.0	47.0	47.0	46.0	47.0	46.0	46.0	46.0	46.0	46.0	47.0	46.0	45.0	46.0	46.0	48.0	47.0	48.0	47.0	47.0	47.0	47.0	47.0	47.0	47.0	47.0	47.0	45.0			
		50.0	47.0	47.0	47.0	47.0	46.0	46.0	46.0	46.0	46.0	46.0	46.0	46.0	48.0	48.0	47.0	47.0	47.0	47.0	47.0	47.0	47.0	47.0	47.0	47.0	47.0	47.0	44.0			
	46.5	48.5	47.0	47.0	46.5	47.0	46.0	46.0	46.0	46.0	46.5	46.0	45.5	47.0	47.0	47.0	47.5	47.0	47.0	47.0	47.0	47.0	47.0	47.0	47.0	47.0	47.0	47.0	46.7			
Day 2 05/04/2012		44.0	44.0	44.0	44.0	45.0	44.0	44.0	44.0	44.0	45.0	44.0	44.0	44.0	45.0	45.0	45.0	45.0	45.0	45.0	45.0	46.0	45.0	46.0	46.0	46.0	48.0					
		44.0	43.0	44.0	44.0	44.0	44.0	44.0	44.0	44.0	45.0	44.0	44.0	44.0	45.0	45.0	45.0	45.0	45.0	45.0	46.0	45.0	46.0	45.0	45.0	47.0						
	44.2	44.0	43.5	44.0	44.0	44.5	45.0	44.0	44.0	44.0	44.5	44.0	44.0	45.0	45.0	45.0	45.0	45.0	45.0	45.0	45.5	45.0	45.0	45.0	45.0	47.5	45.4					
OVERALL AVERAGE	45.3																															46.0





Hotspot effects on PV array

Table 4.5 (a) High Potential Test Resistance Output in mega Ohms (MΩ)

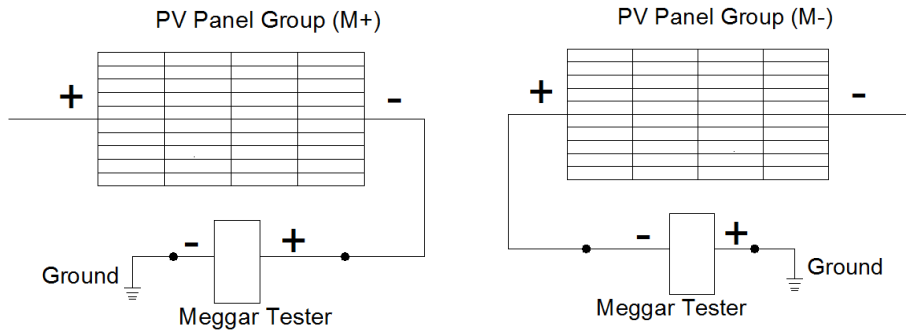
PGs TESTED	DRY CONDITION		VERY WET CONDITION (RAIN)		MILD WET CONDITION (DEW)	
	M +	M-	M +	M-	M +	M-
*14	192.5	371	0.014	0.002	-	-
97	330	190	0.035	0.015	-	-
4	209.4	244.5	0.048	0.08	-	-
*55	177	181	-	-	13.3	36.56
91	183	232	-	-	48	44
58	179	176	-	-	10.5	63.8

* Panel Group has one module with broken glass

Table 4.5 (b) High Potential Test current Output in milliamps (mA)

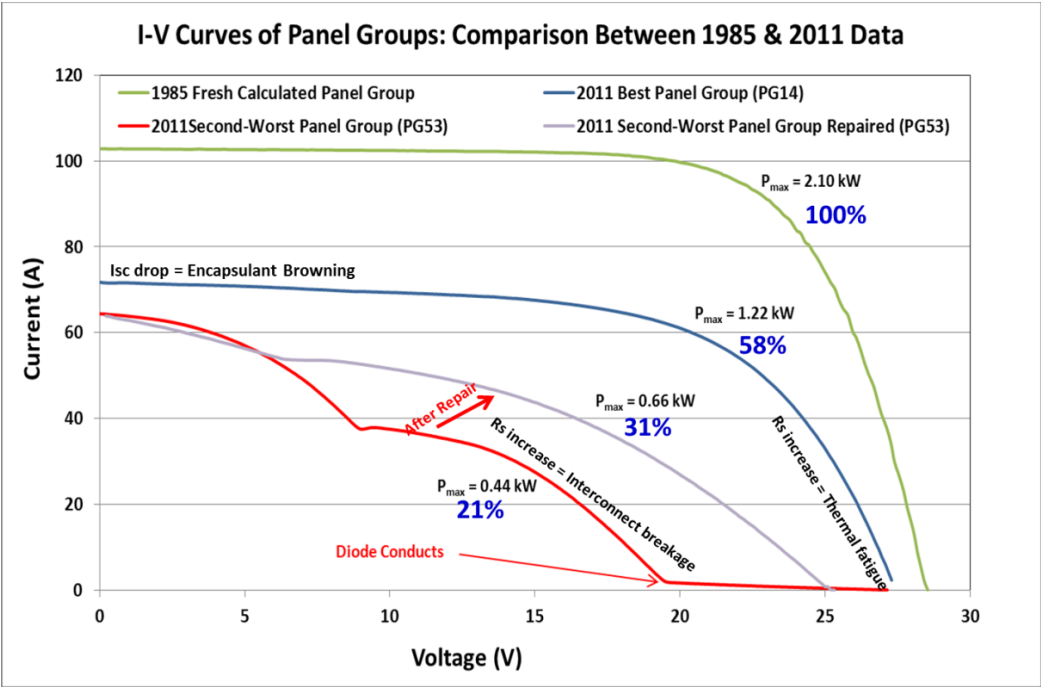
PGs TESTED	DRY CONDITION		VERY WET CONDITION (RAIN)		MILD WET CONDITION (DEW)	
	M +	M-	M +	M-	M +	M-
*14	0.0026	0.0013	35.714	250.000	-	-
97	0.0015	0.0026	14.286	33.333	-	-
4	0.0024	0.0020	10.417	6.250	-	-
*55	0.0028	0.0028	-	-	0.038	0.014
91	0.0027	0.0022	-	-	0.010	0.011
58	0.0028	0.0028	-	-	0.048	0.008

* Panel Group has one module with broken glass

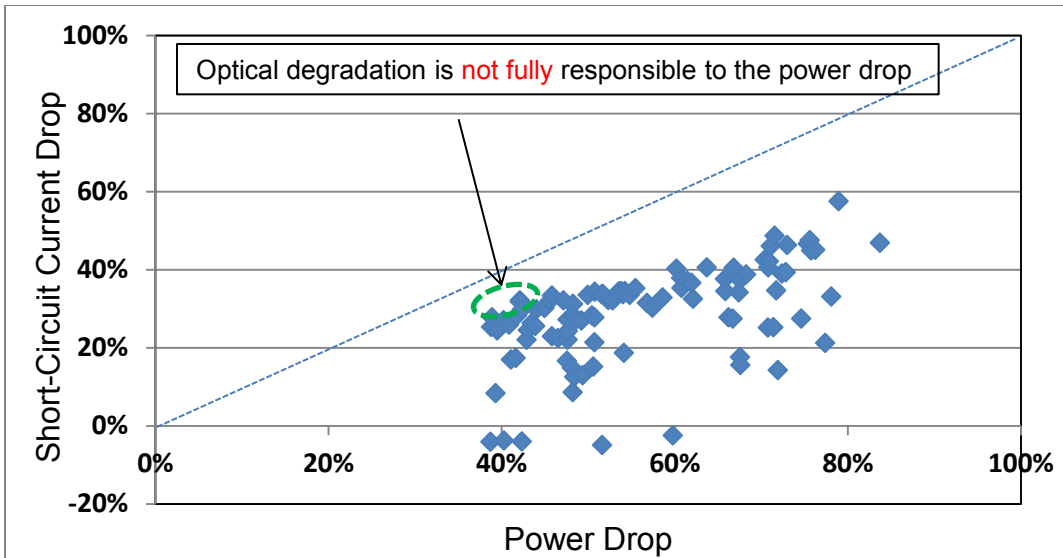
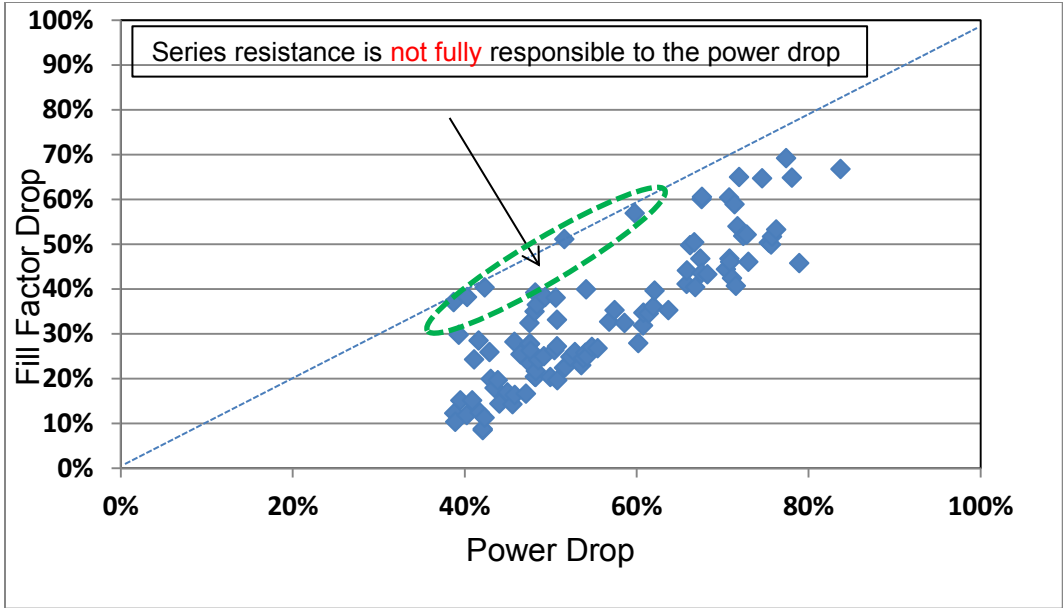


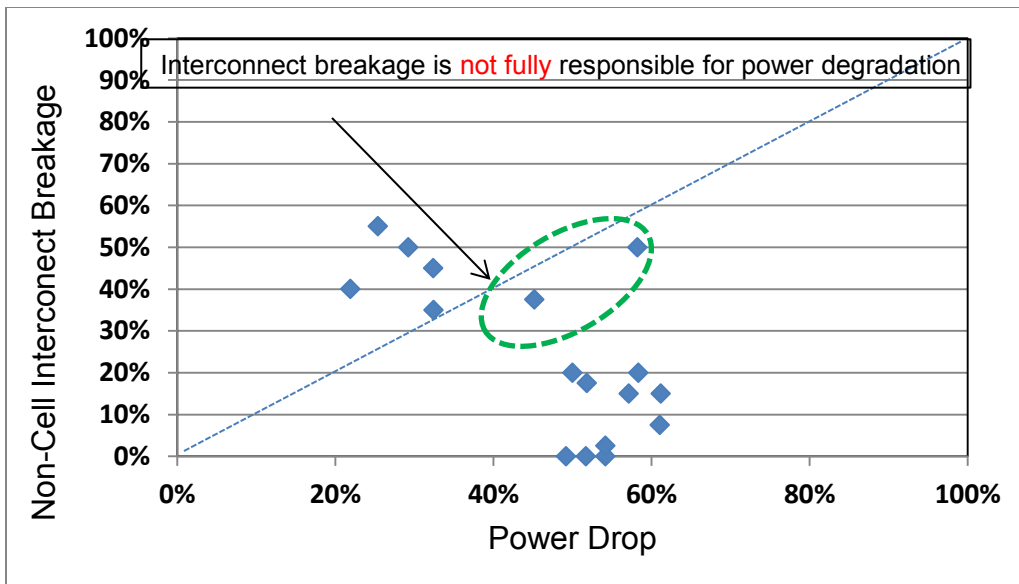
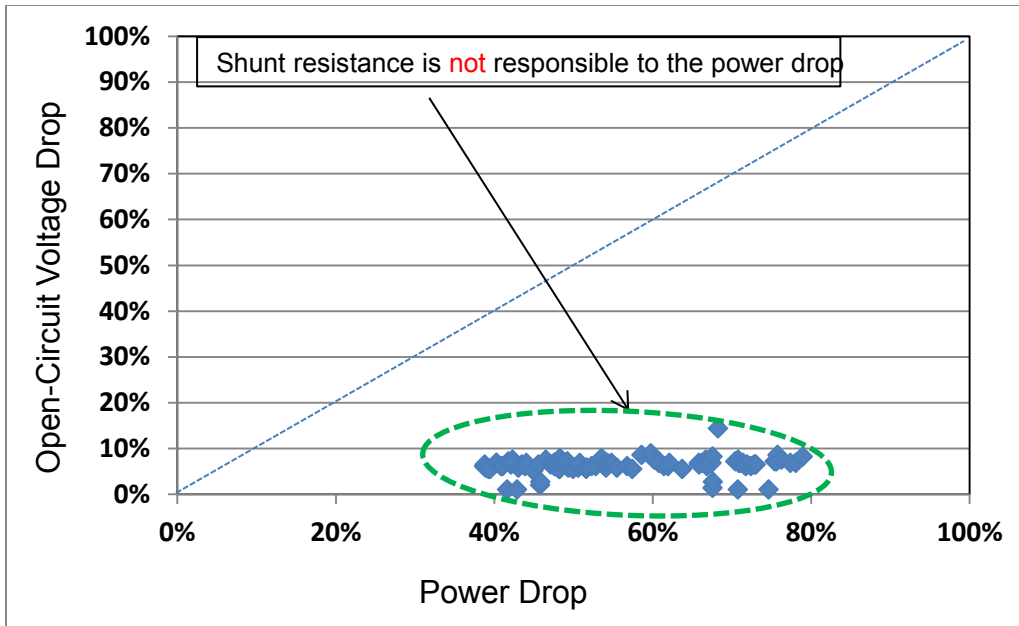
Hi-Pot Insulation Test wiring for positive (left) and negative (right) polarities above ground

I-V Before and After Repair

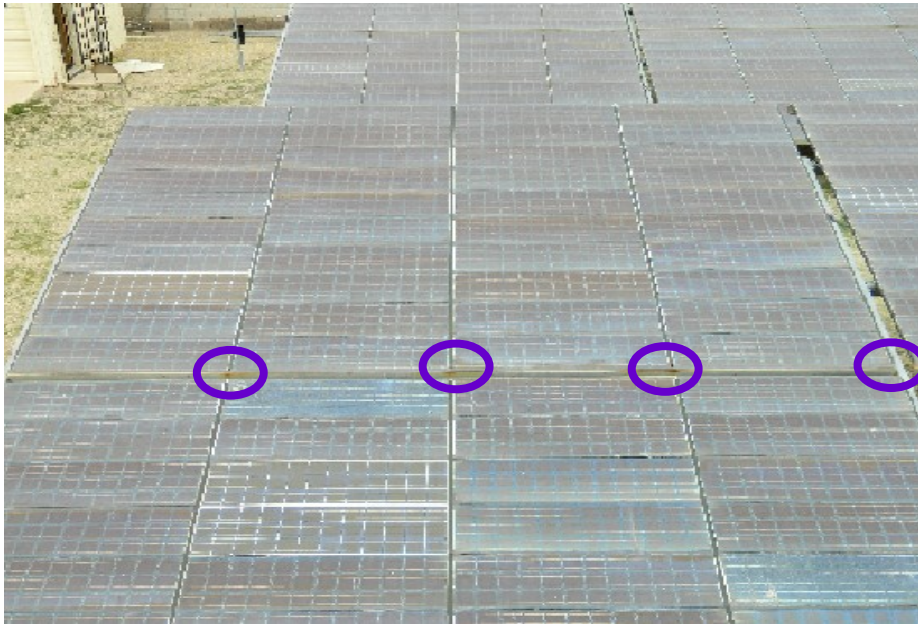


I-V comparison of PG from new to degraded condition





Corrosion of panel group



SUB- ARRAY 3	Panel Group 75	Panel Group 76	Panel Group 77	Panel Group 78	Panel Group 79	Panel Group 80	Panel Group 81	Panel Group 82	Panel Group 83	Panel Group 84	Panel Group 85	Panel Group 86	Panel Group 87	Panel Group 88	Panel Group 89	Panel Group 90	Panel Group 91	Panel Group 92	Panel Group 93	Panel Group 94	Panel Group 95	Panel Group 96	Panel Group 97	Panel Group 98	Panel Group 99	Panel Group 100
	Panel	Panel	Panel	Panel	Panel	Panel	Panel	Panel	Panel	Panel	Panel	Panel	Panel	Panel	Panel	Panel	Panel	Panel	Panel	Panel	Panel	Panel	Panel	Panel	Panel	Panel
SUB- ARRAY 4	Panel Group 75	Panel Group 76	Panel Group 77	Panel Group 78	Panel Group 79	Panel Group 80	Panel Group 81	Panel Group 82	Panel Group 83	Panel Group 84	Panel Group 85	Panel Group 86	Panel Group 87	Panel Group 88	Panel Group 89	Panel Group 90	Panel Group 91	Panel Group 92	Panel Group 93	Panel Group 94	Panel Group 95	Panel Group 96	Panel Group 97	Panel Group 98	Panel Group 99	Panel Group 100
	Panel	Panel	Panel	Panel	Panel	Panel	Panel	Panel	Panel	Panel	Panel	Panel	Panel	Panel	Panel	Panel	Panel	Panel	Panel	Panel	Panel	Panel	Panel	Panel	Panel	Panel
SUB- ARRAY 1	Panel Group 41	Panel Group 42	Panel Group 43	Panel Group 44	Panel Group 45	Panel Group 46	Panel Group 47	Panel Group 48	Panel Group 49	Panel Group 50	Panel Group 51	Panel Group 52	Panel Group 53	Panel Group 54	Panel Group 55	Panel Group 56	Panel Group 57	Panel Group 58	Panel Group 59	Panel Group 60	Panel Group 61	Panel Group 62	Panel Group 63	Panel Group 64	Panel Group 65	Panel Group 66
	Panel	Panel	Panel	Panel	Panel	Panel	Panel	Panel	Panel	Panel	Panel	Panel	Panel	Panel	Panel	Panel	Panel	Panel	Panel	Panel	Panel	Panel	Panel	Panel	Panel	Panel
SUB- ARRAY 2	Panel Group 26	Panel Group 27	Panel Group 28	Panel Group 29	Panel Group 30	Panel Group 31	Panel Group 32	Panel Group 33	Panel Group 34	Panel Group 35	Panel Group 36	Panel Group 37	Panel Group 38	Panel Group 39	Panel Group 40	Panel Group 41	Panel Group 42	Panel Group 43	Panel Group 44	Panel Group 45	Panel Group 46	Panel Group 47	Panel Group 48	Panel Group 49	Panel Group 50	Panel Group 51
	Panel	Panel	Panel	Panel	Panel	Panel	Panel	Panel	Panel	Panel	Panel	Panel	Panel	Panel	Panel	Panel	Panel	Panel	Panel	Panel	Panel	Panel	Panel	Panel	Panel	Panel

Number of Units	Number of Subunits per Unit	Parallel or Series Connection
1	System	NA
2	Arrays per system	Parallel
4	Subarrays per array	Parallel
12 or 13	Panel groups per subarray	Series
4	Panels per panel group	Series
10	Modules per panel	Parallel
Total number of modules = $1 \times 2 \times 4 \times 13 \times 4 \times 10 = 4000$		
Voltage of each module = 7.3 V		
Sytem Voltage = $13 \times 4 \times 7.3 \sim 375$ V (4 positive and 4 negative as shown below)		

<u>PV Module Physical Data</u>	
Manufacturer	ARCO Solar, Inc.
Model Number	M54
Date of Manufacture	1985
Frame Type	unframed
Module Width	13 inches
Module Length	50.9 inches
Weight	11.5 lbs
Solar Cell Technology	single crystal silicon
Solar Cell Shape, Size	Square, 4-in x 4-in
Number of Solar Cells	36
Series	12
Parallel	3
<u>PV Module Specifications*</u>	
Rating Conditions	1,000 W/m ² irradiance 25 C cell temperature
Open-circuit Voltage	7.3 Volts
Max-power Voltage	5.8 Volts
Max-power Current	8.6 Amps
Short-circuit Current	9.6 Amps
Rated Power	50 Watts
Fill Factor	0.71
<u>PV Array Physical Data</u>	
Number of PV Modules	4,000
Mounting Method	Ground-mounted fixed tilt rack
PV Array Width	425 ft.
PV Array Slope Height	22 ft.
Tilt Angle	17°
Azimuth Orientation	due South
* Values obtained from manufacturer's literature	

Subarray – Measured Performance Data:

West Subarrays						East Subarrays					
West Subarray	Panel Groups	Pmax (kW)	Irradiance (W/m ²)	Tamb (°C)	Tarray (°C)	East Subarray	Panel Groups	Pmax (kW)	Irradiance (W/m ²)	Tamb	Tarray
Subarray 3 (-ve)	12	8.88	903	33.8	55	Subarray 3 (+ve)	13	5.32	859	34.3	55
Subarray 4 (+ve)	13	9.48	867	35.1	55	Subarray 4 (-ve)	12	5.27	904	34.4	54
Subarray 1 (-ve)	12	9.43	877	34.6	54	Subarray 1 (+ve)	13	5.83	853	33.5	54
Subarray 2 (+ve)	13	8.78	855	32.9	54	Subarray 2 (-ve)	12	5.88	898	35.4	54
Average		9.1425	875.5	34.1	54.5	Average		5.575	878.5	34.4	54.25
Total	50	36.57				Total	50	22.3			

Table 4A: Measured Pmax of WEST Subarrays

Table 4B: Measured Pmax of EAST Subarrays

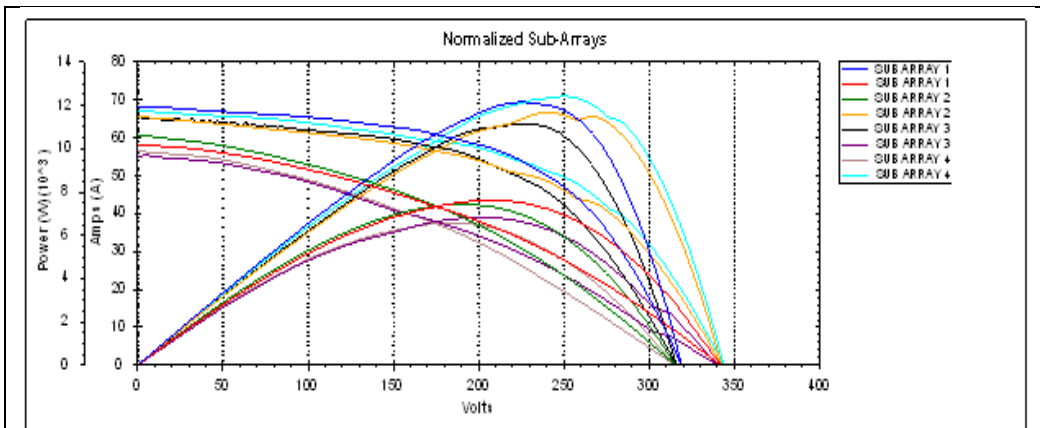


Figure 3: I-V and P-V Curves of 8 Subarrays at STC

West Subarray #	Panel Groups	Date	Pmax (W)	Isc (A)	Voc (V)	I _{max} (A)	V _{max} (V)	FF (%)
Subarray 3 (-ve)	12	10/12/2011	11,139	65	316	50	224	54
Subarray 4 (+ve)	13	10/12/2011	12,427	67	344	49	251	54
Subarray 1 (-ve)	12	10/12/2011	12,155	68	320	54	225	56
Subarray 2 (+ve)	13	10/12/2011	11,672	66	343	49	240	52
Average			11,848	67	331	51	235	54
Total	50		47,393					

Table 5A: STC Pmax of WEST Subarrays

East Subarray #	Panel Groups	Date	Pmax (W)	Isc (A)	Voc (V)	I _{max} (A)	V _{max} (V)	FF (%)
Subarray 3 (+ve)	13	10/12/2011	6,833	55	340	34	199	36
Subarray 4 (-ve)	12	10/12/2011	6,572	57	315	35	185	37
Subarray 1 (+ve)	13	10/12/2011	7,628	58	342	37	206	38
Subarray 2 (-ve)	12	10/12/2011	7,443	61	316	39	192	39
Average			7,119	58	328	36	196	38
Total	50		28,476					

Table 5B: STC Pmax of EAST Subarrays

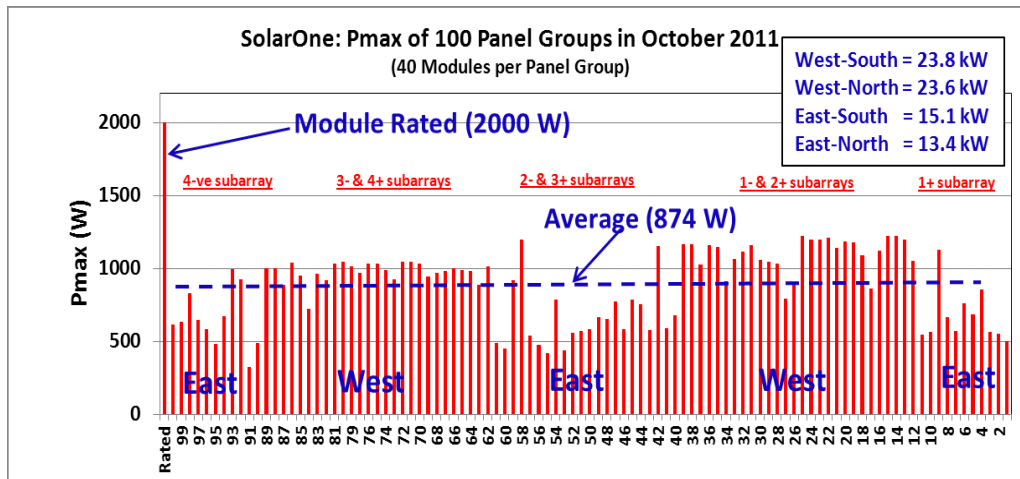
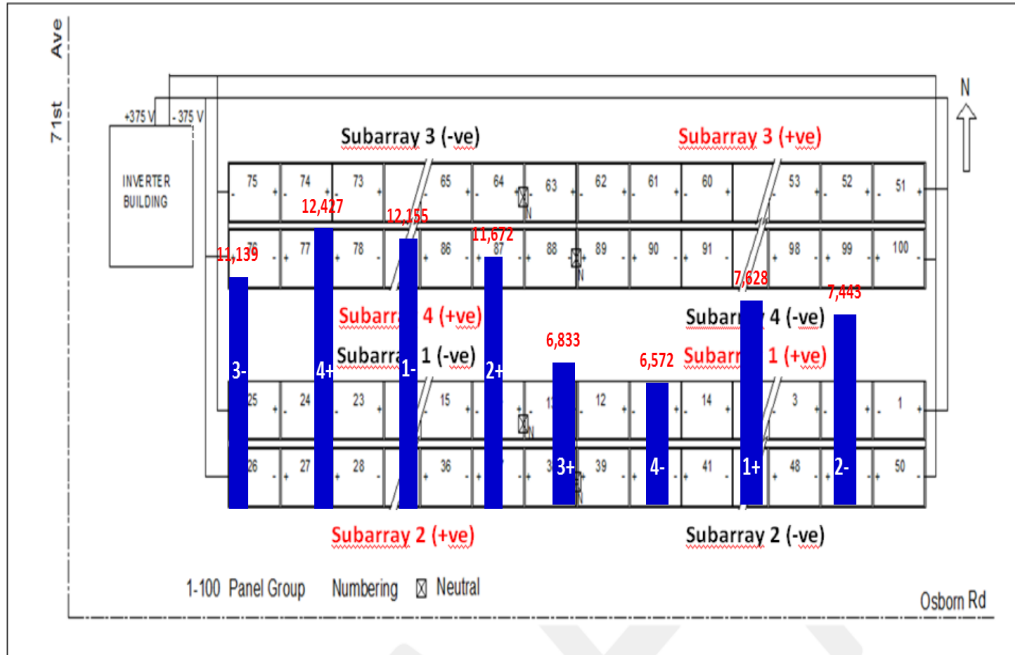


Figure 5: Panel Group Number versus STC Pmax Plot